Investigation of Regulation of Expression of *SKS1* mRNA in *Saccharomyces cerevisiae*

A Thesis submitted for the Degree of Doctor of Philosophy

in the Faculty of Science

2025

By

SOUMITA PAUL

Under the Guidance of

Prof. Biswadip Das

RNA BIOLOGY LAB

DEPARTMENT OF LIFE SCIENCE AND BIOTECHNOLOGY

JADAVPUR UNIVERSITY, KOLKATA-700032

DECLARATION

I hereby declare that the work reported in this thesis entitled **"Investigation of Regulation of Expression of *SKS1* mRNA in *Saccharomyces cerevisiae*"** is entirely original and was carried out by me under the general supervision of **Prof. Biswadip Das**, Department of Life Science and Biotechnology, Jadavpur University, Kolkata, India.

I further declare that the contents of this thesis have not been the basis for the award of any degree, diploma, fellowship, associateship or any other similar title of any University or Institution.

SOUMITA PAUL

Date:

Department of Life science and Biotechnology

Jadavpur University

Kolkata-700032

India

“Discovery consists of seeing what everybody has seen and thinking what nobody has thought”

-Albert Szent-Györgyi

যাদবপুর বিশ্ববিদ্যালয়
কলকাতা-৭০০০৩২, ভারত

*JADAVPUR UNIVERSITY
KOLKATA-700 032, INDIA

DEPARTMENT OF LIFE SCIENCE AND BIOTECHNOLOGY

CERTIFICATE FROM THE SUPERVISOR(S)

This is to certify that the thesis entitled "**Investigation of Regulation of Expression of *SKS1* mRNA in *Saccharomyces cerevisiae***" Submitted by **Smt. Soumita Paul** who got her name registered on 13th September, 2019 for the award of Ph. D. (Science) Degree of Jadavpur University, is absolutely based upon her own work under the supervision of Prof. Biswadip Das and that neither this thesis nor any part of it has been submitted for either any degree / diploma or any other academic award anywhere before.

Biswadip Das 05-05-2025.

Biswadip Das
FRSB, FASc., FAScT.
Professor
Department of Life Science & Biotechnology
Jadavpur University

Biswadip Das
Ph.D., FRSB
Department of Life Science and Biotechnology
Jadavpur University
Kolkata - 700032

ACKNOWLEDGEMENT:

"Believe you can and you're halfway there"- Theodore Roosevelt

With immense joy and profound gratitude, I begin this acknowledgement, thanking Almighty God for transforming my dream of earning a doctoral degree into reality. His unwavering guidance and unrelenting faith have been the driving forces behind my perseverance. As I embark on this major milestone of my Academic career, I offer my deepest gratitude to God, whose divine presence has illuminated my path. His blessings have filled my heart with faith, fortifying me to overcome every obstacle and emerge triumphant. As the first doctorate in my family, I hope He conveys my joy and accomplishments to my beloved father, Late Adv. Biswanath Paul.

Maa look, we have made it till here. I am forever indebted to my mother, Mrs. Tapashi Rani Paul, for her dedication and selfless love, which have shaped me into the person I am today. She instilled in me the values of resilience, sincerity and responsibility, inspiring me to persevere through life's challenges. Her belief that "God is always in our favor" has echoed throughout my journey, fortifying my resolve to overcome obstacles and achieve excellence. I have inherited my straight-forwardness and honesty from my father. He has been my inspiration when it comes to "Love what you do". He is the reason that I believe in "never compromise with honesty, come what may". I remember how he taught me to be confident and content. Baba, your love will surround me forever, beyond the cycle of life and time. Dada, Sourav Paul, you have been by my side even after being miles apart. Dida, Nila Rani Paul & Mama, Anjan Kr. Paul, thank you for supporting us when we needed it the most and now that I have grown up, I wish to reciprocate the same.

I would like to express my sincere appreciation to my supervisor Professor Biswadip Das and Dr. Satarupa Das, for their invaluable guidance and support. Sir, I cannot express enough gratitude for the trust you have shown towards me, without which, this journey would not have started. Your perfectionist nature is an inspiration for me and your insightful expertise have shaped my research mindset. Sir and Madam both have

been kind enough to allow me proceed with my own pace. I am forever grateful for their presence in my academic life.

I have a very small world and my lab-mates have become like a family to me. This family wasn't built in a day, we have all grown up together for the past 6 years. We know each other's strengths and weaknesses. Somewhere between fighting over minor issues to guarding each other during major issues, we all grew up. We have learnt the art of co-existing despite having differences in views. I am glad to be a part of this lab. My seniors Dr. Anusha Chaudhuri and Dr. Subhadeep Das have blindly trusted me when it comes to bench work, they have boosted my confidence level. Anusha Di you are a gem of a person, the most organized and sorted out individual. You are the reason my name was there for the first time in a scientific publication. Sunirmal da is our go-to person whatever be the matter. Dr. Sunirmal Paira has patiently taught me a lot of the experimental procedures. I hope, I too could help you out sometimes with my little knowledge, because I believe, that is the best way to show gratitude. The Post Doctoral Fellows of our laboratory, Dr. Arindam Chakraborty and Dr. Prosanta Saha have introduced me to the path ahead of Ph.D. I wish them good luck for their respective careers. Arindam da has always treated us like younger siblings and guided me with various matters outside lab work. Dr. Shouvik Chaudhuri, I am indebted to you for doing all the MAT-LAB analyses for my paper quietly ignoring my constant nagging. Then comes a group of seniors who have never made me feel like a junior, Mayukh Banerjea, Bhaswar Nandi and Rajlaxmi Gaine. Mayukh da is confused, thoughtful and organized all at the same time. Bhaswar da is a unique combination of a laid-back talented person. He is our very own "mythological story teller" and "tour guide". Rajlaxmi di is the protein deficient girl, sitting silently in a corner and doing the major protein related work of our lab. I wish for each of you, all the success and appreciation that you deserve. From potlucks to seminar-presentations, you all have been great mates. My juniors, Gargi Sirkar and Arnab Kundu, have loved me immensely, for which I am humbled. Arnab is like a clueless sibling without whom the lab feels incomplete. I wish both of you a worthy Ph.D. career ahead. My colleagues have been very compassionate and supportive. I will cherish forever; the warmth and generosity they have shown towards me. I will miss the laughter we shared, the mischievous eye-

contacts, the giggles and the pokes. I can truly say that I have noticed and felt a lot more effort than I could write down here due to my inability to express. Last, but not the least, I am indebted to my trainees Poulomi, Ria, Abhishek, Debojyoti, Biswajit and Siddhartha for allowing the student in me, a chance, to grow into a teacher. I wish good luck to all the new joiners of our lab.

I have had a cordial and co-operative relation with all the other labs of our department, specially ASG Lab and PKD Lab. Shreya Das of ASG lab has been a savior for me as she has taught me various techniques that were required for my research work. PKD lab has been very supportive in time of any need, I am grateful to all the scholars of that lab.

Indraneel Sengupta, you have been a great colleague and friend. Your readily available guidance and support have helped me navigate numerous challenges of life. Your selfless dedication to assisting others, coupled with your remarkable work ethic, has been a constant source of inspiration for me. You have been my best critique and biggest supporter. I wish you continued success and recognition for your outstanding efforts in the field of research. I am grateful to God that I met you.

I would also like to extend my heartfelt gratitude to all the faculties, technician staffs and specially the Department of Life Science and Biotechnology, Jadavpur University; for giving all the facilities that were possible with the limited funding we had.

Lastly, thank you CSIR for providing me with fellowship and making me realize the importance of being financially independent. And for the same reason, I would like to thank all my Graduation and Masters faculties, because it is for their guidance that I could crack the CSIR-NET examination.

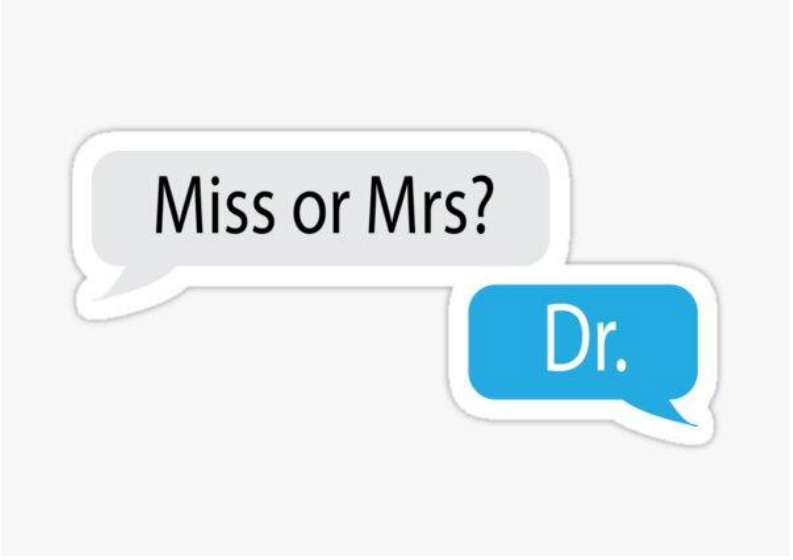

"This achievement is dedicated to those who dared to dream, but circumstances interrupted their path. Your efforts, though unseen, are not unfelt. I dedicate my degree for the acknowledgement of the significance of every effort, every struggle and every step taken towards excellence. May your unfinished journey inspire others to persevere."

~Soumita Paul

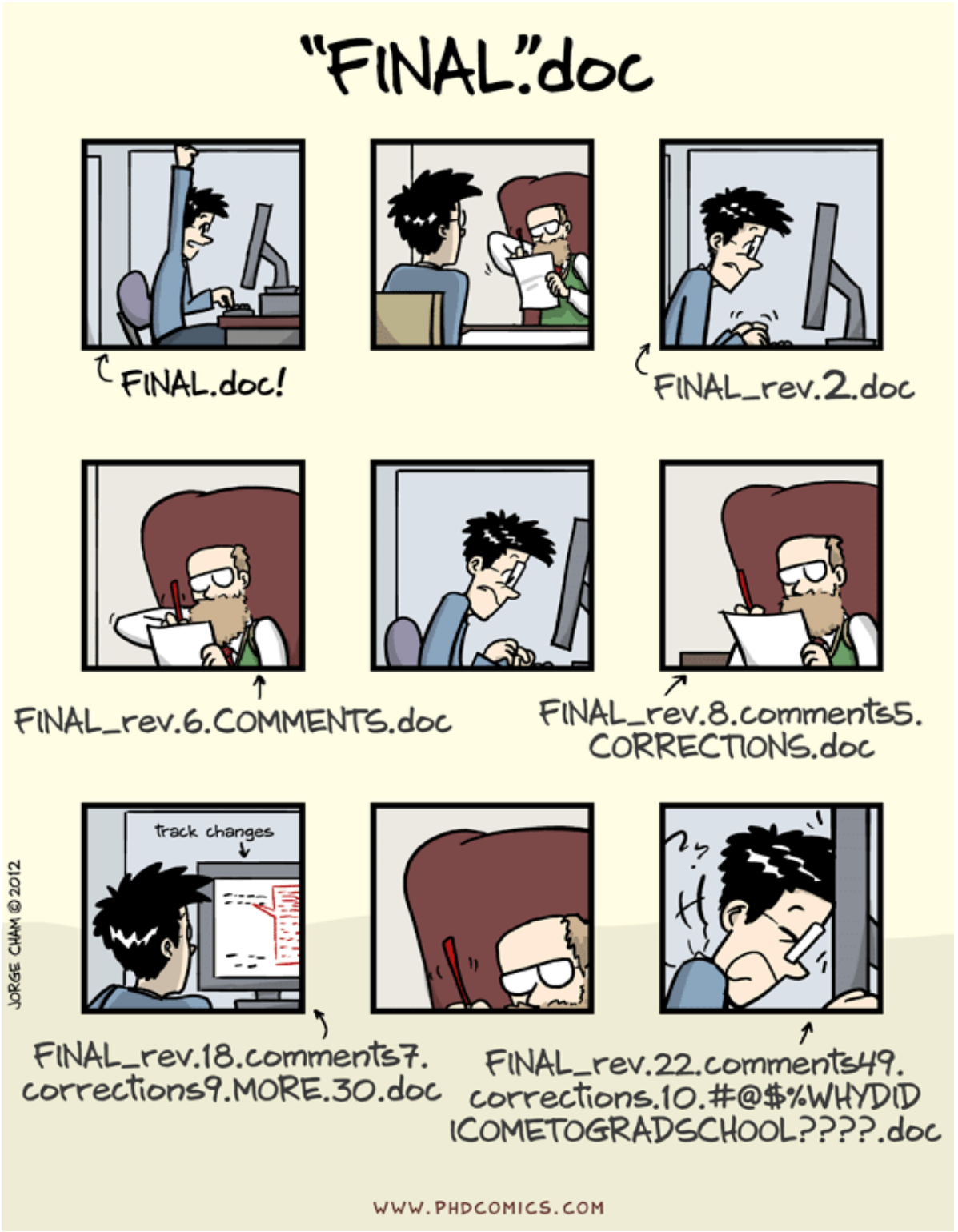
"FINAL".doc
FINAL.doc!
FINAL_rev.2.doc
FINAL_rev.6.COMMENTS.doc
FINAL_rev.8.comments5.
CORRECTIONS.doc
track changes
FINAL_rev.18.comments7.
corrections9.MORE.30.doc
FINAL_rev.22.comments49.
corrections.10.#@$%WHYDID
ICOMETOGRADSCHOOL????.doc
JORGE CHAM © 2012
WWW.PHDCOMICS.COM

TABLE OF CONTENTS:

LIST OF FIGURES:

ABSTRACT:

Regulation of gene expression is the vital activity of all organisms to sustain their life processes under the changing environmental conditions and stress. Nutrient stress is one such situation, in which limiting glucose and nitrogen stimulate a transition of rounded yeast cells to elongated/filamentous pseudohyphal form in pathogenic fungi. It is believed that the filamentous pseudohyphae is the pathogenic and virulent form of these fungal pathogens. However, neither the bona fide master regulator that controls the yeast to hyphal transition nor the detailed mechanistic insight of this transition is known. The protein kinase Sks1p was implicated in the integration of signals for nitrogen and glucose limitation, resulting in pseudohyphal growth in baker's yeast *S. cerevisiae.* The *SKS1* gene being orthologous to *SHA3* gene of pathogenic *C. albicans*, is also associated with the organism's virulent form. In *Saccharomyces cerevisiae, SKS1* mRNA belongs to a special class of "Nuclear Retained mRNAs" (NR mRNAs) representing a subset of otherwise normal transcripts, which typically undergo very slow export and an unusually long intra-nuclear dwell time owing to the presence of a 202 nt "export-retarding" nuclear zip code (NZ) element. However, the regulation of the expression of the *SKS1* gene is entirely unknown. Recent findings in our laboratory indicated that the cellular repertoire of *SKS1* mRNA is regulated at the post-transcriptional level via its Nuclear Zip-code sequence, which leads to its intranuclear retention followed by its rapid degradation by the Exosome and its cofactor CTEXT. This research work focuses on the identification of any Nuclear Zip-code element associated *trans*-acting factor(s), as well as the mechanism involved in the regulation of *SKS1* gene as well as other "NR mRNAs". The final conclusion of this analysis reveals a reversible mechanism of post-transcriptional regulation of these "NR mRNAs" involving modulation of intranuclear decay and nuclear export, which plays a crucial role in the adaptability and viability of the yeast cells. This work would provide a useful knowledge base in hunting the target for therapeutic intervention in pathogenic fungi like *Candida albicans*.

Chapter 1

INTRODUCTION TO THE AREA OF RESEARCH

1.1. Baker's Yeast *Saccharomyces cerevisiae* as a Model Eukaryote:

Baker's yeast *Saccharomyces cerevisiae* is a unicellular fungus, having a 12068 kb long nuclear genomic DNA organized in 16 chromosomes [(1)]. Goffeau *et al.* 1996 had sequenced its complete genome and it was found to contain approximately 6000 genes, of which, 5570 [(2)] are predicted

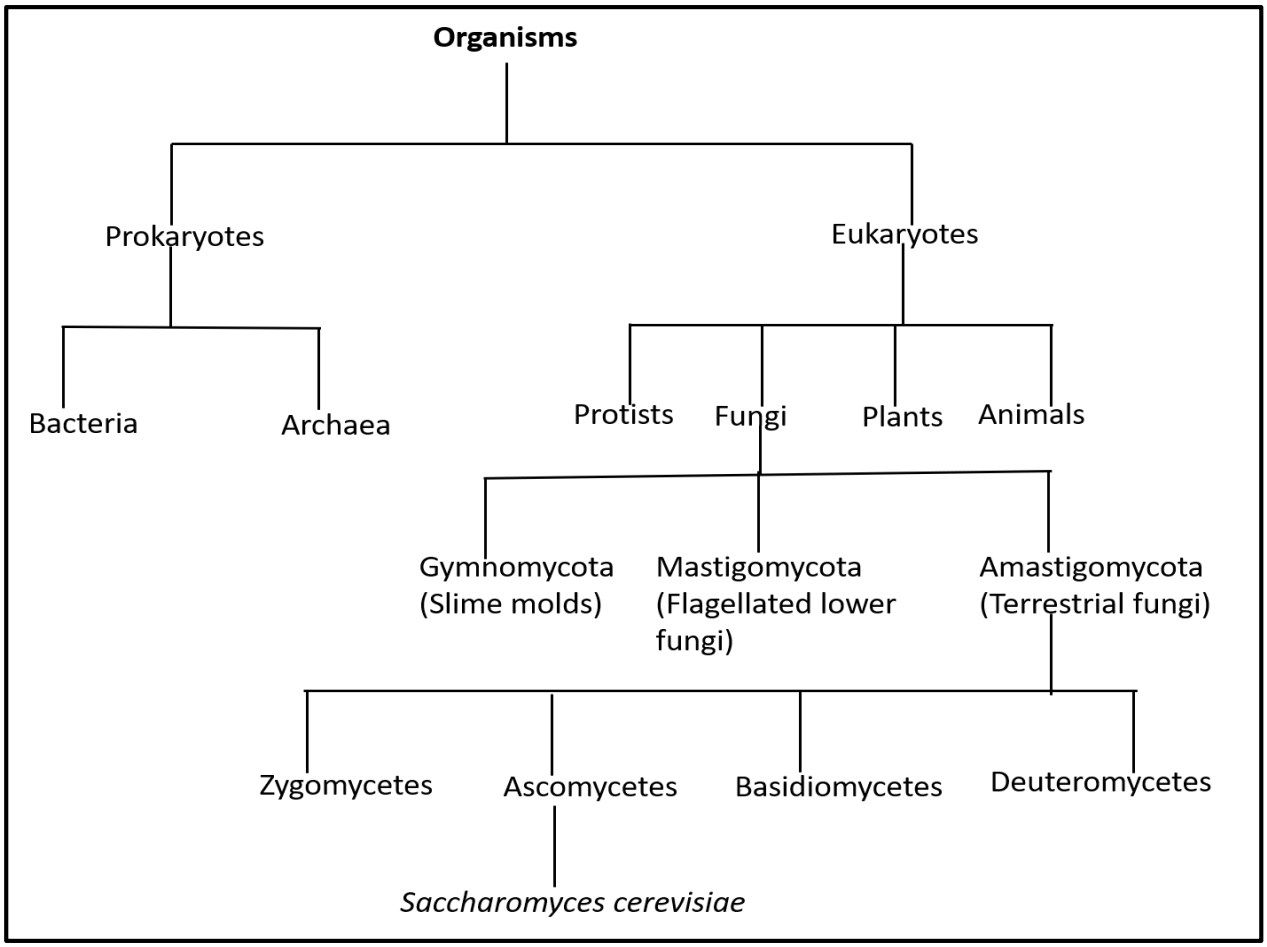

Fig 1.1: Phylogenetic Classification of Saccharomyces cerevisiae

to be protein-encoding genes. *Saccharomyces cerevisiae* is the best studied eukaryote and a valuable tool for most aspects of basic research involving eukaryotic biology. This is due to the fact that in spite of having a simple unicellular nature, *S. cerevisiae* offers most of the eukaryotic biological functions which are well conserved. In addition, it is also easily amenable to genetic manipulation [(3)] while being non-pathogenic to humans. *S. cerevisiae* is being extensively used to produce many industrially relevant chemicals and heterologous protein production apart from traditional applications in alcohol fermentations, baking or bio-ethanol production [(4)]. Hence, *S. cerevisiae* is widely chosen as an ideal model for research work in the field of studying eukaryotic gene regulation.

1.2. Eukaryotic mRNP Biogenesis and mRNA Degradation:

Nuclear mRNP (mRNA associated with proteins) biogenesis events comprise of the capping of the nascent RNA transcript at the 5′-end, pre-mRNA splicing, and cleavage/polyadenylation at the 3′-end of the message. [5-10] All of these events are accompanied by the association of the nascent transcripts with wide repertoire of mRNA maturation factors and heterogeneous nuclear ribonucleoproteins (hnRNPs). [11-16] This vibrant RNA-protein association initiates with the interaction and binding of the heterodimeric nuclear cap binding complex (CBC) to the m^7G cap when the nascent transcript acquires a cap structure and is only 20-30 nucleotide residues long [15]. This event is followed by the deposition of the transcription/export (TREX) complex onto the maturing message that consists of THO proteins, (Hpr1p, Mft1p, Tho2p, Thp2p), mRNA export factor RNA helicase Sub2p (UAP56 in human); RNA binding protein Yra1p (REF/ALY in human).[17-19] Co-transcriptional recruitment of these proteins/factors onto the transcribing/maturing message further aids splicing (if intron is present) and 3′-end maturation processes followed by the consequent association of the transcript with the export receptor Mex67p:Mtr2p (NXF1:p15 in human), various hnRNPs, and poly(A) tail binding protein Pab1p. [14][16] The collective and

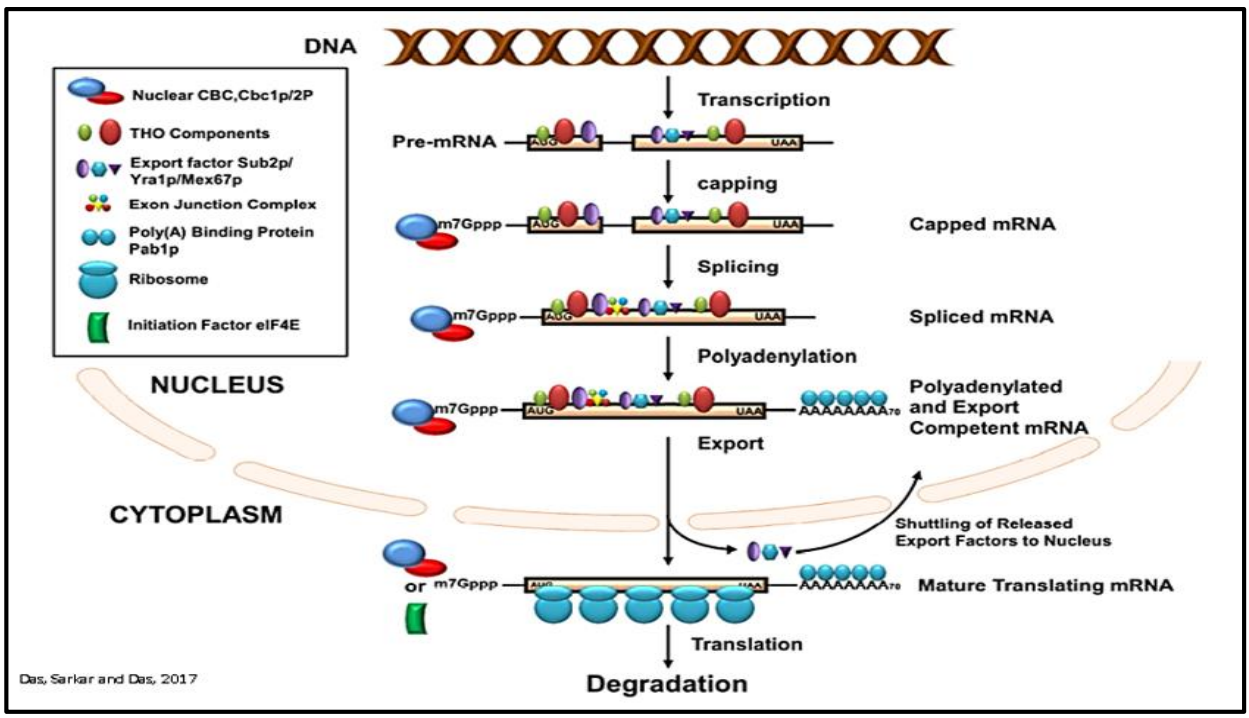

Fig. 1.2: mRNA life-cycle in eukaryotic cells. *Schematic view of the nuclear and cytoplasmic phases of the mRNA life cycle. Various mRNPs which are recruited onto/associated with the maturing transcripts during different stages are schematically indicated by symbols (either annotated directly or denoted in the associated legend box). THO components/maturing factors/mRNA-binding proteins are released from mRNA once the mRNA matures and becomes export-competent. Similarly, export factors are also released from the transcript body once the mRNA arrives at the cytoplasm and shuttle back into the nucleus. In the cytoplasm,*

mRNAs may remain associated either with nuclear CBC (while undergoing a pioneer round of translation) or with eIF4E (while undergoing subsequent steady state translation) which is indicated in the diagram. For simplicity, other mRNA binding proteins remaining associated with translating mRNAs are not shown except for CBC and eIF4E. AUG and UAA and of the open reading frame (ORF) carried by the message.

concerted actions of the whole spectrum of RNA-binding proteins (RBPs) ultimately leads to the formation of a mature export-competent mRNPs [(17)(20-22)] followed by its release from the transcription site at the chromatin and gradual movement through the inter-chromatin space to the nuclear periphery. At the nuclear periphery, the export-competent mRNP docks at the nuclear pore complexes, travels through the nuclear pore complex and is eventually released into the cytoplasm[(8)(23-27)] (Fig. 1.2).

Upon entering the cytoplasm, some of the nuclear mRNPs are shed off before proceeding towards translation. A unique initial round of translation immediately follows this remodelling event while they still carry the nuclear CBC.[(28-29)] During this round, the presence of any potential in-frame premature termination codon (PTC) in the translating mRNA is detected and if found, the mRNA is promptly degraded by the non-sense mediated decay (NMD) pathway to avoid production of any truncated proteins.[(30)] Messages that pass this test undergo another mRNPs remodelling event during which the translation initiation factor eIF4F (consisting

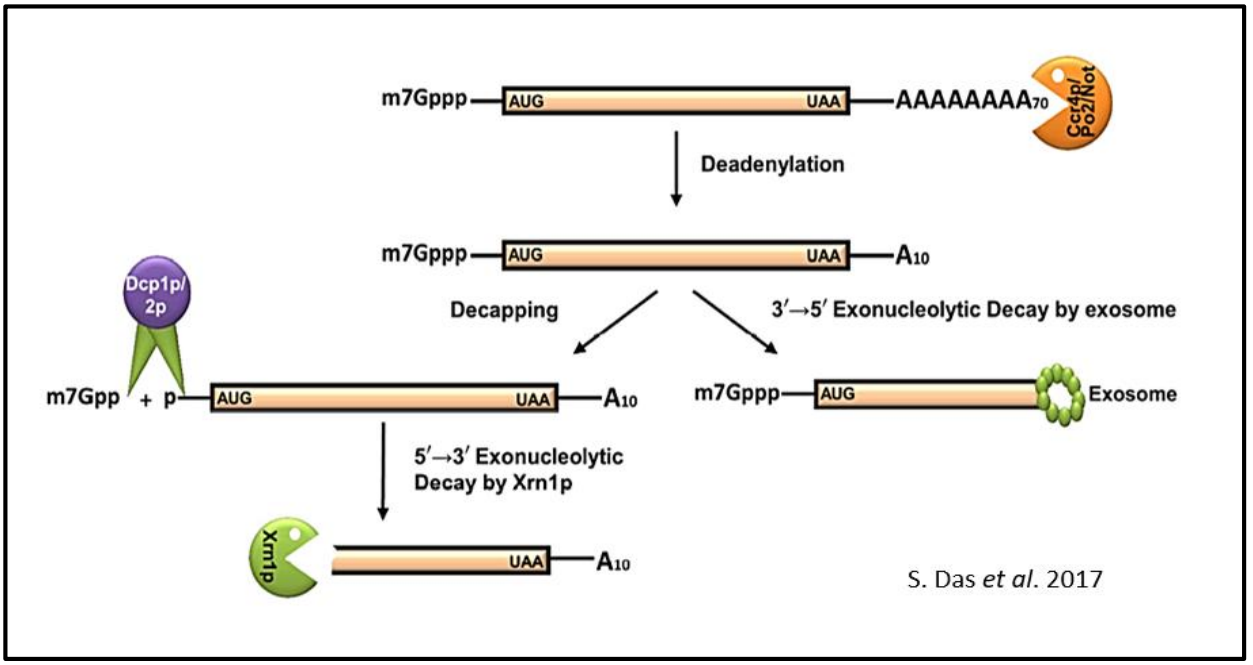

Fig. 1.3: Default pathway of mRNA degradation in S. cerevisiae. *Almost all mRNAs undergo decay by the deadenylation-dependent pathway. Thereby, the poly(A) tail is gradually and progressively shortened by the deadenylase activity of the cr4/Pop2/Not complex. Following deadenylation, the mRNA can be degraded by one of two mechanisms. The major mechanism involves decapping by Dcp1p/2p, following a 5'→3' decay by Xrn1p. The minor mechanism includes a 3'→5' decay by the*

cytoplasmic exosome and Ski7p. AUG and UAA are indicating the beginning and end of the ORF carried by the message. Only relevant decay components are shown by annotated symbols. Proteins which remain associated to translating/degrading mRNAs during different stages of decay are not shown. (Das, Sarkar and Das, 2017)

of eIF4E and eIF4G) replaces the nuclear CBC at the 5'-cap of mRNA. [30] This remodelled message is now ready for the steady productive translation to produce the cellular pool of proteins. [28-29]

However, not all of the exported mRNPs enter the regular translation cycle; instead, they are transported to several special cytoplasmic locations (e.g., stress granules) for future use. [31-32] After a message undergoes ample rounds of translation to suffice for the cell's need of that particular protein, it sheds off the attached polysomes and associates with cytoplasmic stress granules or P-bodies to mark its commitment towards degradation by default decay pathway [33-35]. The first step of default decay pathway is 'deadenylation', which involves shortening of the 60-90 residues long adenylated tail to a 10-15 residue oligo-A state [33] [36-38] either by the Ccr4p/Pop2p/Not complex (major deadenylation machinery) or by the Pan2p/Pan3p complex (subsidiary deadenylation machinery) [39-40] (Fig. 1.3). Thereafter, the 5'-cap structures are removed by the concerted action of the decapping complex consisting of Dcp1p/Dcp2p, which is catalytically stimulated in vivo by Pat1p, Edc1-3p, Scd6p, the Lsm1-7p complex, and the DEAD box helicase Dhh1p [33][41-45] to expose the 5'-monophosphate of the terminal residue which subsequently promotes the degradation of the message in a 5'$\rightarrow$3' direction by the major cytoplasmic exo-ribonuclease Xrn1p.[46] Alternatively, the deadenylation step can also be followed by 3'$\rightarrow$5' degradation by the cytoplasmic exosome and the Ski complex[47-49] (Fig. 1.3) and eventually the leftover residual oligonucleotides structure with the 5'-cap are removed by Dcps.[50]. The highly regulated default mRNA degradation pathway plays a vital role to dictate the basal steady state level of all mRNAs such that the total cellular pool of proteins is well maintained. [33][36-38]

Notably, every mRNP processing event is thought to impact its following step depending on the status of the preceding event(s). This functional interplay improves the possibility of the generation of export-competent and productive mRNPs and lowers the chance of production of the functionally defective and faulty transcripts. [51-56] Ironically, however, numerous aberrant and faulty messages are still produced, which are promptly detected and selectively eliminated by a variety of mRNA surveillance and quality control mechanisms operating in the nucleus. [57-

[66] In the nucleus of the *Saccharomyces cerevisiae*, various classes of aberrant and faulty mRNAs undergo rapid and selective decay by the nuclear exosome in association with its co-factors TRAMP, CTEXT and NNS complex. [10][61-62][66-72] The nuclear exosome consists of nine catalytically inactive (trimeric Cap: Rrp4p, Rrp40p and Csl4p, hexameric ring: Rrp41p, Rrp42p, Rrp43p, Rrp45p, Rrp46p, and Mtr3p) and two functionally active (Dis3p/Rrp44 and Rrp6p) subunits, and a few associated nuclear and cytoplasmic cofactors. [33][62][69][73-79] While Dis3p/Rrp44p is associated with both nuclear and cytoplasmic forms of the exosome, Rrp6p is specifically associated with the nuclear form. [80-81] (Fig. 1.4)

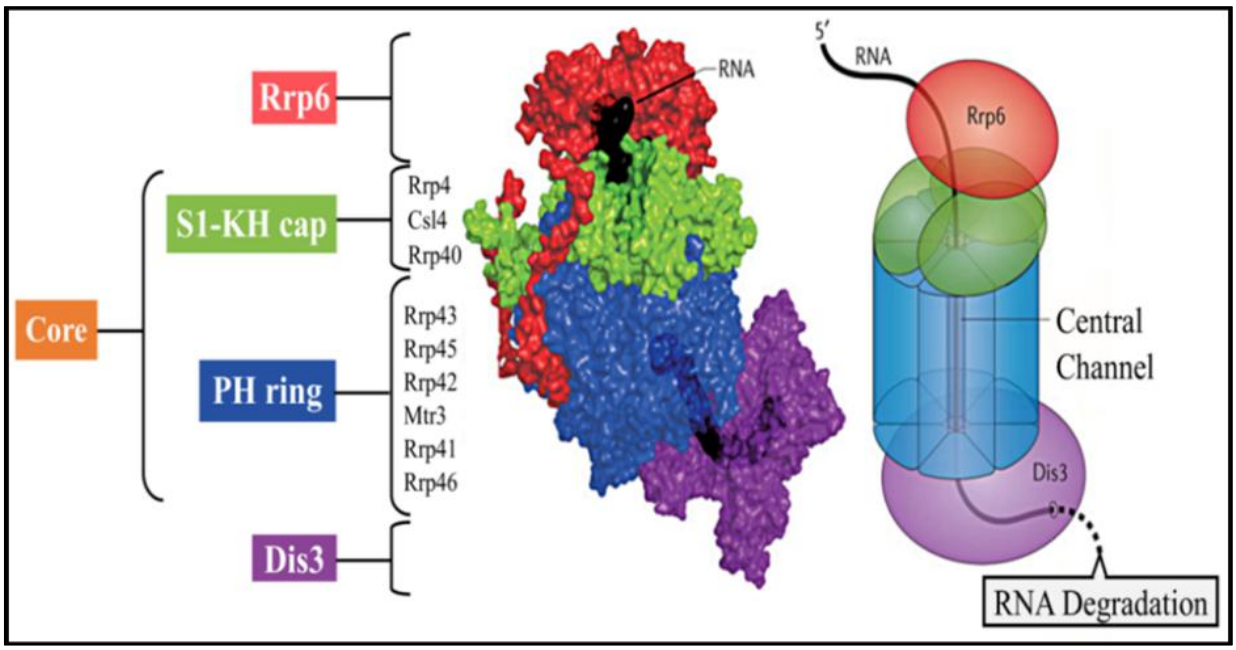

Fig. 1.4. Structure of exosome complex: *Model of the exosome EXO11$^{Dis3+Rrp6}$ complex and its different subunits. Adapted from Kilchert, C., Wittmann, S. & Vasiljeva, L. The regulation and functions of the nuclear RNA exosome complex. Nat Rev Mol Cell Biol 17, 227–239 (2016).*

1.3. COFACTORS OF THE EXOSOME:

The exosome is assisted and guided by a series of cofactors that presumably promote specificity or target the exosome to a particular site of processing or degradation. The exosome, *in vitro*, has weak exonuclease activity but rapid degradation has been noticed *in vivo*. This suggests that cofactors are required to stimulate activity in the presence of targets. [82]

1.3.1. The NNS Complex:

The trimeric NNS complex is composed of three subunits: the RNA-binding protein nuclear pre-mRNA downregulation 1 (Nrd1), nuclear polyadenylated RNA-binding 3 (Nab3) and the helicase splicing endonuclease 1 (Sen1), which helps in recognizing sequence elements that are enriched in unstable Pol II-transcribed ncRNAs. The Nrd1-Nab3-Sen1 complex is important because of its major role in the biogenesis of snRNAs and snoRNAs and in controlled pervasive transcription in connection with the exosome and TRAMP complexes. [83] The CID domain of Nrd1p has the ability to bind the CTD of RNAPII. The Nrd1-CID domain plays important roles in the efficiency of transcription termination and in RNA degradation. Termination of RNA coding genes depends on the cleavage and polyadenylation factor (CPF) that also interacts with the nascent RNA and the CTD. The NNS complex and the CPF have partially overlapping sequence requirements and the same RNA sequence can be used as a terminator by any one of the complexes, depending on the distance from the transcriptional start. [84-85] The early recruitment of the NNS complex via the Nrd1p CID-CTD interaction kinetically favors the appropriate recognition of RNA binding sites that could be bound by the CPF complex, impairing termination by the NNS pathway.

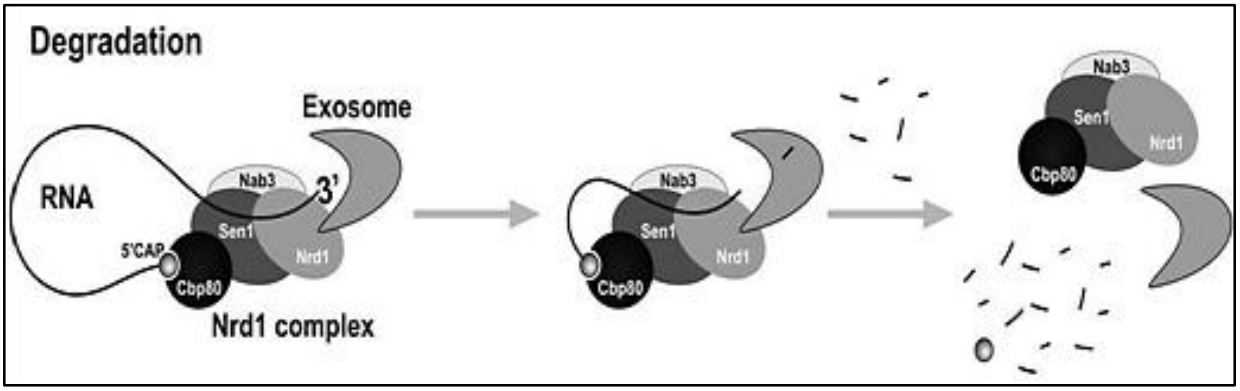

Fig. 1.5: Model for Nrd1-Mediated Degradation by Exosome: *Activity In degradation mode, the Nrd1 complex may recruit exosome to an RNA substrate and promote its degradation. This pathway may be used for the degradation of NRD1 and NAB3 mRNAs and for mRNAs that are not properly polyadenylated (adapted from Vasiljeva, 2006).*

The function of the CID in RNA degradation is dependent on the interaction with a CTD-like motif in Trf4p. The strong interaction between the termination complex and the Trf4p poly (A) polymerase reveals the association of Pap1p with the CPF complex. Trf4p participates in the degradation of CUTs and the processing of snRNAs and snoRNAs. [86] Trf5p lacks a NIM (Nrd1-Interaction Motif), which explains the different target specificity between Tr4p and Trf5p. In contrast, the interaction of Rrp6p and the exosome with the NNS complex *in vivo* is strongly RNA dependent. [87] These two proteins involved in nuclear degradation of mRNA in *Saccharomyces cerevisiae* was inter-bridged by this tri-complex protein, Nrd1p-Nab3p-Sen1p (Fig. 1.5). Nrd1 may normally be involved in exosome-mediated degradation of improperly 3'-processed mRNAs. If this happens then, the processing mode of exosome would simply differ from degradation mode by the presence of a block to complete exosome digestion.[88] Previous research in our laboratory demonstrated that NNS complex is specifically loaded onto the various kinds of aberrant mRNA directly by RNA Polymerase dependent manner and thereby mark the these messages as "aberrant" and subsequently promotes the further recruitment of the CTEXT and the nuclear exosome onto them for their further recruitment. [71]

1.3.2. THE TRAMP COMPLEX:

The TRAMP complex is the major and most well studied cofactor of the nuclear exosome. It was named after the three proteins and comprises of the non-canonical poly(A) polymerases Trf4/5p, putative RNA binding proteins that contain a zinc ring finger domain Air1/2p and a nuclear RNA helicase Mtr4p (Fig. 1.6). [82] Together, these three proteins form two distinct complexes: the TRAMP4 complex which includes Trf4p and the TRAMP5 complex with Trf5p.

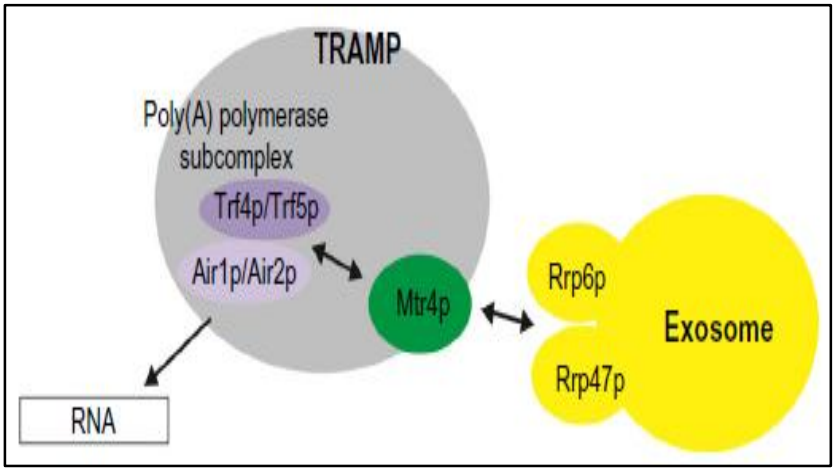

***Fig. 1.6: Model of interactions between RNA, TRAMP, and the exosome**: RNA substrate bound by Air1p or Air2p is oligo-adenylated by poly(A) polymerase Trf4p or Trf5p until sufficient binding sites are generated for the helicase Mtr4p. TRAMP recruits the exosome for RNA degradation through the interaction between Mtr4p and Rrp6p/Rrp47p. Adapted from Pan K, Huang Z, Lee JT, Wong C. Research and Reports in Biochemistry. 2015; 5:111-117*

Each complex is responsible for polyadenylation of different pre-rRNAs,[82][86][89-92] snoRNAs [86][93], snRNAs [82][91-93] , tRNAs [82][94-96], mRNA[97] and CUTs [86][92][93] as well as stimulating degradation by Rrp6p [89- 93][95] and the exosome. Each complex is responsible for distinct degradation and surveillance activity. Each of the TRAMP complexes has some specific role in the surveillance and degradation of RNAs, but not responsible for their maturation. [82] In addition, the complex has a global role in stimulating the exonuclease activity of the exosome and Rrp6p to degrade aberrant RNA. [89]

1.3.3. CTEXT (Cbc1p-Tif4631p-dependent EXosomal Targeting):

Discovered during the investigation of the mechanism of genetic suppression analysis of *cyc1-512* mutation as an independent mRNA degradation pathway (B. Das et al., 2000), CTEXT: Cbc1p-Tif4631p-dependent EXosomal Targeting Complex, is a critical cofactor complex assisting the larger Nuclear Exosome to carry out its function efficiently.[70] (Fig. 1.7) CTEXT defines the second co-factor of the nuclear exosome that consists of nuclear mRNA-cap binding protein, Cbc1p/2p [98-99] two nucleo-cytoplasmic shuttling proteins, Upf3p and Tif4631p [72][99] and the DEAD Box RNA helicase Dbp2p. [72] Previous genetic data and a body of recent findings indicate that CTEXT assists the nuclear exosome to selectively degrade aberrantly long 3'-extended and export-defective messages. [70][72]

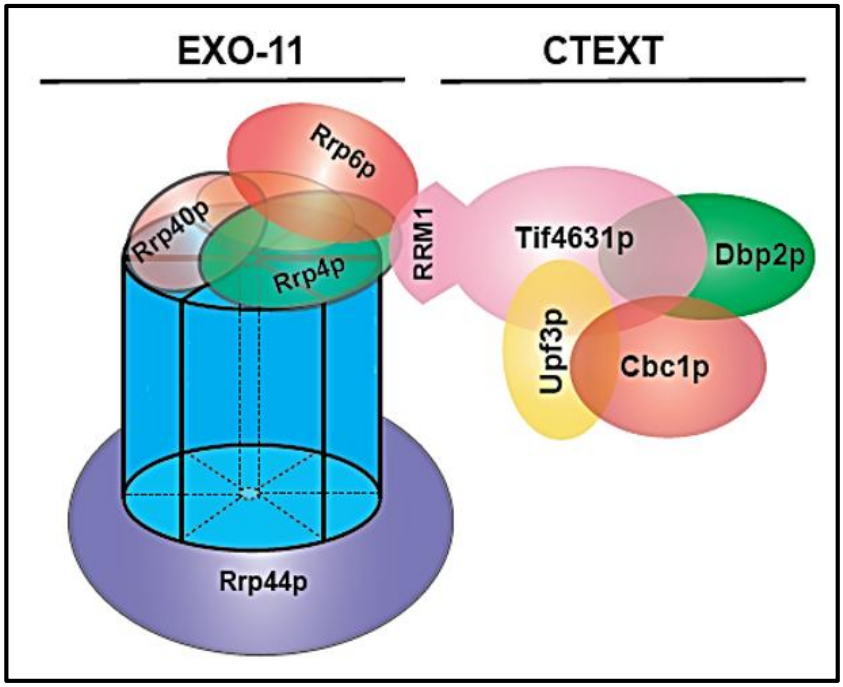

Fig. 1.7: The N-terminal RRM1 domain of Tif4631p specifically mediates the interaction of CTEXT with the core nuclear exosome complex. *Schematic representation of the Proposed model of interaction of CTEXT with the nuclear exosome mediated via the N-terminal RRM1 domain of the Tif4631p. The model portrays the interaction of the CTEXT that is mediated by the RRM1 domain of Tif4631p (indicated as a separate domain) with the core nuclear exosome (mediated presumably via Rrp6p and Rrp4p). Other components of CTEXT are coded with different colours and are also indicated. Adapted from Saha et al. 2024.*

During post-splicing events of mRNA biogenesis, this cofactor complex is hypothesized to feed aberrant mRNAs to the Nuclear Exosome and thus impart directionality to the otherwise non-specific mRNA degrader. The nuclear Exosome along with its cofactor CTEXT, targets a few signature substrates that include aberrantly long 3'-extended read-through *cyc1-512* mRNAs [98] and various kinds of export defective messages. [74-75] [98] [100] mRNAs with export defects include both cis-acting defect (*lys2-187* mRNA) [75] or trans-acting mutation (global cellular mRNAs in export defective *nup116*-Δ strain) are also rapidly degraded by CTEXT. [74] In addition, a group of non-aberrant Nuclear Retained (NR) mRNAs undergo CTEXT dependent accelerated decay. Previous investigations revealed that Dbp2p, the newly identified component of CTEXT was demonstrated to participate in various aspects of the RNA metabolism. [101] For example, this DEAD-box helicase plays a crucial role in the efficient termination of RNAPII transcription, [102] unwinding of RNA duplex *in vitro* that is consistent with its ability to promote the alteration of RNA secondary structure. [103-104] Baker's yeast Dbp2p is also essential for ribosome biogenesis and transcriptional fidelity. [105-107] Moreover, Dbp2 was found to associate with actively transcribed chromatin in an RNA-dependent manner [108] and plays an essential role in pre-mRNA maturation and mRNPs assembly. [104] In addition, Dbp2p was recently demonstrated to be involved in the efficient remodeling of 3′-end of a small subsets of mRNAs thereby promotes recruitment of NNS complex for effective transcription termination by NNS complex. [109] Interestingly, Dbp2p was also shown to be involved in the glucose-dependent gene repression in *Saccharomyces cerevisiae*. [110]

1.4 So, why is it important to understand mRNA degradation in a cell?

- RNA degradation ensures robust gene expression by removing the RNAs arising from any "accidents" during transcription, splicing, export or translation.
- Apart from regulating transcription rate for controlled gene expression, mRNAs must be turned over rapidly for fast changes in transcriptome composition. Coordinated destabilization of an entire class of mRNAs can promote major physiological changes in a cell.
- Specific mechanisms of mRNA decay can serve to regulate gene expression through feed-back control. [111]

Chapter 2

ORIGIN OF WORK:

LITERATURE REVIEW

In order to maintain specific and optimal internal conditions for survival, cellular organisms through evolution have developed unique strategies to cope-up with variable and harsh external conditions. These strategies can be tissue/organ specific in case of multicellular organisms, or can be autonomous mechanisms for unicellular organisms like the Baker's yeast *Saccharomyces cerevisiae*. In order to maintain that optimal or at least basal level of cellular functions, unicellular organisms like Baker's yeast modulate the expression of certain genes rapidly to respond to the abrupt changes in the external environment. The complexity of the yeast cell's system for detecting and responding to environmental variation is only beginning to emerge. Genes whose transcription is responsive to a variety of stresses have been implicated in a general yeast response to stress. [112-113] Several regulatory systems have been implicated in modulating these responses, but the complete network of regulators of stress responses and the details of their actions, including the signals that activate them and the downstream targets they regulate, remain to be elucidated. [114]

Starvation, specially of carbon and nitrogen sources, is a common yet complex stress for microorganisms. Starvation for specific nutrients provides cues for developmental responses throughout the fungi, e.g. nitrogen starvation is frequently required for mating or sexual development. [115-116] Starvation for carbon is the cue for haploid or diploid yeast cultures to enter stationary phase [117-118] and, under certain conditions, for haploid yeast cells to grow invasively. [119] In the presence of a poor carbon source, starvation for nitrogen induces sporulation and in the presence of a good carbon source stimulates pseudohyphal growth. [120-121]

Remarkably, in response to glucose starvation, there are cell surface proteins that detect the absence of glucose and activate signal-transduction pathways in different cellular compartments, [122-123] which govern changes in the phosphorylation, localization, and activity of proteins, changes in gene expression [114] [124] and translation, [125-126] accumulation of stress-protectant molecules, [127] and degradation of proteins and RNA. [128-129] Thus, for the cell to respond effectively, changes in all of the cellular components must be completely integrated. Overall, each genomic expression program is unique to the features of the environment, however comparative analysis of the genomic expression responses to diverse environmental changes revealed that the expression of roughly 900 genes (around 14% of the total number of yeast genes) is stereotypically altered following stressful environmental transitions. [114] A similar set of genes was also identified in a related study, [130] further indicating the commonality of these gene

expression changes. The genes that participate in this response, referred to here as the environmental stress response (ESR), fall into two groups based on their expression patterns: one group is composed of around 600 genes whose transcripts are decreased in abundance following stressful environmental transitions (referred to as repressed genes), and a second group is composed of around 300 genes whose transcripts increase in abundance in response to the transitions (referred to as induced genes). [131] The genes in these two groups display nearly identical but opposite changes in gene expression in response to essentially all of the conditions tested, suggesting that they are components of the same cellular response. The ESR is initiated in response to many different stressful environments in a manner that is sensitive to the degree of cellular stress. When cells are shifted from optimal growth conditions to conditions thought to be stressful for the cell, they respond with changes in ESR gene expression that are proportional to the magnitude of environmental change. [131]

Fungi are omnipresent in nature that parasitizes humans, animals and plants in the form of pathogens. Typically, fungal Pathogenesis is extremely prevalent almost in all parts of the world, which affects large number of human populations. Although a large body of information about the molecular basis of bacterial pathogenesis is known, the mechanisms of fungal pathogenesis remain obscure and poorly understood. [99] [62] Pathogenicity displayed by virulent fungus is a major problem in the field of medical and clinical microbiology. Fungi exhibit alternate morphological forms in response to altered environmental conditions, which leads to the formation of multicellular forms or structures critical to the respective life cycles of these organisms under those environmental cues. [71-72] [132] Some of these morphological transitions have been implicated in the origin and maintenance of the virulence state in several human and plant fungal pathogens, including *Candida albicans*, *Cryptococcus neoformans*, *Aspergillus fumigates*, and *Ustilago maydis.* [133-135] Notably, a critical determinant of virulence in C. albicans is its morphological plasticity which is characterized by its ability to switch reversibly between yeast, pseudohyphal, and hyphal growth forms, and is found in both yeast and filamentous forms in the host. [70] [75] [100] [136-138] It is believed that the hyphal form plays key roles in the infection process, and can promote tissue penetration and escape from host's immune response. [29] [139] Hyphal morphogenesis is coupled with virulence, as genes that control hyphal morphology are co-regulated with genes encoding virulence factors, including adherence [74] [140] secretion of hydrolases [141] and Candida lysin [142] to damage host cells. Remarkably, the budding yeast

Saccharomyces cerevisiae serves an excellent model system to study the transition from yeast to filamentous hyphal state, since (i) multiple powerful genetic tools available in *Saccharomyces* are not available in *Candida* and (ii) the non-pathogenic *Saccharomyces* exhibits similar morphogenetic transition from yeast to hypha under nutrient stress. [143] Strikingly, this dimorphism in *S. cerevisiae* is quite distinct: yeast cells are clearly round/ovoid-shaped, whereas the cells undergoing pseudohyphal growth appear elongated and remain connected after cytokinesis, forming multicellular chains, or filaments. [143-147] These filaments of connected cells can spread out along the surface of a solid growth substrate as well as invade the substrate [143] and are referred to as pseudohyphae, since they resemble the hyphae of other fungal species. [144] Thus, utilizing the power of genetics of *Saccharomyces* it is possible to dissect out the genetic circuitry involved in virulence in *Candida.*

Yeast cells prefer the fermentable sugars glucose or fructose as source of carbon for energy and growth. This preference for glucose over other carbon sources is made possible by allosteric inhibition of catabolic enzymes and transcriptional repression of genes required for respiration and for metabolism of other carbon sources. [148] Given the fact that glucose is the preferred source of carbon, removal or addition of glucose leads to large-scale changes in phosphorylation of proteins and transcription of genes. [139] [149-150] Overlapping signalling pathways modulate changes in proliferation and gene expression in cells upon glucose starvation or upon addition of glucose to starved cells. The PKA pathway modulates changes in growth, metabolism, and stress responses. The Snf1 pathway is required for utilizing alternative sources of carbon. Regulation of glucose intake through transporters is regulated by Rgt3/Snf3. [148] Glucose also regulates levels of hexose transporters present on the cell membrane. [150-151] Rgt1 along with the co-repressors Mth1 and Std1 repress HXT1-4 in the presence of glucose. Glucose sensors Snf3 and Rgt2 respond to external glucose and recruit Mth1 and Std1 to the plasma membrane for degradation, relieving HXT genes from repression by Rgt1. [152-154]

Notably, *SKS1* (Suppressor Kinase of *SNF3*) gene was originally discovered as a multicopy suppressor of *snf3* null mutation that encodes a putative serine-threonine kinase. [155-156] Remarkably, Snf3p/Rtg2p signalling pathway represents a sensory cascade that plays a vital role in detecting the extracellular glucose level [151] and *SNF3* encodes a transmembrane glucose sensor. Consequently, *snf3* null mutant strain exhibits defect in high-affinity glucose transport and are unable to grow fermentatively on medium with low glucose. Overexpression of *SKS1*

was found to suppress the growth defect rendered by *snf3* mutation and the *snf3 sks1* double mutant strains can grow under limiting glucose conditions. [155] Further research shows that Sks1p forms a central kinase involving a signalling cascade controlling the pseudohyphal growth and the expression of *SKS1* undergoes upregulation during glucose/nitrogen liming conditions. [157] However, the molecular mechanism of regulation of expression of physiological level of *SKS1* under limiting glucose and nitrogen conditions is currently obscure.

Previous investigations from our laboratory demonstrated that a subset of normal functional mRNAome consisting of approximately two hundred forty-three mRNAs undergo rapid nuclear degradation by the nuclear exosome and its co-factor CTEXT in baker's yeast *Saccharomyces cerevisiae*. [100] To explain their unexpected susceptibility to the nuclear surveillance system it was postulated that these messages are export-inefficient and spend prolonged dwell time in the nucleus. This postulate was based on a lesson learnt from a previous investigation that a "kinetic competition" exists between the nuclear export of mRNAs and their nuclear degradation. [74] [100] (Fig. 2.1) Further investigation indeed revealed that these subsets of messages display a characteristic slow nuclear export and a propensity to retain in the nucleus for unusually longer time. This cohort of mRNAs were dubbed 'Nuclear Retained' mRNAs (NR mRNAs) as exemplified by *SKS1*, *IMP3*, *NCW2*, *HAC1*, *NCA3*, *SAS4* and *GRE1.* [100] Genetic and cytological analysis of a model NR mRNA *SKS1* suggested that its slow export could be attributed to a 202 nt long *cis*-acting sequence termed nuclear zip-code (*NZ*) element that encompasses 825 to 1026 nt of the *SKS1* ORF. [133] Earlier investigation[157] has shown that, when glucose/nitrogen is limiting in the medium, Sks1p kinase function is absolutely necessary for cell growth. So, we hypothesised that under low glucose/nitrogen condition, the equilibrium of *SKS1* mRNA's "kinetic competition" shifts towards nuclear export compared to nuclear retention (gene off). Thus, *SKS1* mRNA perhaps undergoes rapid nuclear export to arrive in the cytoplasm and subsequently undergo translation (gene on) to produce a copious amount of Sks1p Ser/Thr kinase protein. (Fig. 2.2) However, the mechanism of the *NZ*-dependent nuclear retention and slow export of the *SKS1* remained elusive.

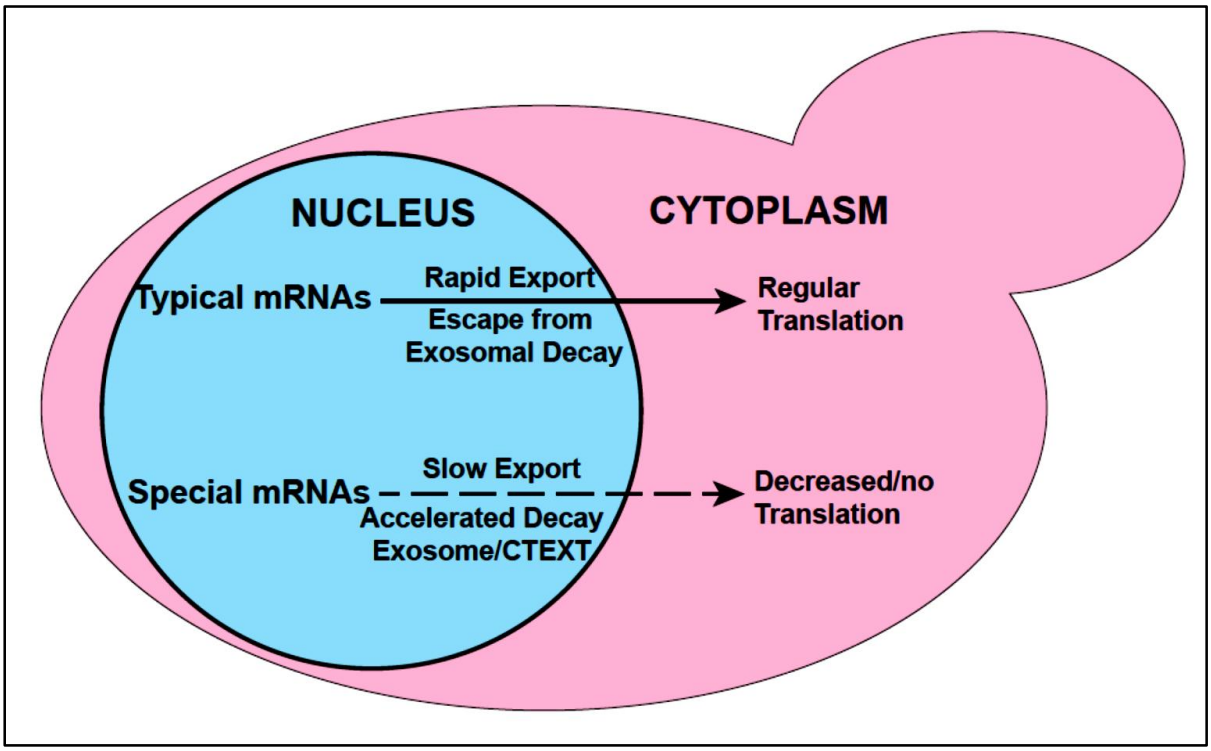

Fig. 2.1: Model of regulation of expression of the genes encoding the NR mRNAs in Saccharomyces cerevisiae*. NR mRNAs display a strong propensity of slow export and a preferential retention in the nucleus when their expression is turned off. This strong nuclear retention leads to their rapid intra-nuclear decay by nuclear exosome/CTExT and the corresponding protein is not synthesized. In contrast, when their expression is required, the model predicts that the export could be modulated to become faster so that they escape the degradative activity of exosome and exported to the cytoplasm and translated*.

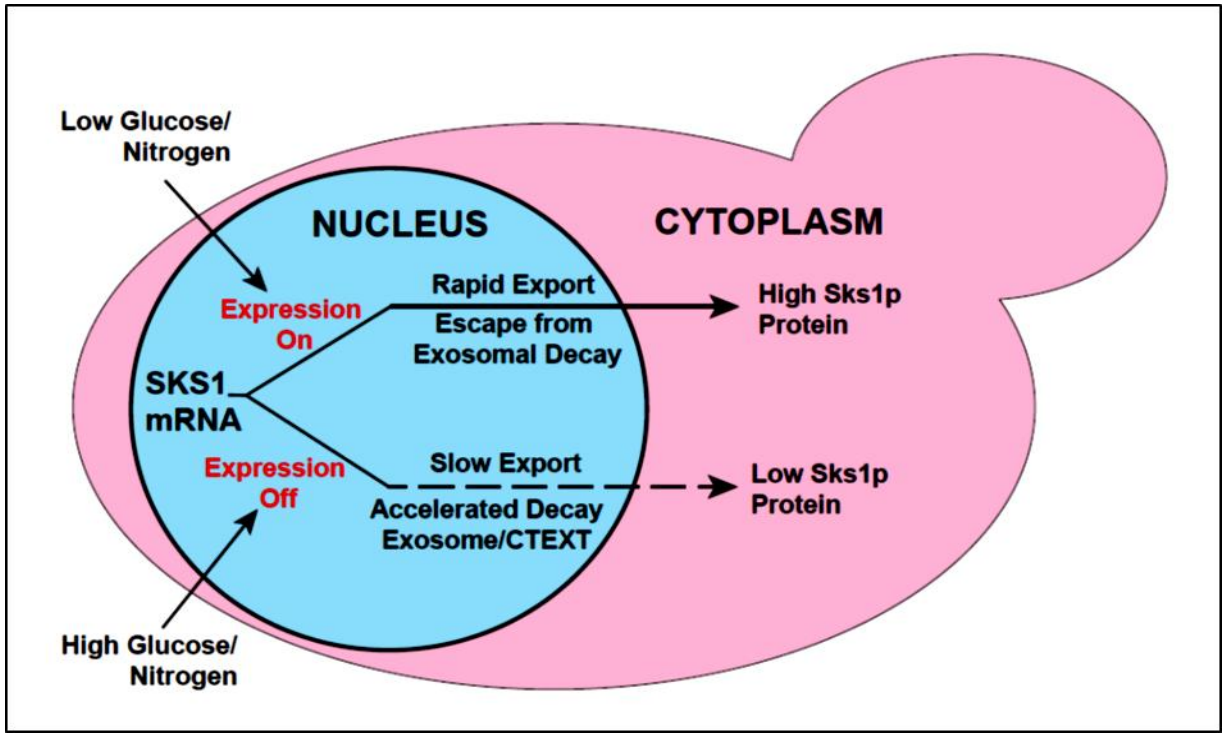

Fig. 2.2: Model of regulation of expression of SKS1 gene in Saccharomyces cerevisiae. *When the glucose/nitrogen levels are high in the medium, the Sks1p protein is not required and the SKS1 mRNA displays a strong propensity of slow export and a preferential retention in the nucleus. This strong nuclear retention leads to their rapid intra-nuclear decay by nuclear exosome/CTEXT and the corresponding protein is not synthesized. In contrast, during low glucose/nutrient supply, when its expression is urgently required, the model predicts that the export would be modulated to become faster so that they escape the degradative activity of exosome/CTEXT and is exported to the cytoplasm and undergoes rapid translation.*

Consequently, we would explore following key questions:

1: What are the molecular mechanisms of nuclear retention of *SKS1* mRNA and other nuclear retained messages in the nucleus? Although, we have previously shown that a 202 nt long *cis*-element plays a key role in the nuclear retention of *SKS1* mRNA, its underlying mechanism is currently unknown. To unravel the mechanism, we postulate that one or more putative trans-acting factor(s) bind(s) to this cis-acting nuclear zip-code element and thereby brings about its nuclear retention.

2: Is activation of transcription of or the diminution of mRNA decay or both, are responsible for the control of expression of nuclear retained messages?

3: Is our proposed mechanism valid with respect to the maintenance of physiological expression of *SKS1* mRNA and Sks1p protein under various concentrations of glucose/nitrogen?

Chapter 3

MATERIAL METHODS

❖ **Yeast Strains, Plasmids, Oligonucleotides and yeast genetics.**

All the strains, plasmids and oligonucleotides are listed in Tables below. Standard genetic nomenclature is used to designate wild-type alleles, as, *SKS1*, *DBP2* etc.; the corresponding disruptants or deletions are designated, for instance, *sks1-N-*Δ, *dbp2-Δ* etc. The protein encoded by a particular gene is denoted, for example, Dbp2p, which is encoded by *DBP2*. Standard YPD, YPG, YPR, SD, SLAD and other omission media were used for testing and the growth of yeast. [158] Yeast genetic analysis was carried out by standard procedures as described. [158] HA tagging of gene using pYM2 plasmid was done as mentioned in Janke *et al.* Yeast 2004. [159] TAP tagging of gene was done by PCR amplification of TAP: URA from pBD44 with gene specific overhang primers followed by one step gene replacement technique in yeast. PCR amplified genes coding for respective mRNAs along with their promoters were used to replace *SKS1* in pBD72 [100] to construct plasmids used for confocal microscopy.

- **List and Genotypes of Yeast Strains used in this study**

Strain No.	Genotype	Source
yBD 5	*MATa cyc1-512 ura3-52 trp2-1*	Das *et al.* 2000
yBD 20	*MATa cyc1-512 lys2-187 leu2-1 his4-166 ura3-52 met8-1*	Das *et al.* 2000
yBD 58	*MATa his3-Δ1 leu2-Δ0 lys2-Δ0 ura3-Δ0*	Kuai *et al.* 2005
yBD 462	*MATa cyc1-512 ura3-52 trp2-1 sks1-Δ::SKS1-N-Δ1*	Das *et al.* 2019
yBD 471	*MATa his3-Δ1 leu2-Δ0 lys2-Δ0 ura3-Δ0 pBD56 pBD72*	Das *et al.* 2019
yBD 477	*MATa cyc1-512 ura3-52 trp2-1 sks1-Δ::SKS1-N-Δ6*	Das *et al.* 2019
yBD 484	*MATa DBP2-3xFLAG:KanMx6 his3Δ1 leu2Δ0 met15Δ0 ura3Δ0*	Beck *et al.* 2014
yBD 515	*MATa DBP2-3xFLAG:KanMx his3Δ1 leu2Δ0 met15Δ0 ura3Δ0 cyc1:: CYC1-NZ*	This work[c]
yBD 518	*MATa DBP2-3xFLAG:KanMx his3Δ1 leu2Δ0 met15Δ0 ura3Δ0 sks1-Δ::SKS1-N-Δ1*	This work[c]
yBD 519	*MATa DBP2-3xFLAG:KanMx his3Δ1 leu2Δ0 met15Δ0 ura3Δ0 sks1-Δ::SKS1-N-Δ6*	This work[c]
yBD488	*MATa cyc1-512 lys2-187 leu2-1 his4-166 ura3-52 met8-1 dbp2::KanMx*	Saha *et al*. 2024
yBD501	*MATa cyc1-512 lys2-187 leu2-1 his4-166 ura3-52 met8-1, pBD 56,pBD57*	This Work[c]
yBD502	*MATa cyc1-512 lys2-187 leu2-1 his4-166 ura3-52 met8-1, pBD 56, pBD72*	This Work[c]
yBD503	*MATa cyc1-512 lys2-187 leu2-1 his4-166 ura3-52 met8-1 dbp2::KanMx, pBD 56,pBD57*	This Work[c]
yBD504	*MATa cyc1-512 lys2-187 leu2-1 his4-166 ura3-52 met8-1 dbp2::KanMx, pBD 56, pBD72*	This Work[c]
yBD523	*Mata ade2-1 can1-100 his3-11,15 leu2-3,112 trp1-1 ura3-1 pep4::HIS3 TRP1-CEN-pCAN1 Upf3:HA*	This Work[c]
yBD555	*MATa cyc1-512 lys2-187 leu2-1 his4-166 ura3-52 met8-1 dbp2::KanMx Mex67-TAP::URA3*	This Work[c]
yBD556	*MATa cyc1-512 lys2-187 leu2-1 his4-166 ura3-52 met8-1 dbp2::KanMx Yra1-HA::His3*	This Work[c]

yBD625	*MATa cyc1-512 lys2-187 leu2-1 his4-166 ura3-52 met8-1 dbp2::KanMx (pDBP2-3XFLAG:KanMx, URA)*	This Work[c]
yBD640	*MATa cyc1-512 lys2-187 leu2-1 his4-166 ura3-52 met8-1 Mex67-TAP::URA3*	This Work[c]
yBD641	*MATa cyc1-512 lys2-187 leu2-1 his4-166 ura3-52 met8-1 Yra1-HA:: HIS3*	This Work[c]
yBD656	*MATa cyc1-512 lys2-187 leu2-1 his4-166 ura3-52 met8-1, pBD56,pBD366*	This Work[c]
yBD657	*MATa cyc1-512 lys2-187 leu2-1 his4-166 ura3-52 met8-1 dbp2::KanMx, pBD56,pBD366*	This Work[c]
yBD658	*MATa cyc1-512 lys2-187 leu2-1 his4-166 ura3-52 met8-1, pBD56,pBD368*	This Work[c]
yBD659	*MATa cyc1-512 lys2-187 leu2-1 his4-166 ura3-52 met8-1 dbp2::KanMx, pBD56, pBD368*	This Work[c]
yBD660	*MATa cyc1-512 lys2-187 leu2-1 his4-166 ura3-52 met8-1, pBD56,pBD367*	This Work[c]
yBD661	*MATa cyc1-512 lys2-187 leu2-1 his4-166 ura3-52 met8-1 dbp2::KanMx, pBD56,pBD367*	This Work[c]
yBD662	*MATa cyc1-512 lys2-187 leu2-1 his4-166 ura3-52 met8-1, pBD56, pBD365*	This Work[c]
yBD663	*MATa cyc1-512 lys2-187 leu2-1 his4-166 ura3-52 met8-1 dbp2::KanMx, pBD56, pBD365*	This Work[c]
yBD664	*MATa cyc1-512 lys2-187 leu2-1 his4-166 ura3-52 met8-1, pBD56, pBD370*	This Work[c]
yBD665	*MATa cyc1-512 lys2-187 leu2-1 his4-166 ura3-52 met8-1 dbp2::KanMx, pBD56,pBD370*	This Work[c]
yBD666	*MATa cyc1-512 lys2-187 leu2-1 his4-166 ura3-52 met8-1, pBD56, pBD371*	This Work[c]
yBD667	*MATa cyc1-512 lys2-187 leu2-1 his4-166 ura3-52 met8-1 dbp2::KanMx, pBD56,pBD371*	This Work[c]
yBD668	*MATa cyc1-512 lys2-187 leu2-1 his4-166 ura3-52 met8-1 Sks1-TAP::URA*	This Work[c]
yBD669	*MATa cyc1-512 lys2-187 leu2-1 his4-166 ura3-52 met8-1 dbp2::KanMx SKS1-TAP::URA*	This Work[c]

[c]Constructed in the laboratory during the period of work.

- **List of Plasmids used in this study**

Plasmid No.	Description	Source
pBD 56	p*GAL-U1A* (1-94) – *GFP*, *LEU2* fusion gene under Galactose control cloned in pRS315	Brodsky and Silver 2000
pBD 57	p*PGK1-PGK1*-U1As-*ASH1* 3'UTR-*ADH1* terminator in pRS426, URA3	Brodsky and Silver 2000
pBD 72	2.5 kb. *Xho*I-*Bam*HI *SKS1* coding region and 1kb upstream replacing *PGK1* in pAB 3123	Kuai *et al.* 2005
pBD325	pYM2 3HA *HIS3*MX6	Janke *et al.* 2004
pBD365	p*NCW2-NCW2* replacing *SKS1* in pBD72, *URA*3	This Work[c]
pBD366	p*NCA3-NCA3* replacing *SKS1* in pBD72, *URA3*	This Work[c]
pBD367	p*IMP3-IMP3* replacing *SKS1* in pBD72, *URA3*	This Work[c]
pBD368	p*SAS4-SAS4* replacing *SKS1* in pBD72, *URA3*	This Work[c]
pBD370	p*CYC1-CYC1* replacing *SKS1* in pBD72, *URA3*	This Work[c]
pBD371	p*CYH2-CYH2* replacing *SKS1* in pBD72, *URA3*	This Work[c]
pBD353	*DBP2*-FLAG: KanMx in PRS316, *URA3*	This Work[c]

[c]Constructed in the laboratory during the period of work.

- **List of Oligonucleotides used in this study**

Oligo ID	Sequence	Purpose
oBD 774	5'-TAATACGACTCACTATAAACTTGCATAAGAAACCCATG-3'	202 nt Streptotag-*SKS1* Amplification
oBD 775	5'-GGATCCGACCGTGGTGCCCTTGCGGGCAGAAGTCCAACGATCCATAGGATTGGAACTTGAGACAA-3'	
oBD 876	5'-AGAATTCTAGGAAGCGGATGTG-3'	Cloning of *SAS4*
oBD 928	5'-CATGCTGATTTTTCACGCA-3'	
oBD 929	5'-CGATATGATTGCTGAGAATGC-3'	Cloning of *NCW2*
oBD 930	5'-CTATAACAAAAGGGCACCA-3'	
oBD 931	5'-TTGAGCTAATTAAGGCGAAA-3'	Cloning of *NCA3*
oBD 932	5'-GACTTAATAGAAAACAAATTCAGCA-3'	
oBD 933	5'-CATGGGAATGTCAAATTCTGAG-3'	Cloning of *CYH2*
oBD 934	5'-TTAAGCGATCAATTCAACAACAC-3'	
oBD 935	5'-GTTCTTCGTCAGACATGTTTTAG-3'	Cloning of *CYC1*
oBD 936	5'-TTACTCACAGGCTTTTTTCAAG-3'	
oBD750	5'-CGAACTCGAGTACGAAAATAACT-3'	Cloning of *IMP3*
oBD 751	5'-GAGTATGGATTCAGAAAACGTAAG-3'	
oBD 776	5'- GATGGATTTATGTGACGTTGTAG-3'	Cloning of *DBP2*
oBD 777	5'-TGCCTGGCAGATAGAATTATTA-3'	
oBD 752	5'-GCAGAAGATGGGTGCATTT-3'	qRT PCR of *NCA3*
oBD 753	5'-ACGACAAGTATGTTTCTCCATTAG-3'	
oBD 836	5'-ATAAGGGAGAGACGCCTAAA-3'	qRT PCR of *SAS4*
oBD 837	5'-CTCAGCTACGATAGCAAACC-3'	
oBD 276	5'-AGCGTCCGTAATGTCCAATTCT-3'	qRT PCR of *NCW2*
oBD 277	5'-CCCGCACCATAAGCTATGTGA-3'	
oBD 184	5'-AAAGGGTGGCCCACATAAGG-3'	qRT PCR of *CYC1*
oBD 185	5'-CTTCAACCCACCAAAGGCCA-3'	
oBD 792	5'-GACTATTTCCGGACACGATATT-3'	qRT PCR of *DBP2*
oBD 793	5'-ACTTTCGATGAAGCTGGTTT-3'	
oBD 160	5'AATGGAAGCAGGACCAAGGC-3'	qRT PCR of *IMP3*
oBD 161	5'TCGTTACGAGGTAGGCTGGA-3'	
oBD 592	5'-GCTCCGGAACTAGACGATAGGA-3'	qRT PCR of *LYS2*
oBD 593	5'-TGTCCATGCGGTGTCTTTCTT-3'	
oBD 565	5'-TTGTGGCAACCGTCTTTCCT-3'	qRT PCR of *SCR1*
oBD 566	5'-CCGAAGCGATCAACTTGCAC-3'	
oBD 280	5'-GTGCAACCAATATGTCGTGTGT-3'	qRT PCR of *CYH2*
oBD 281	5'-GCGCTCTCTACAACCATTTGA-3'	
oBD 268	5'-GCCGAAAGAATGCAAAAGGA-3'	qRT PCR of *ACT1*
oBD 269	5'-TCTGGAGGAGCAATGATCTTGA-3'	
oBD 274	5'-CCTACTGGATCGCAATGACAAC-3'	qRT PCR of *SKS1*
oBD 275	5'-CGCACACATTTGGAGCTAGATATT-3'	
oBD 331	5'-CCTTTTTAACTTCCTCAATGGACAGT-3'	
oBD 332	5'-CAATCTTTGGAAGCACTAACGTCAT-3'	
oBD 695	5'-CTGTTCACAGTGTTGACGAA-3'	
oBD 696	5'-CTTCCCTGGTGAAAGAAGTAAG-3'	
oBD 838	5'-TATCATCATTGGTGGTGGTATG-3'	qRT PCR of *PGK1*
oBD 839	5'-TTGGCATCAGCAGAGAAAG-3'	
oBD 186	5'-AATTCAAGGCCGGTTCTGCT-3'	qRT PCR of *CYC1*

OBD 588	5'-ACGGTGTGGCATTGTAGACATC-3'	
OBD 812	5'-TTTAACAGACGGTCCAAACGAGAAATGGTTACCAGATTATTCCATGGAAAAGAGAAG-3'	TAP tagging *SKS1*
OBD 813	5'-GAACATAAGATAATACAGTGAGTATAAAGGTGAGACCTGCTACGACTCACTATAGGG-3'	
OBD 794	5'-TGGCATCCCTAGAGAAGCATTTGTGCAGTTCTCCATGGAAAAGAGAAG-3'	TAP tagging *MEX67*
OBD 795	5'-TGTGCGGCTGAAACAGGGAACAATATCATTATACGACTCACTATAGGG-3'	
OBD 796	5'-CAAGGAAATGGCGGACTATTTCGAAAAGAAACGTACGCTGCAGGTCGAC-3'	HA tagging *YRA1*
OBD 797	5'-AAATCAAACAAAAAATTGACAATTAATTAATCGATGAATTCGAGCTCG-3'	

❖ Transformation of *S. cerevisiae* by Lithium Acetate ($LiAc^-$) Method.

50ml YPD culture was inoculated with 1ml O/N culture (starting o.d. = 0.1), incubated at 30°C with shaking till $O.D._{600}$ reaches 0.6. Cells were harvested by centrifugation at 5000rpm for 5mins at 4°C and washed once with 20ml sterile water followed by pelleting. The cell pellet was resuspended in 1.5ml of 1X TE/ $LiAc^-$ and centrifuged at 12000rpm for 15seconds. Cell pellet was again resuspended in 0.4ml of 1X TE/ $LiAc^-$ and incubated at 30°C for 30mins with shaking. Next, a transformation mix was prepared by adding: Cells in 1X TE/LiAc- = 50µl, 50% PEG = 240µl, 1(M) 10X LiAc- = 36µl, Sonicated and boiled (5 mins boil, then stored in ice) Salmon sperm DNA = 25µl, transforming DNA Sample (5-50µgram) dissolved in TE = 50µl. The mix was incubated again at 30°C for 30mins with shaking followed by heat shock at 42°C for 20mins. The cells were pelleted down at 5000rpm for 1 min to remove the supernatant, washed once with 1000µl of sterile water. Finally, pellet was dissolved 200µl water and plated on desired agar medium plate.

❖ *In-vitro* Transcription of *SKS1-NZ* element fused to StreptoTag aptamer.

The *SKS1-NZ* element (825 to 1026 nt) was amplified using a forward primer containing the T7 promoter sequence in the 5′ region and a reverse primer containing the StreptoTag aptamer sequence in the 3′ region. Using this PCR product as template, the mRNA (e.g. *SKS1*)-*cis*-acting element-StreptoTag hybrid RNA was produced in large quantities using *in vitro* transcription technique with T7 RiboMAX™ Express Large Scale RNA Production System (Promega Inc.) following manufacturer's recommendation.

❖ **Preparation of Cell Lysate from *Saccharomyces cerevisiae*.**

Appropriate yeast strains were grown till the OD_{600}=2.7-3.0 followed by the harvesting and washing of the cells. The cells were resuspended in 1 ml of Buffer A containing 50 mM Tris-HCl pH - 7.5, 150mM NaCl, 5mM EDTA, 1mM DTT, 1mM PMSF,1.5mM MgCl2, 1x RNAse inhibitor and 1x Protease Inhibitor Cocktail (Abcam Cat No: ab201111). Cells were lysed by vortexing in presence of glass beads (Unigenetics Instruments Pvt. Ltd Cat No: 11079105). The protein containing supernatant fraction was collected after centrifugation at 12000g for 20minutes at 4℃ and was quantified using Coomassie plus (Bradford) Assay Kit (Thermo Scientific) according to standard protocol.

❖ **StreptoTag Affinity Chromatography.**

The Strepto-Tag (a streptomycin-binding aptamer) affinity purification was essentially carried out as described before (Bachler *et al.* 1999[163]; Windbichler and Schroeder 2006[164]). Briefly, 5grams of epoxy-activated Sepharose 6B was incubated with stirring in 1lt of DEPC treated water at room temperature. After passing the suspension through a sintered glass filter, the beads were washed once with 50ml of 96% ethanol and then four times with 50ml coupling solution (10mM NaOH). The beads were then incubated with 0.055grams of dihydrostreptomycin in 25ml of coupling solution in a shaker at 37 ℃ overnight. Then beads, next day, were again passed through the sintered glass filter and washed four times with coupling solution. Then the beads were washed four times alternatively with 50ml each of wash buffer pH 4 (0.1M Sodium acetate, 0.5M NaCl) and wash buffer pH 8 (0.1M NaHCO3, 0.5M NaCl). Finally, the beads were washed four times with DEPC treated water and resuspended in 50ml of DEPC treated water with 250µl 10% sodium azide for storage at 4 °C.

For preparing the column, the suspension of activated beads was inverted the tube a few times and 3ml from it was loaded on a column (should yield around 1 ml of settled column material). After washing the column three times with 1 ml column buffer, the column opening was closed from bottom and 20 µg tRNA in 1 ml column buffer was added to block nonspecific RNA binding sites. 15minutes later, the column was washed thrice with 1 ml column buffer.

Next step is to refold the hybrid RNA and incubate in with the protein isolate. First, 50-500 pmoles hybrid RNA was incubated at 56 °C for 5 minutes followed by 37 °C for 10 minutes in 100 µl column buffer (50 mM Tris HCl, pH 7.5, 5 mM $MgCl_2$, 250 mM NaCl) and then, 1mg of total cellular protein extract was incubated with the refolded hybrid mRNA for 1.5 hours at 4°C. The mixture was then loaded onto the column and was incubated within the column for 45 minutes for binding. The column outlet was then opened for removal of any excess unbound proteins with 1ml column buffer in 5-10 washes. The proteins that bind to this hybrid RNA was then eluted with 1 ml column buffer containing 10 µM streptomycin. The eluted proteins were then precipitated with one volume of 100 % Trichloroacetic acid (TCA) followed by incubation for 10 minutes at 4 °C and centrifugation at 10000 rpm for 5 minutes. The protein pellet was then washed with 200µl cold acetone followed by centrifugation at 15000 rpm for 5 minutes. The pellet was then dried in 95°C heat block for 5 minutes and was finally dissolved in suitable buffer solution and was run on SDS-PAGE.

- **SDS-PAGE and Western Blot.**

<table>
<tr><th>Sl. No.</th><th>Primary Antibody</th><th>Source</th><th>1º Ab Dilution</th><th>2º Antibody</th><th>2º Ab Dilution</th></tr>
<tr><td>1</td><td>Anti-Rrp6</td><td rowspan="2">Dr. Scott Butler, University of Rochester</td><td rowspan="5">1:1000</td><td rowspan="4">Anti-Rabbit</td><td rowspan="5">1:3000</td></tr>
<tr><td>2.</td><td>Anti-Cbc1</td></tr>
<tr><td>3.</td><td>Anti-TAP</td><td rowspan="4">Commercially Procured, Thermo Scientific</td></tr>
<tr><td>4.</td><td>Anti-FLAG</td></tr>
<tr><td>5.</td><td>Anti- HA</td><td rowspan="2">Anti-Mouse</td></tr>
<tr><td>6.</td><td>Anti-α Tubulin</td><td>1:3000</td></tr>
</table>

80-100 µg of the protein sample was mixed with 2X SDS sample loading dye to make a volume of 20µl followed by boiling for 5 minutes and separated in a denaturing 12 % SDS-PAGE gel. The gel can then be either used for Western blotting or stained with silver nitrate using standard procedure. For Western Blotting, proteins were subjected to overnight electro-transferring at 35volts to a PVDF membrane and immunoblotted with 1:1000 dilution of anti-TAP/ anti-FLAG/

anti-α-Tubulin antibody (Invitrogen). Blots were then incubated with a 1:3000 dilution of horseradish peroxidase-coupled secondary antibody, and the signal was detected on X-ray films using ECL reagent (Abcam).

❖ **Silver staining procedure.**

After performing SDS PAGE, the bands on the gel were fixed by adding 5 to 10 gel volume of Fixing solution A (50% methanol) and agitated for 30 minutes on a shaker. Pouring off solution A, fixing solution B (5% methanol) was added and agitated for 30 minutes on a shaker. After discarding solution B, 50ml of 10% glutaraldehyde was added and agitated for 10 minutes on a shaker. Then the gel was washed 8 times with 5 to 10 gel volume of autoclaved MiliQ water and agitated for 15 minutes on a shaker. The gel was then agitated for 30 minutes on a shaker with 5 gel volume of 5µg/ml of DTT after which 5 gel volume of 0.1% silver nitrate (0.1g silver nitrate in 100ml water) without rinsing DTT. Following agitation for 30 minutes on a shaker, the gel was quickly rinsed off once with MiliQ water and twice with a few milliliters of Carbonate developing solution. Finally, 100ml of carbonate developing solution was added (0.1ml 37% formaldehyde, 3% sodium carbonate and water till 200ml) and incubated till proper staining of bands was attained. Once done, 5ml of 2.3M citric acid was added directly to carbonate developing solution, and agitated for 10 minutes. (Always use 1:20 ratio of citric acid to carbonate developing solution for proper staining, if the pH is too high then color development will continue and is the pH is too low color will bleach away.) Finally, the gel was washed 4 times with MiliQ water with intermittent agitation for 30 minutes.

❖ **LC/MS-MS analysis.**

After analyzing in the SDS-PAGE gel, the eluates were then subjected to Acquity Waters UPLC Systems (Facility run by Sandor Lifesciences Pvt. Ltd.) for LC/MS-MS analysis. For this experiment liquid chromatography was performed on a ACQUITY UPLC system (Waters, UK). This was followed by the separation of all samples was performed on ACQUITY UPLC BEH C18 column (Waters, UK) (150mm X 2.1mm X 1.7µm). A gradient elution program was run for the chromatographic separation with mobile phase A (0.1% Formic Acid in WATER), and mobile phase B (0.1% formic Acid in ACETONITRILE). The raw data which was subsequently acquired from the instrument was processed using PLGS software 3.0.2 within which Data Processing and

Database search was performed. The source of the sample being *Saccharomyces cerevisiae* proteins for samples: YBAC the protein database was downloaded from Uniprot database (Saccharomyces cerevisiae Proteins) and used for searching the proteins present in the sample. The mass spectrometry proteomics data have been deposited to the ProteomeXchange Consortium via the PRIDE [(165)] partner repository with the dataset identifier PXD030639.

❖ **RNA Isolation, cDNA Preparation and Determination of Steady State of mRNAs.**

Total RNA was isolated by harvesting respective yeast cells from 10ml cultures (O.D.600 = 0.8) by centrifugation at 6000rpm for 5minutes and at 4°C. The cell pellet was then washed once with 500µl of Cell Washing Buffer and then resuspend in 500µl of RNA extraction buffer and 500µl of ice-cold PCI (pH 4) mix. The vials should always be placed in ice for RNA isolation. To the suspension, 0.1 grams of sterile RNase free glass beads were added and vortexed 4 times for 20 seconds each time, while intermittent incubating in ice for 20 seconds. The lysate was harvested by centrifugation at 10000rpm for 10minutes at 4°C. The top aqueous phase was separated and RNA was extracted by vortexing in same manner with PCI in ice followed by centrifugation at 10000 rpm for 10mins at 4°C. This step was repeated thrice. Finally, the aqueous phase was separated, mixed with 2.5 volume of chilled 100% ethanol and stored at -80°C overnight. The precipitated RNA was collected by centrifugation at 12000rpm for 15-20minutes at 4°C. The RNA pellet was then washed with 200µl of 75% ethanol, centrifuged at 11000 rpm for 15mins. After drying the pellet at 37°C for 30minutes, it was dissolved 25µl of DEPC water by incubating at 37°C for 1 hour and finally stored at -80°C.

- **200ml Cell Washing Buffer Preparation**:

20ml autoclaved 1(M) LiCl, 40µl autoclave 0.5(M) EDTA, 160 ml DEPC treated water and 180 µl DEPC were incubated together by stirring overnight. The mixture was then autoclaved, cooled and then 20ml of autoclaved 1 (M) Tris-HCl pH 7.5 (made in autoclaved DEPC water) was added,mixed and stored at 4°C

- **200ml RNA Extraction Buffer Preparation:**

20ml autoclaved 1(M) LiCl, 40µl autoclave 0.5(M) EDTA, 5ml of 20% SDS (Do NOT autoclave, made in DEPC water), 155ml DEPC treated water and 180 µl DEPC were incubated together by stirring

overnight. The mixture was then autoclaved, cooled and then 20ml of autoclaved 1 (M) Tris-HCl pH 7.5 (made in autoclaved DEPC water) was added,mixed and stored at room temperature.

For cDNA preparation, the RNA samples were treated with one µl RNAase free DNase I (Fermentas Inc.) at 37ºC for 30 minutes, followed by incubating it with 10 mM EDTA at 65 ºC for 10 minutes. This is followed by cDNA synthesis using iScript Reverse Transcriptase (Biorad) using either random oligodeoxynucleotide primers or oligo-dT primer by incubating it at 25 ºC for 5 mins (priming), 46 ºC for 20 mins (Reverse Transcription) and 95 ºC for 1 minute (Reverse Transcriptase inactivation).

End-point semi-quantitative PCR reaction was carried with 1-2 ng cDNA samples using target gene specific primer sets by Taq DNA polymerase (Thermo Fisher Scientific Inc., Waltham, MA, USA), followed by electrophoresis in 3% agarose gel for visualization of bands using UV Tech-Gel Doc System (Germany) using UVI Band software analysis program.

Real-Time qPCR analyses done in Applied Biosystems StepOne Real-Time PCR machine (StepOne^{TM} software version 2.2.2) with 2ng of cDNA samples and Bio-Rad SYBR Green mixture. The signals for each target mRNA were normalized against control mRNA's signal for relative abundance analysis.

- **Determination of stability of mRNAs by RNA decay.**

The stabilities of the various RNAs were determined by the inhibition of transcription with transcription inhibitor 1, 10-phenanthroline(Sigma-Aldrich) (for RNA-Pol II transcripts) at 30°C as described previously (Maity *et al.* 2016; Sarkar *et al.* 2017). Briefly, specific yeast strains were grown at 30°C till the cultures attained mid-logarithmic phase (OD_{600} = 0.8), when any the transcription inhibitor 1, 10-phenanthroline was added to the growing culture at 100µg/ml final concentration. 10 ml aliquots of cultures were withdrawn at various time intervals after transcription shut-off followed by harvesting of the cells and snap-freezing the pellets in dry ice. Total RNA was then isolated as described above and the mRNA levels were quantified by RT-qPCR assay from random-primed cDNA, and the signals associated with the specific mRNA were normalized against control mRNA's signal. Specific mRNAs' decay rates and half-lives were estimated with the regression analysis program (Graph-pad Prism version 7.04) using a single

exponential decay formula (assuming mRNA decay follows first-order kinetics); $y = 100e^{-bx}$ was used.

❖ **RNA-Immunoprecipitation**.

This procedure is done to isolate RNAs having their bound proteins fixed on them. We used UVP HL-2000 Hybri-Linker Hybridization oven/UV crosslinker with 254nm UV light source for this procedure. 100ml of respective yeast culture (OD_{600}= 1) was poured on glass Petri-dishes (14cm wide, 2cm thick), kept inside the UV crosslinker on icepack without lid and exposed thrice for 10minutes with intermittent gap of 5 minutes in dark. After the procedure, cells were pelleted down at 5000rpm for 7minutes followed by protein isolation for further immunoprecipitation. Protein was then isolated from the cells by above mention method. After estimation, 2mg protein extract was incubated for 1 hour with 5µl of appropriate antibody and 100 µl of protein A+ agarose beads at 4°C in a rotating wheel. After incubation the beads were pelleted by centrifugation at 1500g and washed four time with buffer A used for the protein lysate preparation. Then these beads with immunoprecipitated proteins and the neat protein preparations (input) were subjected to RNA isolation followed by cDNA synthesis to analyze the RNAs bound to that particular protein.

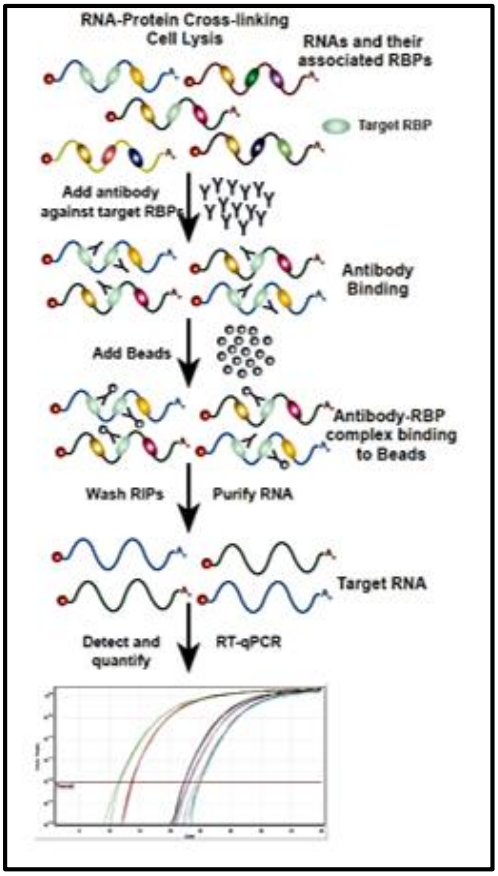

Fig. 3.1: Schematic representation for RNA – Immunoprecipitation Assay

❖ **Genomic DNA isolation from *S. cerevisiae*.**

From the freshly streaked plate one loop full of cells were taken and dissolved 1ml autoclaved water in an eppendorf. Then, this cell suspension was diluted by 10 folds and $O.D._{600}$ was measured. To find out the volume of cells from original suspension that would give $O.D._{600}$ =1.5, a formula 150/ ($O.D._{600}$) was followed. The required volume of cells was centrifuged at 6000rpm for 5mins and dissolved in 100 µl Lysis buffer (100mM Tris HCl 7.5, 30mM EDTA, 0.5 % SDS),

vortexed 5seconds, and boiled for 15mins. The contents of the eppendorf are spun down at 12000 rpm for 5 seconds to pull down DNA. To this pellet, 50 µl of chilled 5(M) KAc^- was added and centrifuged at 12000 rpm for 10mins. To the supernatant 150 µl CHCl3: IAA (24:1) was added and again pulled down by centrifugation at 5000rpm for 10mins to allow phase separation. To the aqueous phase equal volume of isopropanol was added and pulled down with a quick spin at 12000rpm for 20 seconds. The pellet was then washed with 300µl of 95% ethanol, dried at 37°C and finally dissolved in 20 µl of T.E.

❖ **Analysis of transcription rate by Chromatin Immunoprecipitation Assay (ChIP).**

The yeast cultures were grown at 30℃ till the $O.D_{600}$ reaches 0.6. Crosslinking, sonication and incubation with the antibody was done according to the manufacturer's protocol (ChIP assay kit, Upstate Biotechnology, Lake Placid, NY). Anti-RNA polymerase II antibody was provided along with the kit.

❖ **RNA-sequencing analysis.**

In order to validate the results obtained from qRT-PCR or other experiments that was performed we a previously deposited RNA-seq data (GEO accession: GSE58097) was performed**.** The raw reads for GSM1400756 (WT) and GSM1400757 (*dbp2*-Δ) were downloaded from SRA and standard RNA-seq data analysis pipeline was followed to find the differential expression levels of our RNAs of interest in *dbp2*-Δ strain compared to WT. The obtained result was then presented via volcano plot and heat map. To create the Venn diagram, we referred to previously submitted datasets. For *cbc1- Δ*, microarray data from [100] and for *rrp6*- Δ, RNA seq data from (Victorino *et al.* 2020) [166]. The *dbp2*-Δ data was obtained from RNA seq data deposited by (Beck *et al.* 2014). [110]

❖ **Cytological distribution of various RNAs by confocal microscopy.**

Cytological distribution of various RNAs was done by GFP RNA imaging technique as essentially described earlier (Brodsky and Silver 2000). [161] Briefly, the yeast strains harboring various RNA expression plasmids and the U1A-GFP expression plasmid were grown till O.D.600 = 0.3 in their respective glucose medium followed by transfer into 2% raffinose medium and was further grown to $O.D._{600}$ of 0.8. At this point, a 2% Galactose induction was given for 1 hour in order to

induce the expression of U1A-GFP, followed by 1 hour incubation in initial glucose media to clear background noise due to unbound GFP. Nucleus was then stained with Hoechst dye followed by 4 washes with 1X PBS. Images were obtained by using an OLYMPUS FV10-ASW confocal microscope equipped with HCX PL APO 63X/1.2 NA water immersion objective lens. Image processing was done using OLYMPUS FLUOVIEW Ver.2.0b Viewer software. In order to determine the co-localization value of the mRNA within the nucleus of *Saccharomyces cerevisiae* based on captured images, a three-step algorithm is designed in MATLAB, as described below in brevity.

Step 1. Image channel separation

Each image set consists of three images, described as,

(a) Image 1 – Image of the mRNA distribution (dyed in *green*).

(b) Image 2 – Image of the nuclear distribution (dyed in *blue*).

(c) Image 3 – Image of the merged mRNA and nuclear distribution from Image 1 and 2.

Each of these three images of each set were read into the MATLAB script file in the form of a three-dimensional matrix. Subsequently, each image was separated into its respective red, green and blue channels, where each channel represents one dimension of the 3D Image matrix.

Step 2. Image Thresholding and Locating pixels

An Intensity cutoff value was identified and used for thresholding the blue (b_{thresh}) and green (g_{thresh}) channels of the three images. This step is carried out in three hierarchical sub-steps as described below.

A. Determination of percentage of pixel representation in the merged image (Image3)

In order to determine the percentage of pixels being faithfully represented in the merged Image 3 formed by the combination of Image 1 and Image 2, a quantity termed as the representation ratio (RR) is defined such that,

$$RR_g = \frac{Number\ of\ Green\ pixels\ in\ Image\ 3\ \left(N_{g_{merge}}\right)\ in\ the\ green\ channel}{Number\ of\ Green\ pixels\ in\ Image\ 1\left(N_{g_{initial}}\right)\ in\ the\ green\ channel}$$

$$RR_b = \frac{Number\ of\ Blue\ pixels\ in\ Image\ 3\ \left(N_{b_{merge}}\right)\ in\ the\ blue\ channel}{Number\ of\ Blue\ pixels\ in\ Image\ 2\left(N_{b_{initial}}\right)\ in\ the\ blue\ channel}$$

The number of pixels in each case is found by detecting the number of matrix cells having intensity values greater than the threshold values b_{thresh} or g_{thresh} for the corresponding channel of the respective images under investigation. If the RR ratios are 100% for the image set under investigation, then it can be interpreted that the merging process has no error and the next sub-step can be carried out.

B. Determination of the number of combined pixels in the merged image (Image3)

C. In this sub-step, the number of pixels having both blue and green intensities (N_{gb}) in the Image 3 is determined by using the *find* function for the respective image indices which have intensity values greater than b_{thresh} and g_{thresh}.

Step 3. Calculation of co-localization Index

Two co-localization indices are then defined and determined as,

$$CI_{g\_merge} = \frac{Number\ of\ combined\ pixels\ in\ Image\ 3\ \left(N_{gb}\right)}{Number\ of\ Green\ pixels\ in\ Image\ 3\ \left(N_{g_{merge}}\right)}$$

Here, CI_{g_merge} indicates the percentage of mRNA which remains within the nucleus of the yeast cells.

❖ **Separation of Nuclear and cytoplasmic fractions.**

This method of separating nuclear and cytoplasmic fractions from yeast culture was essentially carried out as described before Kizer *et al.* 2006. [160] Cells from 200ml yeast culture ($O.D._{600}$ = 1) were pelleted at 4000g for 10mins at 4^{o}C and washed with sterile water. The pellet was then

resuspended gently in 3ml spheroplasting buffer (1M sorbitol, 500mM K2HPO4 (pH 6.5) with 0.018% β-mercaptoethanol) and centrifuged at 3500g for 10mins at 4^{o}C. The pellet was next resuspended in 3ml spheroplasting buffer containing 40units/ml Lyticase, and incubated at 30^{o}C for 30 mins to allow 90% of cells to form spheroplasts. The spheroplasted cells were centrifuged at 4000g for 5mins at 4^{o}C and washed again with 3ml of spheroplasting buffer. The pellet was resuspended in 8ml of lysis buffer (18% ficol 400, 20mM K2HPO4, 1M MgCl2, 0.5mM EDTA (pH =8), 2mM PMSF) with protease and RNase inhibitor. The cells were then lysed with 20 strokes of small Dounce homogenizer with pestle A in ice. The samples were centrifuged at 3500g to remove cell debris which forms the pellet. The supernatant was then centrifuged at 31,800g for 45mins to pellet the nuclei. The nuclear fraction was finally resuspended in 200ul NP buffer (0.34M sucrose, 20mM Tris-HCl (pH =7.4), 50mM KCl, 5mM MgCl2 with protease and RNase inhibitor) while the remaining supernatant was cytoplasmic fraction.

- **Statistical Analyses.**

The quantitative experiments that are reported in this paper (mRNA steady-state levels, co-localization index) were performed using at least three independent sample size (biological replicates) (N=3). However, for calculating the co-localization index, we used a sample size of 20 cells (N=20). A given yeast strain was grown and treated under the same experimental conditions independently before a given experiment was conducted for each biological replicate. In the case of technical replicate, repetition/analyses of the same biological replicate sample was conducted many times. All the statistical parameters such as mean, standard deviations, P-values, standard error of the mean, median were calculated using GraphPad Prism version 7.04 (GraphPad Software Inc., San Diego, CA, USA). P-values were calculated using Student's two-tailed t-test (unpaired) using the same program.

Chapter 4

RESULTS (I)

4.1 Introduction:

As discussed earlier, the hyphal morphogenesis in many pathogenic fungal species (such as opportunistic pathogen *C. albicans*) is coupled to their virulence. It is therefore, utmost important to have an insight into the detailed mechanism of pathogenic transition of *Candida* and other virulent fungi to develop the possible approaches of therapeutic interventions for the disease caused by them. Recent study revealed that a serine/threonine kinase Sks1p in *Saccharomyces* and its corresponding orthologue Sha3p in *Candida* is involved in the growth and adaptation of the *Saccharomyces/Candida* cells under glucose/nitrogen limiting conditions by integrating multiple signal transduction pathways involved in the pseudohyphal development [(157)]. This observation prompts us to investigate the physiological regulation of SKS1 gene under normal and nutrient depleted conditions in this model organism to have an insight into the control and dynamics of the production Sks1p kinase at various nutrient limiting conditions.

Our laboratory's previous research has revealed that *SKS1* mRNA stands out as one of the "special" mRNAs, exhibiting remarkable nuclear retention and accelerated nuclear degradation—processes intricately dependent on the nuclear exosome and its cofactor, CTEXT. Our preliminary observations suggest an intriguing possibility: the regulation of SKS1 gene expression is intricately tied to the modulation of mRNA nuclear export and the selective intranuclear degradation of the *SKS1* message by both the nuclear exosome and CTEXT.

What's particularly fascinating is that when glucose and nitrogen concentrations are abundant in the medium, the necessity for the Sks1p Ser/Thr kinase diminishes [(157)]. As a result, *SKS1* mRNA is retained in the nucleus. This prompts us to consider an intriguing scenario: during times of nutrient limitation, when the function of Sks1p becomes critical, *SKS1* mRNA likely undergoes swift nuclear export into the cytoplasm, where it is translated into a substantial quantity of Sks1p (Ser/Thr kinase protein).

Thus, gaining a profound understanding of how SKS1 gene expression is regulated is essential for uncovering the intricate mechanisms controlling Sks1p protein production under normal and nutrient-stressed conditions. Such insights will illuminate the compelling connections between glucose-responsive cell signaling and the phenomenon of pseudohyphal growth, enhancing our understanding of these vital biological processes.

4.2. Understanding the Expression Pattern of SKS1 mRNA under nutrient stress:

We initiated our study by revalidating the previous findings [157] where Sks1p has been identified as a key integrator of glucose and nitrogen responsive cell signaling to pseudohyphal growth. To revalidate the previous results showing yeast cells exhibit various cell morphology in growth media with different concentrations of glucose and nitrogen, we tested the growth pattern of a WT yeast cell in various growth media with high and low glucose and nitrogen. As evident from Fig 4.1, indeed the baker's yeast undergoes morphological transition from rounded cells in nutrient rich YPD medium to filamentous form in Low Dextrose (LD) and Synthetic Low Ammonium Dextrose (SLAD) medium. Previously, Johnson *et al*. [157] had shown that *sks1*-Δ yeast strains fail to form any pseudohyphae under glucose/nitrogen stress. Hence combined with the previous studies, we can say that pseudohypha formation is a strategy that baker's yeast adopts to survive nutrient stress and *SKS1* mRNA plays a significant role in this transition.

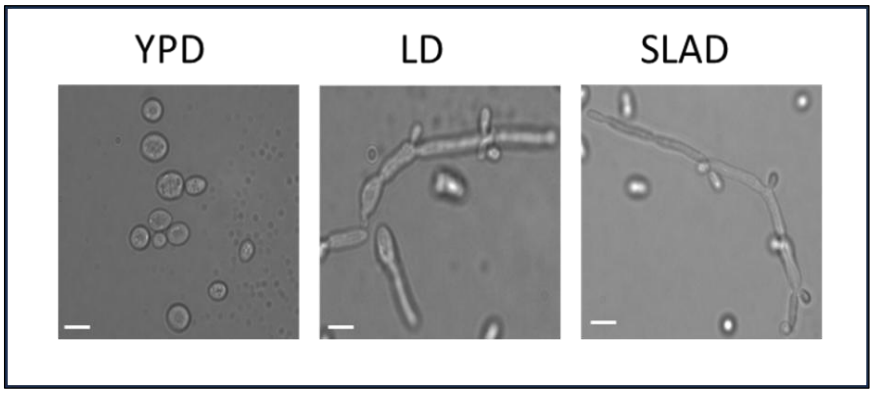

***Fig 4.1*: Morphology of yeast cells grown in different media with various concentrations of glucose and nitrogen.** *Yeast cells showing round cell morphology when grown in YPD (nutrient rich condition). Filamentous yeast cells when grown in LD (low dextrose 0.2%) and SLAD (synthetic Low Ammonium Dextrose medium with 50 µM ammonium sulphate) media. Scale=4µm.*

Having confirmed this, we proceed with the characterization of expression pattern of *SKS1* mRNA in *Saccharomyces cerevisiae* in response to nutritional changes. Preliminary studies [100] revealed that the physiological levels of *SKS1* and *CBC1* mRNAs bear an inverse relationship under nutrient starved conditions. To get a preliminary idea, we analyzed the steady state levels of *SKS1* and *CBC1* mRNAs after growing the yeast cells in YPD and Low Nitrogen (50 µM ammonium sulphate) media for prolonged period. The results of this experiment revealed that with increasing time (from 0 hour to 5days), as the key nutrients in the growth medium started getting depleted resulting in a stressed condition, the steady state level of *SKS1* mRNA increased up to 4-5-fold while that of *CBC1* mRNA decreased to 5-fold (Fig. 4.2), *SCR1* was used as the normalizer and *ACT1* was used as a negative control.

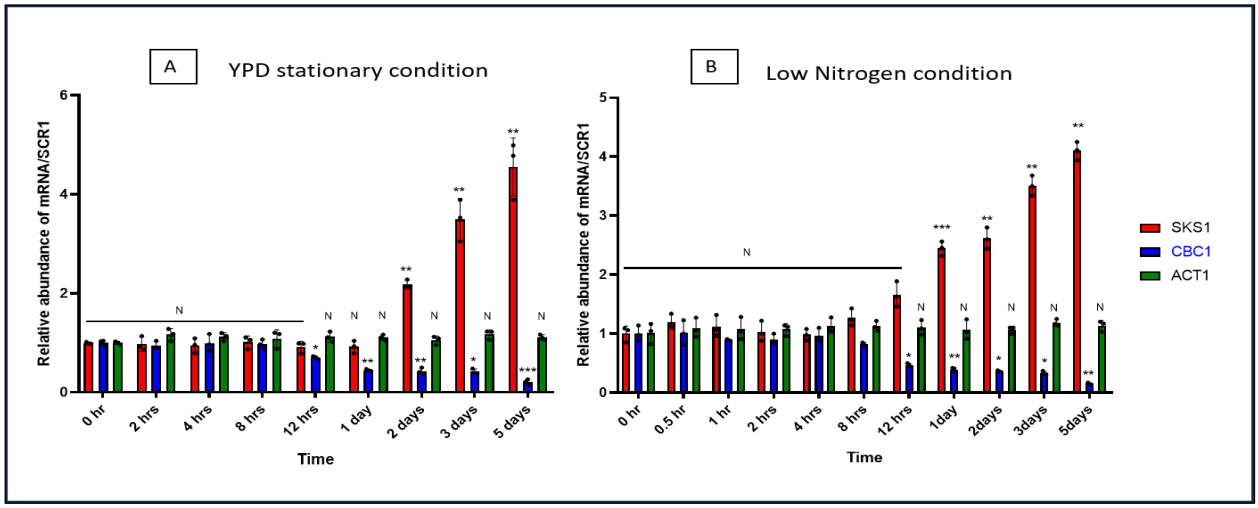

***Fig. 4.2**: Steady state level analysis for SKS1 and CBC1 mRNAs from yeast cells grown under (A) YPD stationary and (B) Low Nitrogen Growth conditions for time points ranging from 0 hour to 5days. Histogram plotted from qRT-PCR analysis (with 2ng of each cDNA) shows SKS1 mRNA is upregulated while CBC1 mRNA is downregulated after 5days of growth in respective media, thus indicating an inverse physiological abundance. The steady state level of ACT1 mRNA is used a control and remains unaffected under the experimental conditions. Significance: *=P value<0.05, **=P value<0.005, ***=P value<0.001, N=Not significant, n=3, internal normalizer= SCR1 mRNA.*

Since these preliminary data are in good agreement with the previous findings, we aim towards analyzing the expression patterns of *SKS1* and *CBC1* mRNAs during the growth under defined concentrations of glucose (2%-0.04%) and nitrogen (378 mM-25 µM Ammonium sulphate). Defining the conditions would enable us with more control over the downstream analyses. For this study, the cells were grown in respective media until $O.D._{600}$ reaches 0.8 followed by RNA isolation and qRT-PCR. Though the Results showed the same inverse relationship between the physiological levels of *SKS1* and *CBC1* mRNAs with increasing stress, yet it gave a clear insight towards the genetic expression pattern with respect to defined nutrient concentrations. From Fig. 4.3, it is clear that *SKS1* mRNA starts getting upregulated when glucose concentration reaches 0.125% and Ammonium sulphate concentration reaches 369 µM. But, *CBC1* mRNA, not only shows a drop in its abundance level, but starts doing so at a comparatively higher concentration of 0.5% glucose and 1.47mM Ammonium sulphate. This finding indicates towards a cause-and-effect relationship between the two genes, because Cbc1p is an important component of the CTEXT complex which acts as a cofactor with nuclear Exosome for the degradation of these NR mRNAs. But before considering the possibility of altered mRNA degradation rate as the cause of this increased level of *SKS1* mRNA we should also take into account the involvement of altered transcription rate.

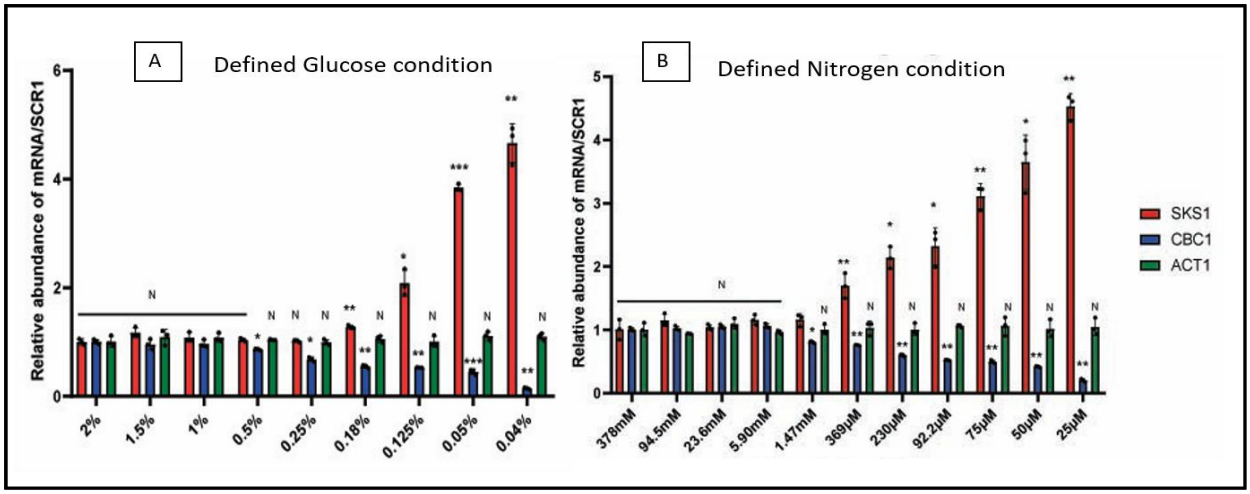

***Fig. 4.3*: Steady state level analysis for SKS1 and CBC1 mRNAs from yeast cells grown in (A) Defined Glucose concentrations (2% to 0.04%) and (B) Defined Ammonium sulphate concentrations (378mM to 25µM).** *Histograms plotted from qRT-PCR analysis (with 2ng of each cDNA) shows that CBC1 mRNA starts getting downregulated at concentrations higher than that where SKS1 mRNA gets upregulated during growth of yeast cells in respective media. This downregulation of CBC1 mRNA could have an impact on the upregulation of SKS1 mRNA. The steady state level of ACT1 mRNA is used a control and remains unaffected under the experimental conditions. Significance: *=P value<0.05, **=P value<0.005, ***=P value<0.001, N=Not significant, n=3, internal normalizer= SCR1 mRNA.*

4.3 Defining the cause of the particular expression pattern of *SKS1* mRNA under nutrient stress:

The steady-state level of any given mRNA is dicatated by both of its rates of transcription (synthesis) and the degradation (destruction). Since *SKS1* mRNA has been found to undergo upregulation during nutrient stress condition for the yeast cells to survive in the previous experiment, the said increment could be brought about either by enhanced transcription or diminished degradation or by both that could be induced during the nutrient deleted condition. Therefore, we went ahead in testing the first hypothesis that increased transcription rate of *SKS1* gene induced by nutrient stress causes its upregulation.

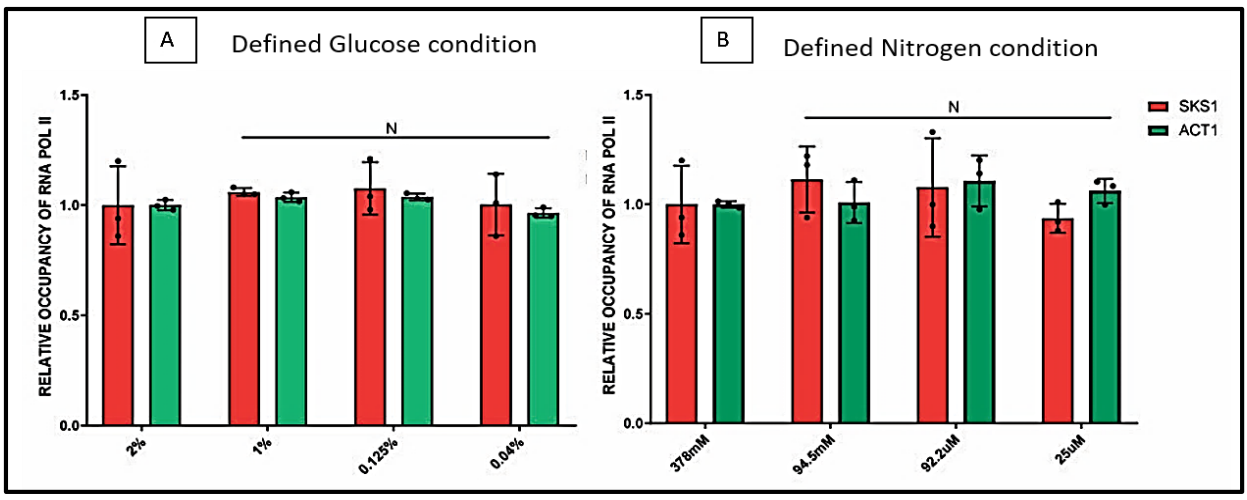

Fig 4.4. Chromatin Immuno-precipitation assay to analyze the relative occupancy of actively elongating RNAPol II on the SKS1 Chromatin from yeast cells grown under (A) Defined Glucose concentrations and (B) Defined Ammonium sulphate concentrations. *Histograms plotted from qRT-PCR analysis shows that the transcription rate SKS1 mRNA under the respective defined nutrient concentrations remain unaltered, hence eliminating the involvement of increased transcription hypothesis behind the upregulation of SKS1 mRNA under nutrient stress. The Transcription rate of ACT1 mRNA is used a control and remains unaffected under the experimental conditions. Significance: *=P value<0.05, **=P value<0.005, ***=P value<0.001, N=Not significant, n=3, internal normalizer= SCR1 mRNA.*

Now, having defined the glucose and Ammonium sulphate stress concentrations, we would be carrying out further analyses of estimating the transcription rate of *SKS1* gene only in some selected concentrations of glucose/nitrogen. The yeast cells were grown in respective media with decreasing concentrations of glucose/nitrogen followed by induction of DNA-protein cross-linking and isolation of crosslinked chromatin, which was then subjected to ChIP analysis (as mentioned in material methods section) to determine the amount of occupancy of elonagating RNA Polymerase II (RNAPII) in SKS1 gene locus. The rationale of this experiment involves if any gene undergoes increased transcription under an induced state, then increased number of elongating RNAPII (hyperphosphorylated) will be bound to it under such condition compared to the control/uninduced condition when the said gene~~s~~ would undergo basal level transcription. Moreover, the transcriptionally elongating active RNAPII always remain hyperphosphorylated at its Ser2 and Ser5 position at CTD of Rpb1 [(196)]. Thus to avoid targetting inactive RNAPolymerases, the antibody we used was raised against the hyperphosphorylated active RNAPII. However, under both the nutrient conditions, the transcription rate of *SKS1* mRNA showed no significant change (Fig. 4.4).

With the elemination of the possibility of involvement of increased transcription rate in the upregulation of SKS1 mRNA under nutrient stress, we moved towards our next hypothesis of diminished degradation rate for the mRNA. This hypothesis was developed due to from the previous finding of downregulation of CBC1 mRNA with increase in nutrient stress. If Cbc1p level falls drastically, then conceivably there will be a resultant decrease in the level of functionality of the CTEXT complex and hence incompetency of the nuclear Exosome to degrade SKS1 mRNA will increase. With this idea, we first checked the levels of Sks1p and Cbc1p under defined glucose and nitrogen growth conditions to confirm if the change in mRNA levels were reflected in their protein levels too. Yeast strain was grown in respective media overnight under increasing stressed conditions and total cellular protein extract was isolated from them and subjected to western blot analysis using antibody against Cbc1p and Sks1p. The blots strongly indicated towards decrease in the level of Cbc1p and increase in the level of Sks1p with increasing nutrient stress (Fig.4.5). Sks1p level is highest when the Cbc1p level is lowest under both conditions. And thus, we have a strong ground to hypothesise that there might be an alteration of degradation rate to cause the upregulation of *SKS1* mRNA.

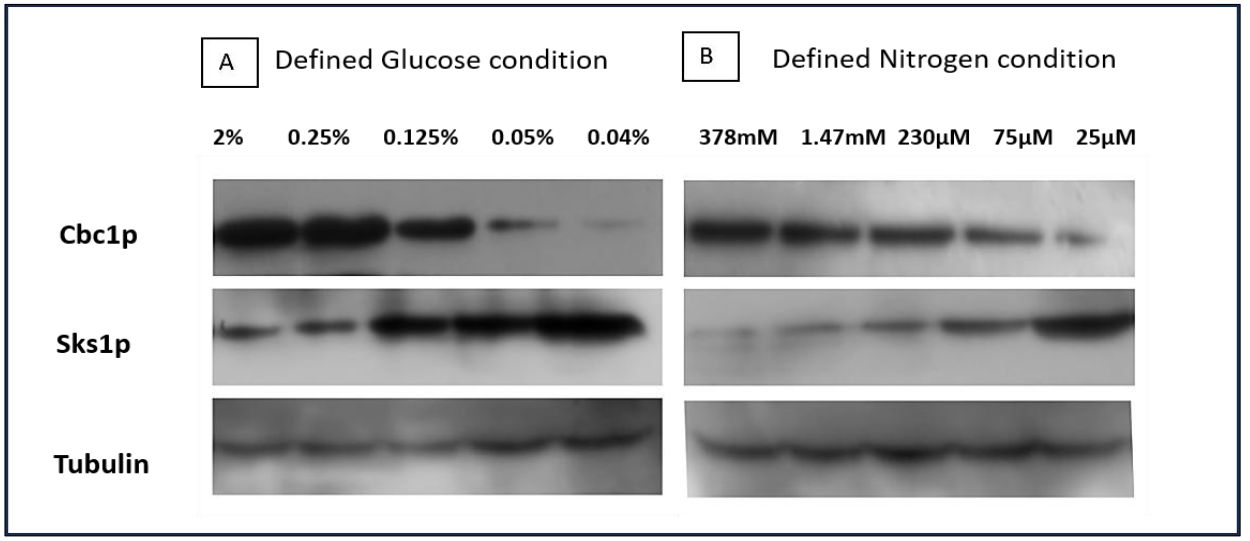

Fig. 4.5: Western blot analysis of yeast cells grown in defined concentrations of nutrients*: (A) The blots reveal that with increase in glucose stress, Cbc1p level starts going down from 0.125% glucose with a simultaneous increase in the Sks1p level. (B) Under defined Ammonium sulphate growth conditions, Cbc1p level starts going down from 1.47mM of Ammonium sulphate, with concomitant increase in Sks1p level. Thus, there could be a cause-and-effect relation between the two genes. α-Tubulin is used as a loading control. Protein loaded is 80µg. Both the Sks1 and Cbc1 proteins are TAP tagged.*

To strongly confirm that decrease in the overall Cbc1p level alters its interaction status with *SKS1* mRNA we analyzed the binding efficiency of Cbc1p to *SKS1* mRNA as well as other typical messages under selected glucose and nitrogen concentrations. This experiment was necessary to interpret whether decrease in Cbc1p level under nutrient stress altered its association to mRNAs irrespective of their nature. We first crosslinked each culture with 254 nm UV light as this will result in crosslinking of proteins and nucleic acids which are in close proximity. Then we pulled down Cbc1p using its Antibody following immuno-precipitation protocol and finally isolated RNA bound to the pulled protein. This RNA was then used for qRT-PCR analysis to find the relative enrichment of *SKS1* mRNA in each of those immuno-precipitated protein samples. This study revealed that with increasing nutrient stress of glucose and nitrogen, the interaction of Cbc1p to *SKS1* mRNA decreased gradually but significantly (Fig. 4.6A), though there was no significant change in binding efficiency of Cbc1p to typical mRNAs under same conditions (Fig. 4.6B). At 0.125% Glucose level from where Cbc1p level starts falling (Fig. 4.5A), its interaction with *SKS1* mRNA is reduced by ≈50% (Fig. 4.6A), while at 369 µM Ammonium sulphate the interaction is reduced by 60-70% (Fig. 4.6A) considering the drop in Cbc1p level at a higher concentration of 1.47mM Ammonium sulphate (Fig. 4.5B). Thus, this finding indicated that the reduced degradation of the *SKS1* mRNA under nutrient stress can be attributed to the transcript specific diminished interaction of CTEXT/Exosome complex.

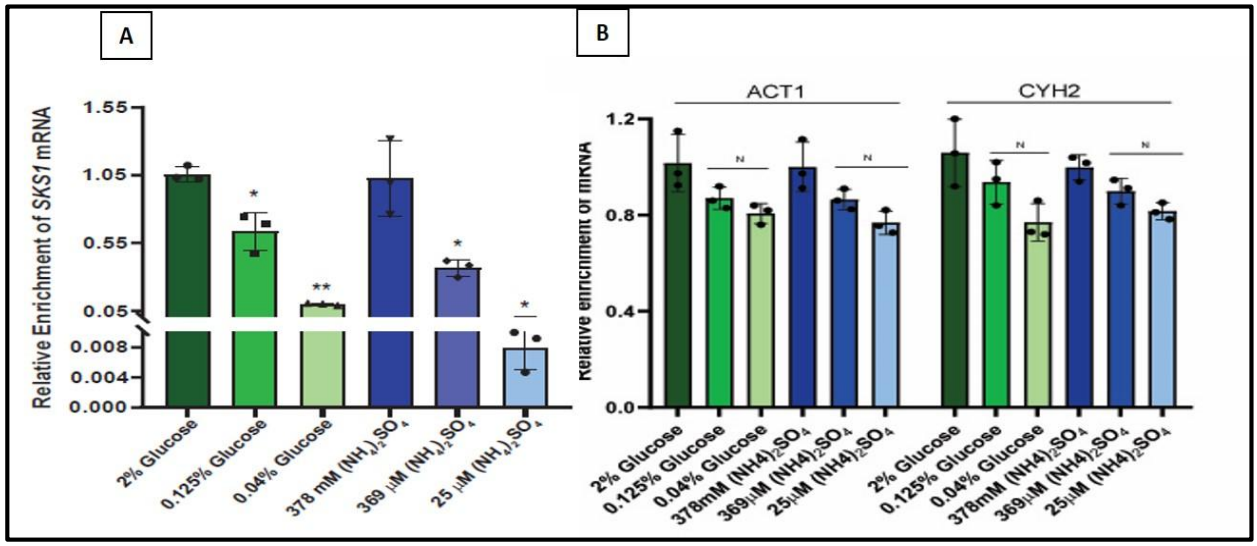

Fig. 4.6: RNA Immuno-precipitation assay (RIP) to analyze binding efficiency of bound mRNAs and Cbc1p: *Yeast strains carrying CBC1-TAP were grown till O.D.= 0.8 in media with defined concentration of glucose and Ammonium sulphate as mentioned. UV crosslinking of cultures resulted in crosslinking of closely situated nucleic acids and proteins. When Cbc1p is pulled down by antibody, the bound RNAs were also precipitated and isolated. These RNAs were converted to cDNAs for performing qRT-PCR (with 2ng of each cDNA) analysis which revealed the relative binding efficiency of (A)SKS1 mRNA as well as (B) two typical messages ACT1 and CYH2 to Cbc1p. Histograms show gradual decrease in the binding efficiency of Cbc1p to SKS1 mRNA with*

*increasing glucose and nitrogen stress. At 0.04% Glucose and 25µM Ammonium sulphate the interaction is decreased by more than 90% compared to 2% Glucose and 378mM Ammonium sulphate respectively. On the other hand, however, there is no significant change in the binding efficiency of Cbc1p to ACT1 and CYH2 mRNAs. Significance: *=P value<0.05, **=P value<0.005, ***=P value<0.001, N=Not significant, n=3, internal normalizer= SCR1 mRNA.*

To assess the degradation rates of SKS1 mRNA under various nutrient deprived conditions, we performed transcription shut-off experiment using 1, 10-phenanthroline to shut off any de-novo synthesis of mRNA by RNAPII. Yeast cells were grown in their respective media with varying concentrations of glucose and nitrogen. When $O.D._{600}$ reached 0.8, an aliquot of 15 ml culture was withdrawn to serve as 0 min sample. Thereafter, following the addition of 1, 10-phenanthroline to arrest RNAPII, aliquots were withdrawn at regular time intervals of 3 mins, 5 mins, 10 mins, 20 mins, 30 mins and 40 mins. RNA isolated from each of these aliquots was subjected to qRT-PCR analysis to detect the rate of degradation of *SKS1* mRNA or in other words half-life of the mRNA under various nutrient conditions. Half-life values of *SKS1* mRNA usually ranges around 7 minutes (±0.68) under glucose rich condition (2%) and 5 minutes (±0.81) under nitrogen rich condition (378mM). (Fig. 4.7) But with increase in nutrient stress, the half-life values show a gradual increase up to 27 minutes (±0.18) under 0.04% glucose and 24 minutes (±0.47) under 25µM Ammonium sulphate. (Fig. 4.7) Thus, the findings indicate towards the involvement of diminished degradation rate of *SKS1* mRNA resulting from reduced interaction with Cbc1p and hence with nuclear Exosome/CTEXT.

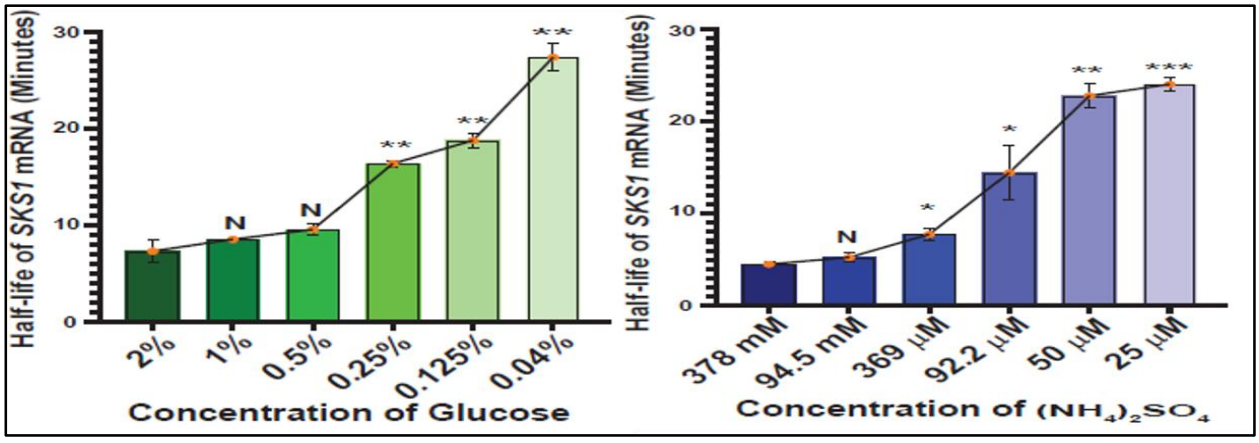

Fig. 4.7: Transcription shut off assay using 1,10-phenanthroline to analyze the half-life of SKS1 mRNA under various glucose (Left histogram) and Ammonium sulphate concentrations (Right histogram). *After growing each culture in media with defined concentrations of glucose and nitrogen, to $O.D._{600}$=0.8, an aliquot was withdrawn from each to serve as 0 min sample, then from the time of adding 1,10-phenanthroline aliquots were withdrawn at regular time intervals as mentioned followed by RNA isolation from each aliquot. Histograms prepared from qRT-PCR (with 2ng of each cDNA) show the increase in half-life of SKS1 mRNA from 7 minutes under 2% glucose rich condition to 27 minutes under 0.04% glucose stress condition (Left histogram) and from 5minutes under 378mM Ammonium sulphate condition (nitrogen rich) to 24 minutes under 25µM Ammonium sulphate condition (nitrogen stress) (Right histogram). q-RT PCR values of SKS1 mRNA are normalized by that of SCR1 mRNA under respective experimental*

*conditions. ACT1 mRNA was analyzed as a control sample and showed almost unaltered half-life under all conditions (data not shown). Significance: *=P value<0.05, **=P value<0.005, ***=P value<0.001, N=Not significant, n=3.*

We know *SKS1* mRNA has a tendency to accumulate inside nucleus under normal condition, where their cellular repertoire is maintained by rapid nuclear degradation. But, under nutrient stress conditions we have found that the mRNA is not only upregulated but also has increased half-life. So, what is their fate inside the cell under nutrient stress? According to our previously published data [133], *SKS1* mRNA is stabilized inside the cell when they escape degradation by means of rapid export from nucleus to cytoplasm. Hence, we proceeded towards checking the cellular distribution of *SKS1* mRNA under some defined nutrient growth conditions.

4.4 Investigating the intra-cellular localization of *SKS1* mRNA and the mechanism behind it:

To investigate the cellular localization of *SKS1* mRNA we took two different approaches: one was by fractionating nuclear and cytoplasmic portions of the yeast cells grown in various concentrations of glucose and nitrogen, and the second method is fluorescence microscopy. For the first approach, RNA was isolated separately from the nuclear and cytoplasmic fractions of each culture and subjected to qRT-PCR. Since typical mRNAs like *ACT1* mostly localize within cytoplasm, so using *ACT1* as the normalizer we checked the abundance of *SKS1* mRNA in each isolated fraction. The analysis revealed that though under nutrient rich conditions (2% glucose and 378mM Ammonium sulphate) about 90% of *SKS1* mRNA population localized within the nucleus, but with increasing nutrient stress the mRNA gradually moved out into the cytoplasmic fraction to an extent of 80-85%, leaving only 15-20% of the mRNA population inside nucleus (Fig. 4.8).

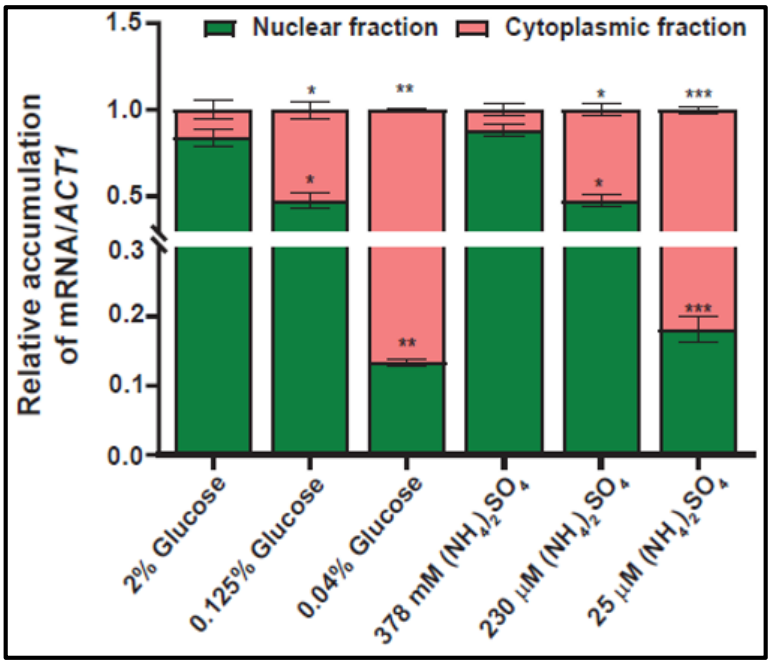

Fig. 4.8: Intracellular localization of SKS1 mRNA under various concentrations of glucose and Ammonium sulphate from RNA isolated separately from nuclear and cytoplasmic fractions: *RNA from separated fractions of Yeast cells grown under defined*

*concentrations of glucose and nitrogen was subjected to qRT-PCR (with 2ng of each cDNA). The analysis revealed that though SKS1 mRNA mostly localized in the nuclear fraction of yeast cells grown in 2% glucose and 378mM Ammonium sulphate containing media, but it gradually moved into the cytoplasmic fraction with increase in nutrient stress. When the media comprises of 0.04% glucose and 25µM Ammonium sulphate almost 80-85% of the SKS1 mRNA had moved out into the cytoplasm. Significance: *=P value<0.05, **=P value<0.005, ***=P value<0.001, N=Not significant, n=3, internal normalizer= ACT1 mRNA.*

This finding was further validated using fluorescence microscopy which required co-transformation of yeast cells with two plasmids (Fig. 4.9): the first plasmid carries a reporter SKS1-U chimeric gene that harbors sixteen tandem repeat modules of U1A RNA hairpin loop between the ORF and 3'-UTR of *SKS1* gene, the second plasmid harbors a human hU1A-GFP fusion gene placed under the control of pGAL1. [161] Notably, the hU1A-GFP fusion gene, which consists of first N-terminal 94 amino acid residues of human U1A RNA binding protein (binds to a small hairpin loop, which does not exist in yeast, [162] fused in frame to GFP. [100] [133] [161] GFP signal that is detected following the co-expression of these two plasmids specifically represents the distribution of the reporter mRNA and not of just the GFP. [100] [133] So, whenever Galactose induction was given to these cells, U1A-GFP proteins were produced that would bind to the U1A loops due to specific affinity and in turn move along with the mRNA fused with the U1A loops. After 2% Galactose induction, the media was changed to Glucose to stop the induction and clear out background noise due to unbound U1A-GFP proteins. For our investigations, yeast cells were harvested after growing in YPD, then these cells were inoculated in their respective media ($O.D._{600}$= 0.1 at the time of inoculation) comprising varying glucose and nitrogen concentrations and grown till $O.D._{600}$ = 0.3. Cells were then kept resuspended in media with Raffinose of same concentration as Glucose till $O.D._{600}$ = 0.8, followed by 2% Galactose induction for 1 hour and finally media was changed to initial percentage of glucose and nitrogen. After incubating for an hour, Nucleus was stained with Hoechst dye followed by 4 washes with 1X PBS before observing under microscope (100X).

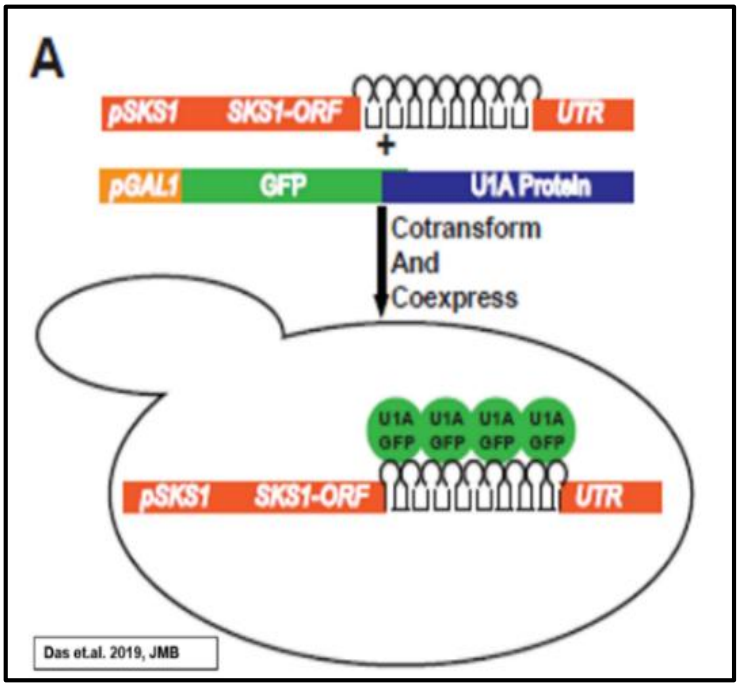

Fig. 4.9: Rational behind construction of yeast strain for visualization of mRNA localization via fluorescence microscopy. *Co-transformation of*

yeast strain with two plasmids, one bearing the mRNA's promoter and ORF fused with U1A protein binding loops and the other plasmid has U1A protein-GFP under GAL Promoter, together results in the construction of a yeast strain that can be induced by Galactose for formation of U1A-GFP protein to bind specifically onto U1A loops and in turn with the fused mRNA and move along with it. Thus, fluorescence microscopic analysis can reveal the intracellular localization of the mRNA.

Using fluorescence microscopic imaging technique, we first observed the intra-cellular localization of *PGK1* mRNA for yeast cells grown separately in three compositions: media with 2% Glucose and 378mM Ammonium sulphate (Nutrient rich), media with 0.04% Glucose media (Glucose stress) and media with 25µM Ammonium sulphate media (Nitrogen stress). Under all growth conditions, the *PGK1* mRNA was found to be distributed throughout the cell cytoplasm (Fig. 4.10, shown in green fluorescence while the nuclei appear blue), hence the mean co-localization indices were below 0.1 under all conditions (Table 4.1 and Fig. 4.12) (indicating that the mRNA-GFP signal and Hoechst-stained nuclei do not co-localize). This observation is consistent with the usual intra-cellular distribution pattern of general mRNAome under nutrient rich condition and remained unaffected by nutrient stress.

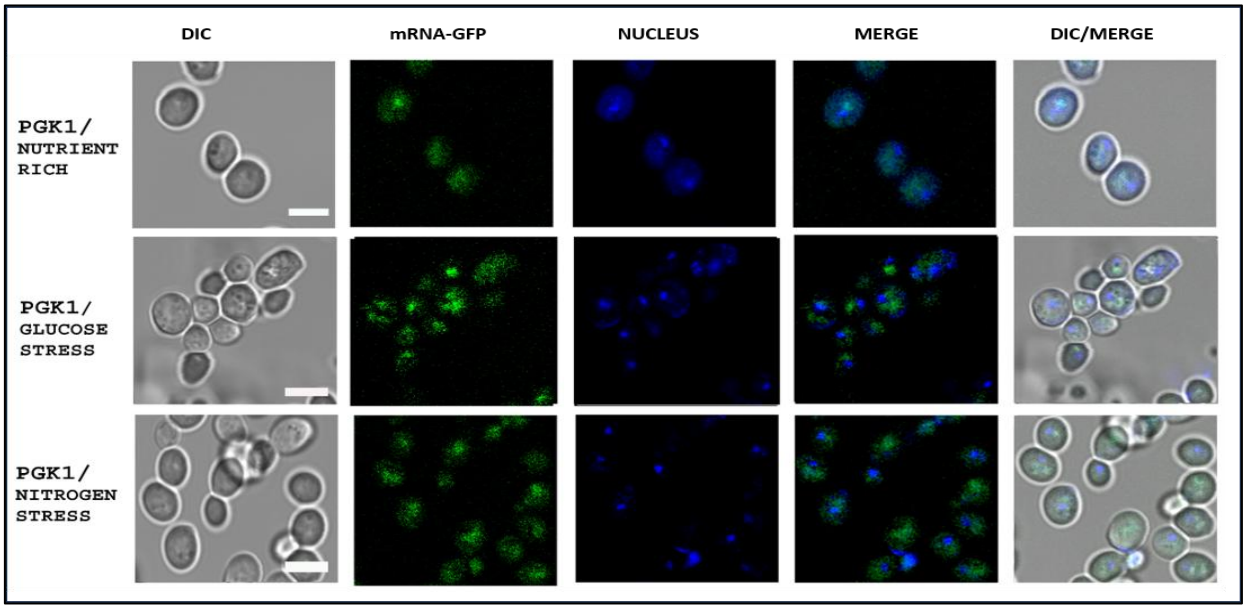

Fig. 4.10: Fluorescence microscopic image showing In situ distribution of PGK1-mRNA under various growth conditions: *2% glucose with 378mM Ammonium sulphate (nutrient rich), 0.04% Glucose (Glucose stress), 25µM Ammonium sulphate (Nitrogen stress). Yeast cells grown in YPD were pelleted down and washed with water for inoculation into media with defined concentrations of glucose and nitrogen. At $O.D._{600}$ =0.3, the cells were resuspended in media having same concentration of Raffinose as that of Glucose and grown till $O.D._{600}$ = 0.8. Then 2% galactose induction was given for 1 hour followed by resuspension in media with initial compositions of glucose and nitrogen, and incubated for an hour before staining the nucleus with Hoechst for observation under confocal microscope (100X). The images showed cytoplasmic distribution of PGK1 mRNA under all conditions of glucose and nitrogen concentrations, as the mRNA is unaffected by nutrients in the media. In the merge panel we could see the green GFP fluorescence of the PGK1 mRNA did not co-localize with the Hoechst-stained nucleus, indicating the mRNA's cytoplasmic distribution (mean co-localization indices being below 0.1 under all conditions). Scale= 4µm.*

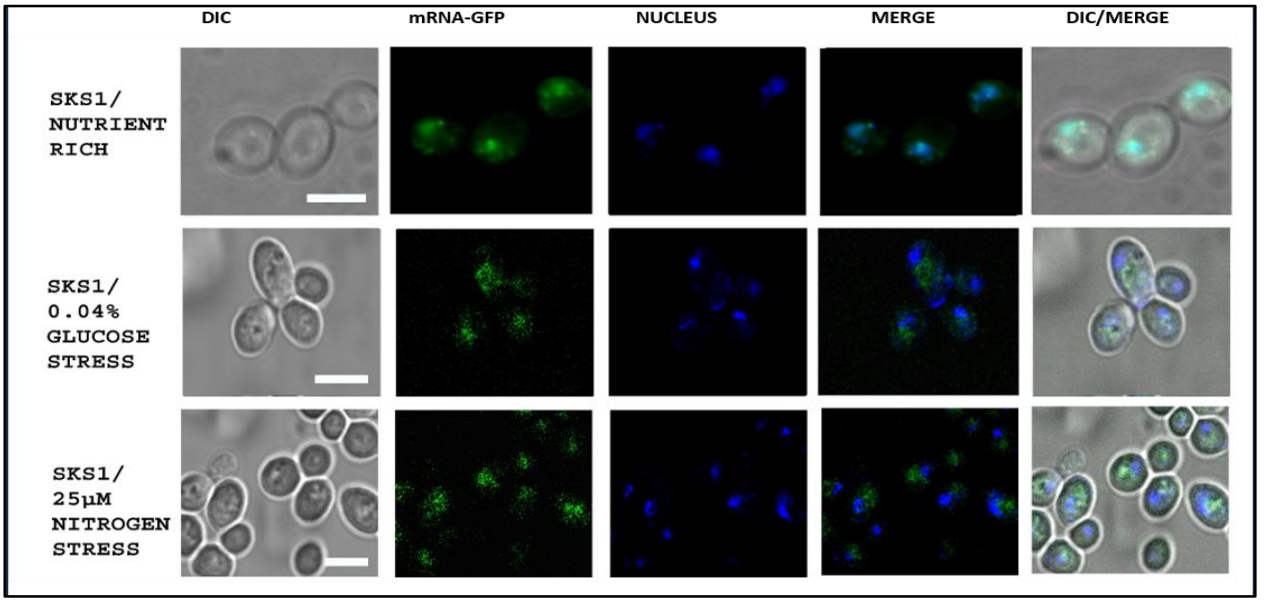

Fig 4.11: Fluorescence microscopic image showing In situ distribution of SKS1-mRNA under various growth conditions: *2% glucose with 378mM Ammonium sulphate (nutrient rich), 0.04% Glucose (Glucose stress), 25µM Ammonium sulphate (Nitrogen stress). Yeast cells grown in YPD ($O.D._{600}$ =0.3) were pelleted down and washed with water for inoculation into media with defined concentrations of glucose and nitrogen. When $O.D._{600}$ reached 0.8, an induction of 2% galactose was given for 1 hour followed by resuspension in media with initial compositions of glucose and nitrogen, and incubated for an hour before staining the nucleus with Hoechst for observation under confocal microscope (100X). The images showed clear nuclear accumulation and hence co-localization of SKS1 mRNA and the nucleus under nutrient rich condition (mean co-localization index being 0.92) while cytoplasmic distribution with no co-localization of SKS1 mRNA with nuclei was observed under both glucose and nitrogen stress conditions (mean co-localization indices being around 0.1 under both glucose and nitrogen stress conditions). Scale= 4µm.*

After testing the intra-cellular localization of *PGK1* mRNA, we proceeded towards analyzing the same for *SKS1* mRNA. (Fig. 4.11) We observed a clear nuclear accumulation of *SKS1* mRNA in nutrient rich media, where the Hoechst-stained nucleus and the GFP signal of *SKS1* mRNA co-localized (Fig. 4.12 and Table 4.1, mean co-localization index = 0.92) but this co-localization was not found in case of glucose and nitrogen stresses as the mRNA was mostly localized outside the nucleus into the cytoplasm (mean co-localization indices being 0.12 for glucose stress and 0.09 for nitrogen stress) (Fig. 4.12 and Table 4.1).

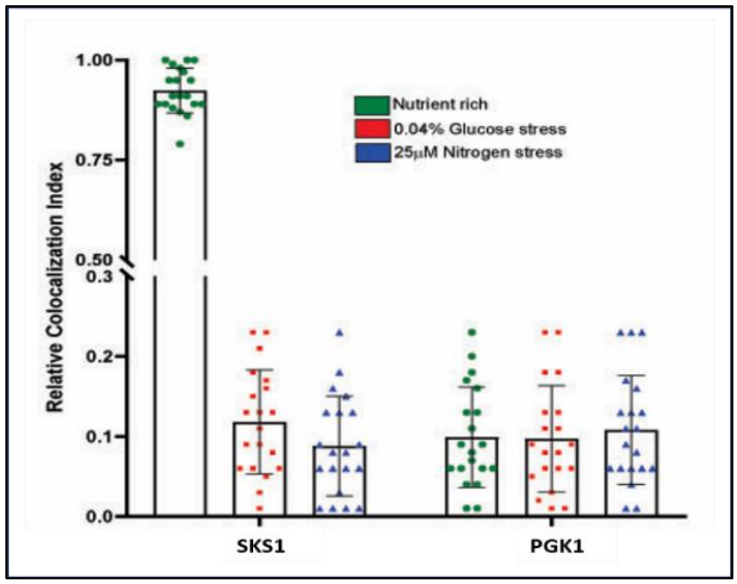

Fig 4.12: Histograms showing co-localization indices of Hoechst-stained nucleus with GFP signal of SKS1/PGK1 mRNAs for each of the growth conditions. *CI (Pearson correlation coefficient, PCC) were determined as described in the method section. Higher CI indicates towards better co-localization of the nucleus and mRNA-GFP. n=20.*

TABLE 4.1: Co-localization index for *SKS1* and *PGK1* messages under various nutrient-rich and nutrient-limiting conditions:

mRNA	Nutrient Rich		0.04% Glucose		25µM Ammonium sulphate	
	CI Mean (+/- SEM)	N	CI Mean (+/- SEM)	N	CI Mean (+/- SEM)	N
SKS1	0.924(+/- 0.013)	20	0.118 (+/- 0.015)	20	0.088(+/-0.014)	20
PGK1	0.099(+/- 0.014)	20	0.097 (+/- 0.015)	20	0.108(+/-0.015)	20

Collectively our data till now reveal that *SKS1* mRNA is retained in the nucleus under nutrient rich conditions, and gets rapidly exported into the cytoplasm under nutrient stress conditions and thus escape the nuclear degradation as evident from RNA Immunoprecipitation assay and fluorescence microscopic imaging. But still, it is not clear why with change in glucose and nitrogen concentrations in the media, there is better export *SKS1* mRNA into the cytoplasm and increased stability. This query led us to hypothesize the presence of one or more putative *trans*-acting factor(s) (*NZ* binding protein or *NZBP*) that bind(s) to the *SKS1-NZ* element and thereby retard(s) its export. If there is any NZBP associated in the regulation, then its involvement needs to be essential for the regulation of other NR mRNAs (see next chapter).

Chapter 5

RESULTS (II)

5.1 Introduction:

In an attempt to understand the mechanism of *SKS1* mRNA's nuclear retention, previously we had uncovered a 202 nt long *cis*-acting element in the 1502 nt long transcript body of *SKS1* mRNA that spans from 825 to 1026 nt residues. [133] Elimination of this 202 nt *cis*-element (dubbed as the nuclear zip-code element or *NZ* element) leads to rapid export of resultant mRNA and its quick relocalization into the cytoplasm. [133] Though the *cis*-acting *NZ* element was implicated to be responsible for *SKS1* mRNA's nuclear retention under nutrient rich condition, the regulation under nutrient depleted conditions cannot be explained. To unravel the mechanism, we postulate that one or more putative *trans*-acting factor(s) bind(s) to this *cis*-acting nuclear zip-code element and thereby brings about its nuclear retention. In the subsequent section we would extend this investigation by evaluating if, binding of the trans-acting retention factor(s) prevents binding of this mRNA with the export factors and thereby inhibiting its nuclear export. Thus, in turn, we need to systemically investigate the regulation of that *trans*-acting factor(s) (if any) under nutrient rich and depleted conditions to answer the physiological expression pattern of *SKS1* mRNA. Moreover, if there is evidence of a *cis-trans* regulation being involved, then we need to verify if it is true for other members of the Nuclear Retained mRNAs.

5.2 The DEAD-box RNA helicase Dbp2p represents one of the top interactors that associates with 202 nt *SKS1-NZ* element immobilized to Streptotag affinity purification column:

To explain the putative mechanism of the nuclear retention of *SKS1* (and other NR mRNAs), we hypothesized that one or more *trans*-acting factor(s) must bind to this *cis*-acting export retarding *NZ* element, which somehow brings about the inefficient export and strong nuclear retention of *SKS1*. To validate this hypothesis, we next proceeded towards purifying the hypothetical *NZBP* by employing the Streptotag affinity purification technique. [163-164] For this assay, a Hybrid-RNA molecule having a streptomycin-binding aptamer, termed 'StreptoTag,' fused to the 202nt *NZ* element (Fig. 5.1A) was synthesised using *in-vitro* transcription (Fig. 5.1A-B).

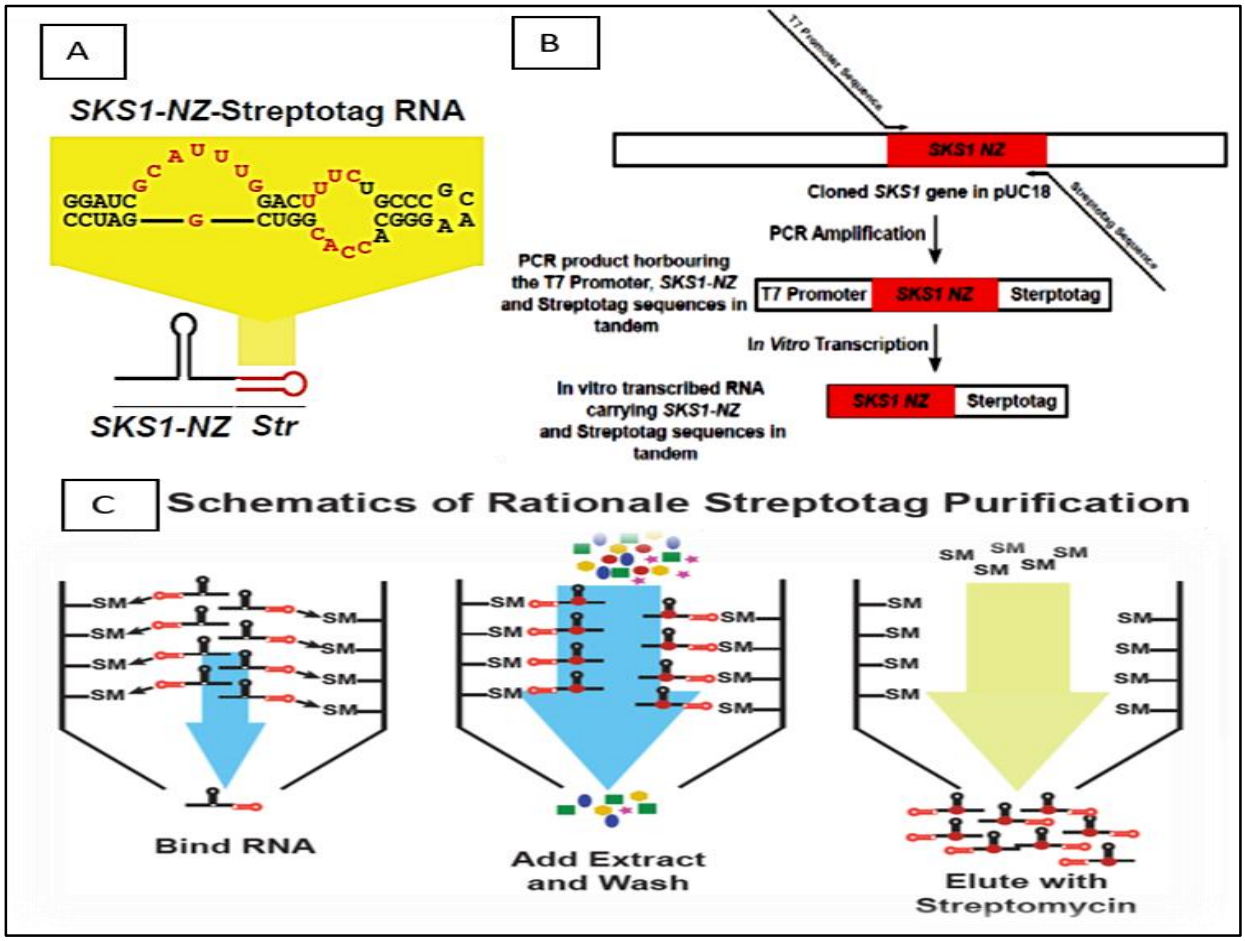

Fig. 5.1: Schematics of the in-vitro synthesis of SKS1-NZ-Str and rationale for Strepto-tag affinity purification assay. *A. Structures of the Streptotag aptamer fused to the 3'-end of the SKS1-NZ element (SKS1-NZ-Str). B. Schematic representation for in-vitro synthesis of SKS1-NZ-Str. The SKS1-NZ element is first PCR amplified with primers such that the forward primer has T7 promoter and the reverse primer has Strepto-tag aptamer bound to it. The amplified product is then used as template for in-vitro transcription of the SKS1-NZ-Str. C. Rationale of the Streptotag based affinity purification scheme showing the basis of purification of protein(s) binding to nuclear zip-code that involves immobilization of the SKS1-NZ-Str aptamer to the epoxy activated column followed by binding and elution of the protein(s) bound to SKS1-NZ-Str. For details of the procedure see materials and methods.*

The resulting hybrid RNA was then immobilized on a dihydro-streptomycin coated epoxy-activated Sepharose 6B matrix and allowed to interact with whole cell protein extract from wild type cells. After washing the column off its unbound proteins, finally the *NZ* element with its bound proteins were eluted out from the affinity matrix using streptomycin (affinity of the aptamer towards streptomycin is higher compared to dihydrostreptomycin) (Fig. 5.1C). Analysis of the eluate had two aspects (i) First was to confirm that the eluate from the Streptotag column contained the *NZ* element and (ii) second eluate also contain the bound proteins, which needs to be identified in the subsequent step.

We initially addressed if the eluate from the Streptotag affinity column contains the 202 nt *SKS1-NZ* element. Consequently, the eluate was subjected to cDNA preparation, followed by end-point PCR amplification using three sets of primer pairs corresponding to three different amplicons located at different positions, R1, R2, and R3 in the *SKS1* transcript body as indicated in Fig. 5.2A. During analysis of the products obtained from these PCR amplification reactions we obtained only amplicon R3 (corresponding to the *SKS1-NZ* element), but no PCR product corresponding to R1 and R2 was detectable under the same condition (Fig. 5.2B). All these amplicons, however, yielded PCR products of appropriate sizes when the cDNA sample prepared from the total RNA from the wild-type yeast strain was used as template that contains full-length *SKS1* cDNA (Fig. 5.2B, lowest panel). Furthermore, the PCR product obtained with amplicon R3 when subjected to sequencing reaction uncovered an identical sequence that perfectly matched the 202 nt *SKS1-NZ element* (data not shown). This was necessary to confirm the binding site because we did not initially analyse our PCR amplified template used for *in-vitro* transcription. All these data strongly demonstrated that the elution of the bound RNA aptamer from the Streptotag affinity column using streptomycin yielded the 202 nt *SKS1-NZ* element.

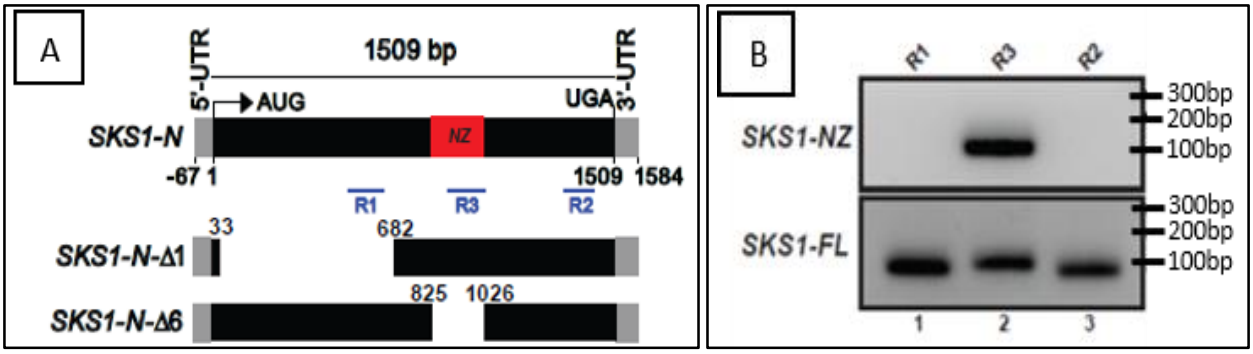

Fig. 5.2A-B: Analysis of the SKS1-NZ from Strepto-tag eluate. *(A) Schematic presentation of SKS1 mRNA (SKS1-N, N stands for the native full-length mRNA) and its two deletion constructs SKS1-N-Δ1 and SKS1-N-Δ6 used in this study. The ORF of full-length*

mRNA (1509 nt), translational start, stop site, the nuclear zip-code (NZ) and amplicons (R1, R2 and R3) are indicated. (B) Amplification profiles of the three amplicons R1, R2, and R3 using the cDNA template prepared from Streptotag-eluate (top panel) and the total cellular RNA from the same yeast strain (bottom panel).

To analyse the proteins, present in the eluate, an aliquot of the eluate was run on SDS-PAGE followed by silver staining of the gel, which revealed a consistent pattern of five bands (Fig. 5.3A). Candidate interactors of *SKS1-NZ* present in the eluate from the Streptotag column was further subjected to the LC-MS/MS analysis. Subsequent examination of the highly abundant peptide fragments led to the identification of several proteins of which Dbp2p was identified as one of the top interactors, which is a member of an ATP-dependent DEAD box RNA helicase. [(101)] To validate the proteomic data obtained from LC-MS/MS analysis further, an aliquot of the input sample prepared from yeast strain expressing Dbp2p-FLAG that was loaded to the Streptotag column and the eluate from the same column was further subjected to western blotting using the anti-FLAG, anti-Cbc1p and anti-α-tubulin antibodies respectively. Notably, the band corresponding to Dbp2p-FLAG appeared in both the input and the eluate samples from Streptotag column but the bands corresponding to α-tubulin and Cbc1p were detectable only in the input sample but not in the eluate sample (used as a negative control) (Fig. 5.3B).

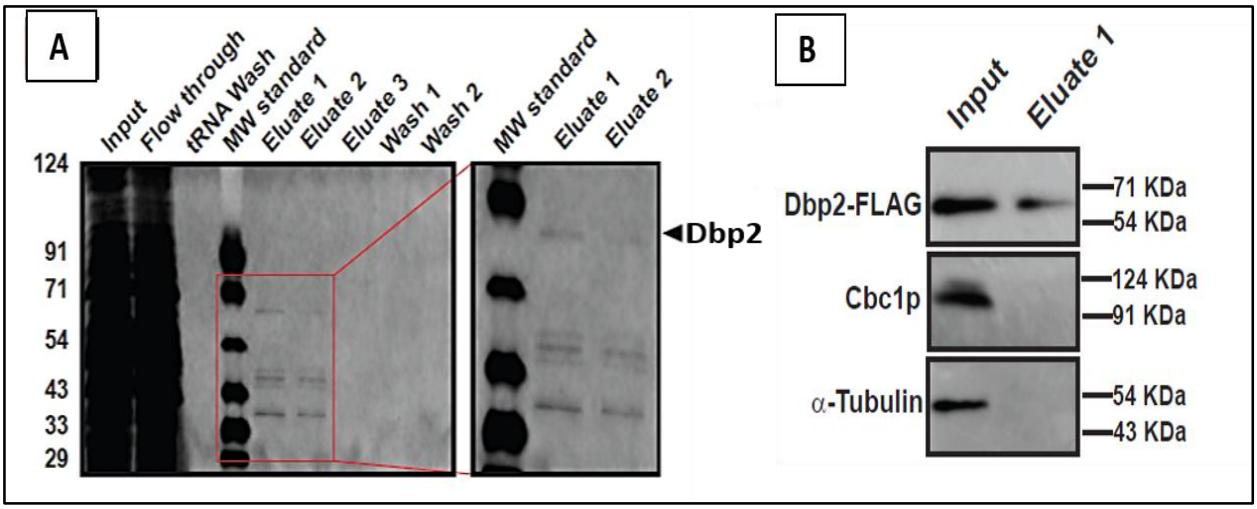

Fig. 5.3A-B: Identification of DEAD-box RNA helicase Dbp2p as a protein that binds to 202 nt SKS1-NZ element*. A. Electropherogram (silver stained SDS-PAGE) showing the input, eluate and wash fractions from a representative experiment involving the purification of proteins bound to the SKS1-NZ element. The protein extract was prepared from wild type yeast strain (yBD 5). The location of Dbp2p was shown in the magnified inset. B. Western blot analysis with the input to the Streptotag column and the eluate from the column using the antibody against FLAG. Cbc1p and α-Tubulin has been used as control which is present only in the input fraction and not eluate.*

Collective data, thereby, affirm that Dbp2p is an interactor that binds to the 202 nt *SKS1-NZ* element in vitro.

Notably, Dbp2p was previously implicated in various aspects of mRNA metabolism such as efficient termination of RNAP II dependent termination, [102] mRNA maturation and assembly, [104] regulation of glucose-dependent gene expression, [110] and RNA structural remodelling during transcription termination. [109] Furthermore, another recent independent investigation from our laboratory also identified Dbp2p as a novel component of CTEXT complex, [72] which prompted us to investigate if Dbp2p plays any crucial functional role in promoting the nuclear retention of the *SKS1* mRNA by binding to the 202 nt *NZ*-element.

5.3 Dbp2p binds to *SKS1* mRNA *in vivo* specifically at its *NZ* element:

Having shown that Dbp2p binds to the isolated *SKS1-NZ* element *in vitro*, we evaluated if Dbp2p binds to *SKS1* by binding to its *NZ* element *in vivo*. We performed RNA immunoprecipitation (RIP) (Fig. 3.1) with wild type strain expressing Dbp2p-FLAG and extracted total RNA bound to the immunoprecipitated proteins followed by qRT-PCR analysis of the sample with the primer sets defining the amplicons R3 and R2 relative to the *SKS1* ORF as indicated in Fig. 5.2A. To assess the specificity of the RIP procedure, we first quantified the *SKS1* R3 or R2 amplicon-specific qRT-PCR signal obtained from the wild-type yeast cells expressing either a FLAG-tagged Dbp2p, an untagged Dbp2p or HA-tagged Upf3p. As shown in left histograms of Fig. 5.4A, using both the *SKS1* specific R3 and R2 amplicons, the *SKS1*-RIP signals obtained from the yeast cells expressing Dbp2p-FLAG were the highest, whereas those obtained from the cells expressing unatagged-Dbp2p or HA-tagged Upf3p were significantly lower (Fig. 5.4A, left histograms). This data indicates that Dbp2p binds to the *SKS1* mRNA *in vivo* as well as affirms the specificity of RIP procedure in assessing the Dbp2p binding to *SKS1* mRNA transcript. This finding prompted us to resolve if Dbp2p associates itself with the *SKS1* mRNA *in vivo* and whether the Dbp2p binding site centers around the 202 nt *NZ*-element of this mRNA by employing RIP procedure. Subsequently, cell extracts from strains co-expressing Dbp2p-FLAG and any one of the full-length and two specific deletion constructs of *SKS1* mRNA [133] (deletions are indicated Fig. 5.2A) were independently subjected to RIP analysis (Fig. 5.4A). The RIP signals from either the native (*SKS1-N*) or artificially made mRNAs (*SKS1-N*-Δ1) harboring the 202 nt *SKS1-NZ* element are significantly higher than *SKS1-N*-Δ6 construct, which does not carry this element, thereby indicating that Dbp2p specifically binds to *SKS1* mRNA and most likely binds to its *NZ* element. To further

validate the notion that Dbp2p binds to any heterologous mRNA carrying *NZ* element, we performed the RIP assay to examine the binding profile of Dbp2p-FLAG with full-length *CYC1* and *CYC1-NZ* chimeric mRNAs (carrying the *SKS1-NZ* fused to *CYC1* mRNA) *in vivo* (Fig. 5.4C-D). qRT-PCR analysis using the *CYC1*-specific C1 amplicon (as indicated in Fig. 5.4C) revealed a similar binding profile of Dbp2p-FLAG (Fig. 5.4D).

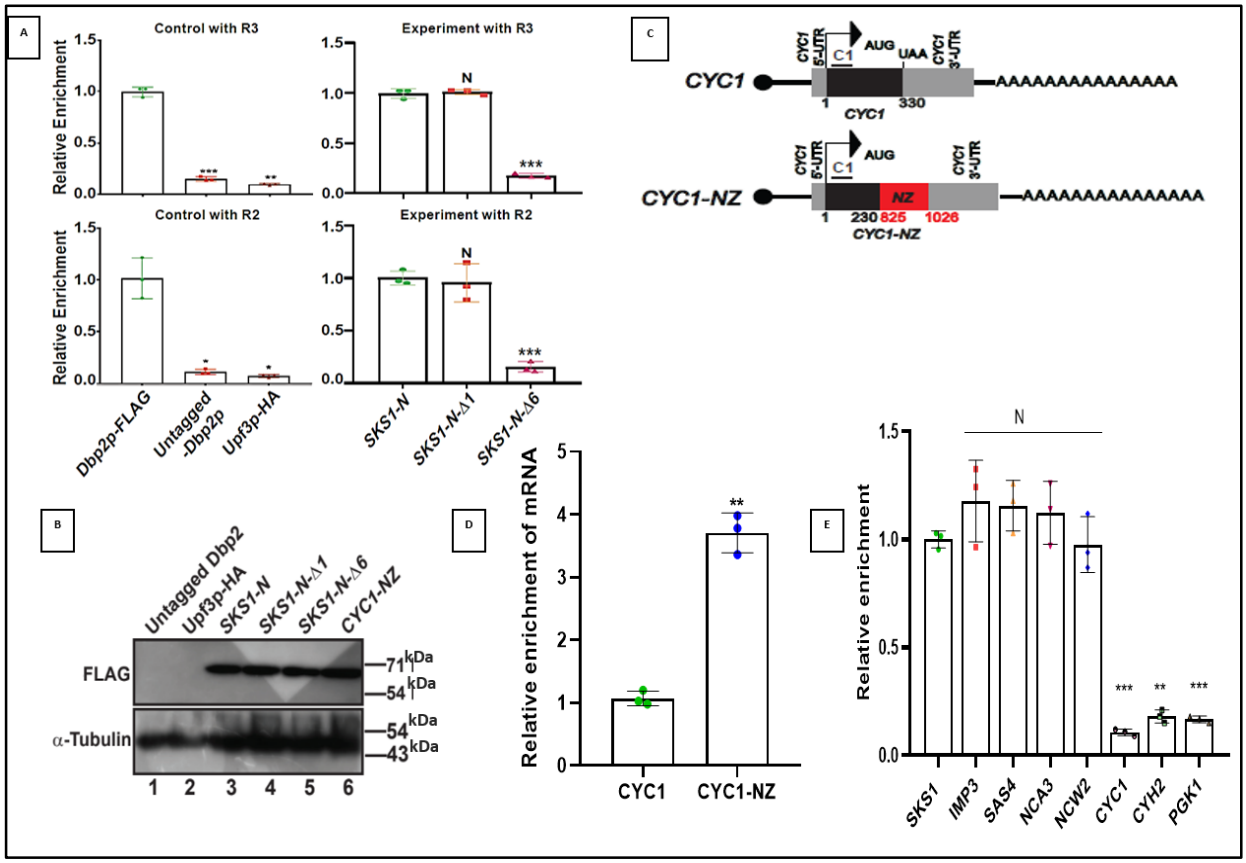

Fig. 5.4A-E: Analysing the interacting affinity and specificity of Dbp2p to NR messages. *A. Bar graphs depicting relative enrichment of the full length SKS1 mRNA (SKS1-N), its two deletion constructs (SKS1-N-Δ1 and SKS1-N- Δ6). The left histograms present the control experiments demonstrating the relative enrichment of the SKS1 mRNA bound with Dbp2-FLAG, untagged Dbp2p and Upf3p-HA using RIP assay. The right histograms show the relative enrichment of the SKS1 mRNA bound with Dbp2p-FLAG in a strain expressing either a native full-length SKS1 (SKS1-N) or its two deleted variants. The levels of enrichment of the SKS1 mRNA in yeast strains expressing Dbp2p-FLAG (in control) and SKS1-N allele (in experiment) are set to one. B. Western blot analysis showing the levels of Dbp2p-FLAG in the yeast strains expressing untagged Dbp2p, Upf3-HA, SKS1-N, SKS1-N- Δ1, SKS1-N- Δ6 and CYC1-NZ mRNAs. α-Tubulin has been used as loading control. C. Schematic presentation of the CYC1, and CYC1-NZ mRNA used in this study. The SKS1-NZ, CYC1 ORFs, and location of the amplicon C1 are indicated by red, black rectangles and black line respectively. D. Bar graphs from RIP analysis showing the relative enrichment of CYC1 and CYC1-NZ element upon binding with Dbp2p. E. Bar Graphs revealing relative enrichment of the five NR and three typical mRNAs bound to Dbp2p-FLAG determined by RIP assay. For the data presented in panels A, D and E, three independent cDNA preparations (biological replicates, n=3) from RIP assays prepared from respective yeast strains were used to determine the levels of these mRNAs. The statistical significance of difference reflected in the ranges of p-values estimated from Student's two-tailed t-tests for a given pair of test strains for each message are presented with following symbols, * <0.05, **<0.005 and ***<0.001, N= not significant.*

This data, suggests that Dbp2p binds to the *SKS1* and other heterologous mRNAs (such as *CYC1-NZ* chimeric mRNA) *in vivo*, which harbor the 202 nt *NZ* element either naturally (*SKS1*) or artificially (*CYC1-NZ*). To rule out the possibility that observed variation of RIP signals in various yeast strains in the experiments described in Fig. 5.4A is associated with the altered/lower expression/cellular levels of Dbp2p, we evaluated the levels of the FLAG-tagged Dbp2p protein using anti-FLAG antibody in all of these yeast strains. Note that while the tagged protein could not be detected in strains expressing no Dbp2-FLAG or expressing Upf3p-HA (Fig. 5.4B, top panel, lanes 1-2), the levels of the FLAG-tagged Dbp2p is very similar and comparable in yeast strains expressing Dbp2p and any one of the *SKS1-N*, *SKS1-N*- Δ1, *SKS1-N*- Δ6 and chimeric *CYC1-NZ* (Fig. 5.4B, top panel, lanes 3-6). The lower panel shows the levels of α-tubulin that were used as the internal loading control (Fig. 5.4B, bottom panel, lanes 1-6). Data from the experiments described in this section is therefore consistent with the argument that Dbp2p binds to *SKS1* mRNA *in vivo* and *in vitro* and the binding is specifically targeted to the 202 nt *NZ* element even if this element is artificially appended to any heterologous message (e.g. *CYC1*). However, it remains to be seen if the Dbp2p-binding to the *NZ* containing *SKS1* and other heterologous mRNAs are direct or it binds to these messages in presence of other proteins.

To explore further if Dbp2p binds the other NR mRNAs *in vivo*, we examined the association of Dbp2p-FLAG with four additional arbitrarily selected NR mRNAs, *IMP3, SAS4, NCA3* and *NCW2* using RIP assay. We analyzed the RIP signals from the yeast strain expressing Dbp2p-FLAG with anti-FLAG antibody using the primer sets corresponding to each of the message. As shown in Fig. 5.4E, the RIP signals obtained for the four other NR mRNAs, *IMP3*, *SAS4*, *NCA3*, *NCW2* were significantly high and were comparable to that obtained for the *SKS1* mRNA. In contrast, the RIP signals for the three typical mRNAs (those, which are exported rapidly and are not sensitive to the nuclear exosome/CTEXT) *CYH2*, *PGK1,* and *ACT1* were significantly lower than those obtained for the NR mRNAs (Fig. 5.4E). This data, thus, suggests that Dbp2p binds strongly to all the NR mRNAs *in vivo*, which suggests that these NR mRNAs may harbor *SKS1-NZ* like cis-acting export retarding element, which favors specific binding of Dbp2 protein to these messages. However, neither had we dissected of the putative *NZ* elements present in other messages experimentally nor we had addressed if association of Dbp2p to these NR-mRNAs is direct or require ancillary factors (see discussion).

5.4 Dbp2p plays a vital role to promote the characteristic nuclear localization/retention of the *SKS1* and other NR mRNAs:

Having shown that Dbp2p binds to the 202 nt "nuclear zip code" element of the *SKS1* (and several other NR mRNAs), we address whether Dbp2p binding is crucial for the characteristic nuclear localization and nuclear arrest of *SKS1* and other NR messages. This quest let us determine the intracellular localization and distribution of these representative NR mRNAs in a wild-type and its isogenic *dbp2-Δ* yeast strains. We speculate that if Dbp2p plays a crucial role in maintaining its intra-nuclear distribution of *SKS1* mRNA, the depletion of this protein would be expected to lead to the redistribution of these messages from the nuclear compartment into the cytoplasm. We substantiated this speculation by determining the intracellular distribution of *SKS1* mRNA in a wild-type and a *dbp2-Δ* yeast strains by using the GFP imaging technique as described previously. [100) (133) (161)]

As shown in Fig. 5.5A, the cytological distribution of *SKS1* mRNA was found to be largely nuclear in the wild-type yeast strain. In contrast, its cellular distribution is largely cytoplasmic in the *dbp2-Δ* strain thereby strongly suggesting that indeed Dbp2p plays a vital role in facilitating the characteristic nuclear retention of *SKS1* mRNA (Fig. 5.5A). We further evaluated the intracellular distribution of a few arbitrarily chosen NR mRNAs: *IMP3, SAS4, NCA3* and *NCW2* in WT and a *dbp2-Δ* strains to assess if Dbp2p plays a central role in promoting their nuclear retention. As shown in the same figure Fig. 5.5A, the *in-situ* localization of these mRNAs in WT and *dbp2-Δ* strains revealed that, indeed their distribution becomes largely cytoplasmic in a *dbp2-Δ* strain relative to a wild-type yeast strain. As a negative control, we also analyzed the in-situ distribution patterns of three arbitrarily selected typical messages *CYC1, CYH2* and *PGK1* which are expected to display a principally cytosolic distribution in both the strains since they are export efficient and Dbp2p is not expected to play any role in their rapid export and/or nuclear retention. As expected, analyses of their distribution pattern revealed that while a very minor fraction of these typical messages are nuclear, majority of these messages are principally cytoplasmic in both WT and *dbp2-Δ* strains thereby indicating that Dbp2p does not play any role in the cellular distribution of these typical messages (Fig. 5.5B).

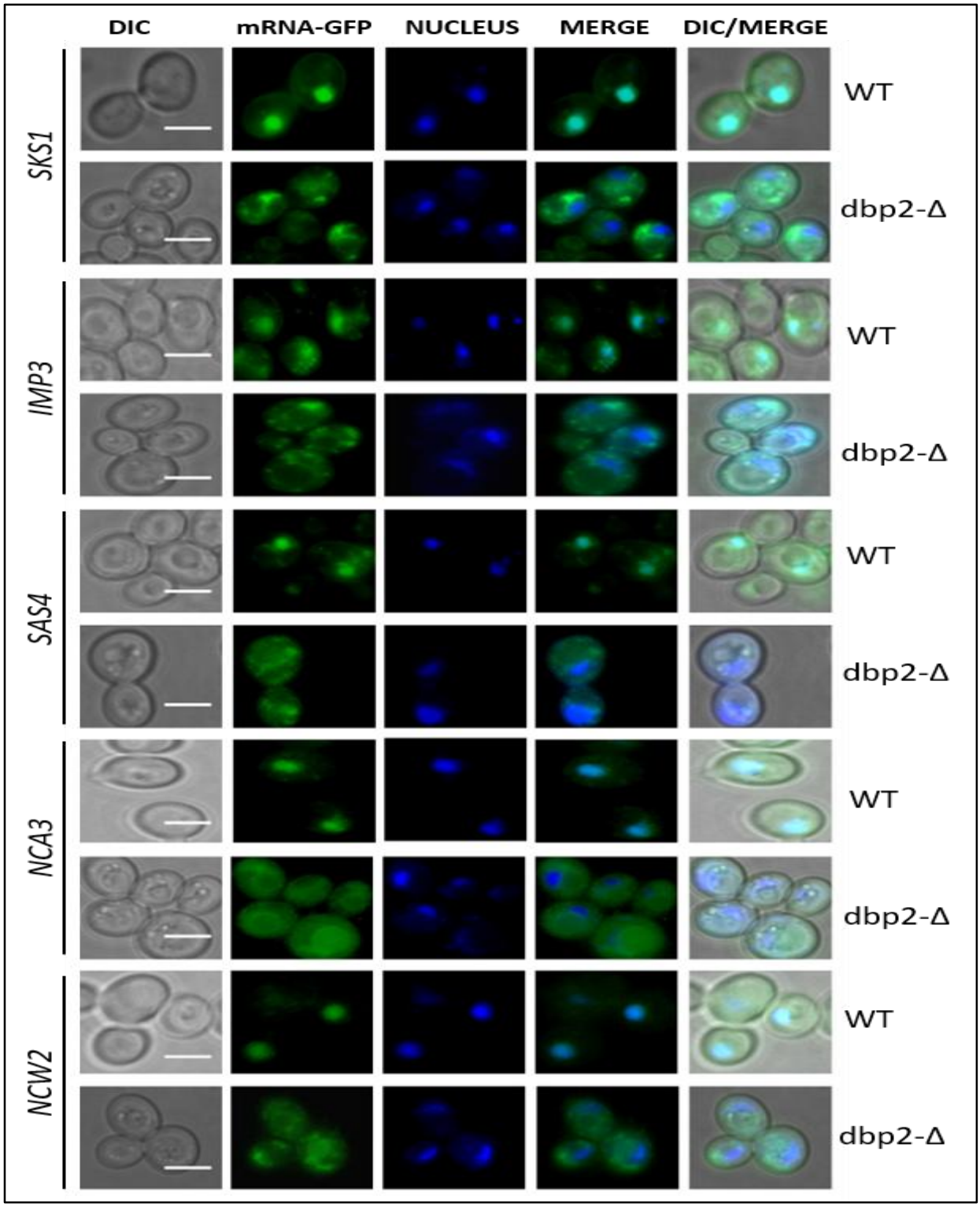

Fig.5.5A: Confocal microscopic image showing In situ localization of the five arbitrarily chosen NR mRNAs (SKS1, IMP3, SAS4, NCA3 and NCW2) bound to U1A-GFP in a wild type (DBP2+) and dbp2-Δstrains*: Yeast cells grown in YPD till O.D.$_{600}$ reached 0.5, the cells were resuspended in media having 2% Raffinose and grown till O.D.$_{600}$ = 0.8. Then 2% galactose induction was given for 1 hour followed by incubation in 2% glucose media for an hour before staining the nucleus with 5 µg/ml Hoechst for observation under confocal microscope (100X). The images revealed clear nuclear retention of the selected NR mRNAs in WT cells while in dbp2-Δ cells, the same mRNAs are distributed mostly in the cytoplasm. Scale= 4µm. The data denotes one representative experiment out of three biological replicates (n=3).*

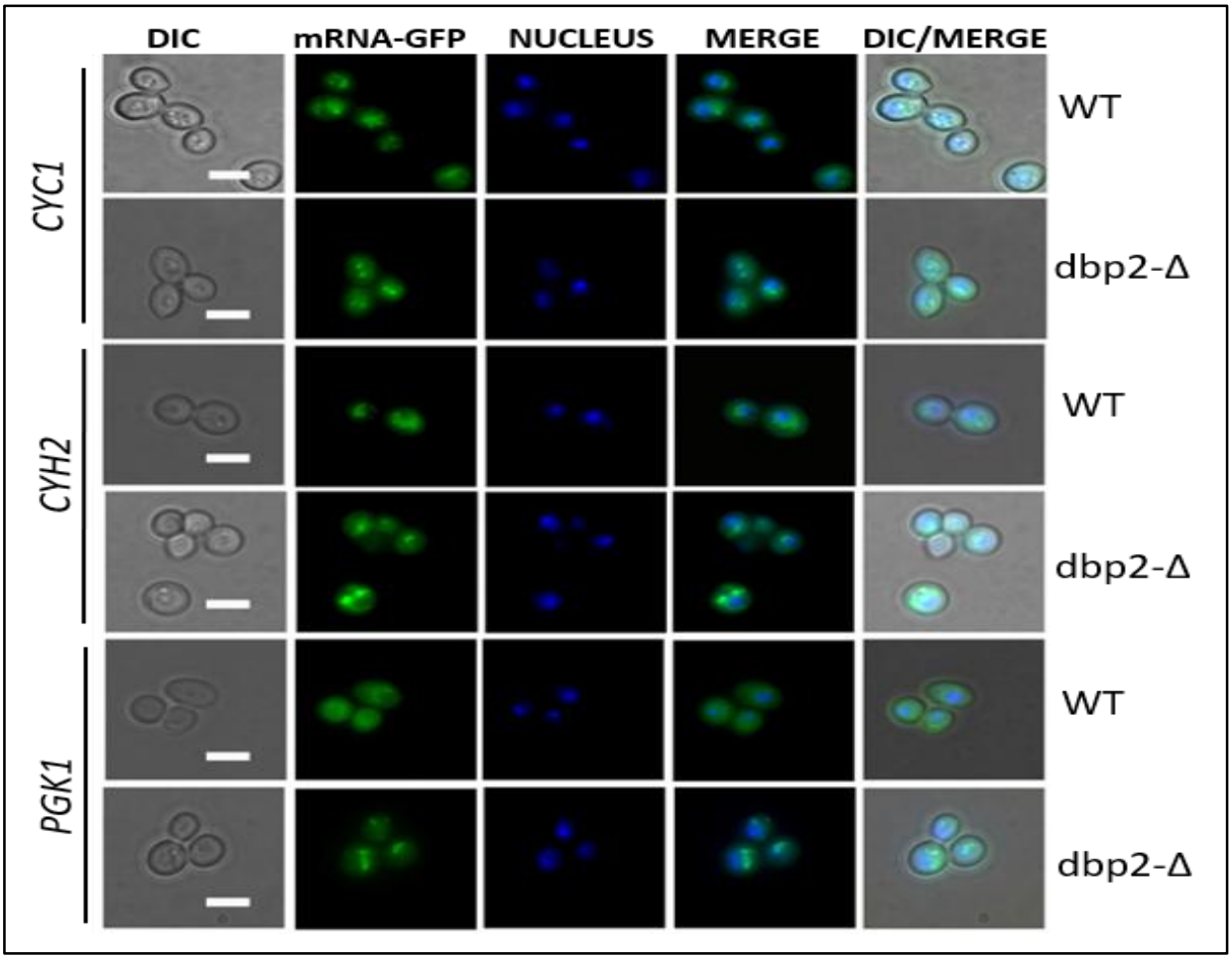

Fig.5.5B: Confocal microscopic image showing In situ localization of three typical messages (CYC1, CYH2 and PGK1) bound to U1A-GFP in a wild type (DBP2+) and dbp2-Δstrains*: Yeast cells grown in YPD till O.D.$_{600}$ reached 0.5, the cells were resuspended in media having 2% Raffinose and grown till O.D.$_{600}$ = 0.8. Then 2% galactose induction was given for 1 hour followed by incubation in 2% glucose media for an hour before staining the nucleus with 5 µg/ml Hoechst for observation under confocal microscope (100X). The images revealed clear cytoplasmic localization of the typical messages in both the yeast strains, thus indicating that Dbp2p has no role in the distribution of typical messages. Scale= 4µm. The data denotes one representative experiment out of three biological replicates (n=3).*

Taken together, thus, our finding supports the argument that the Dbp2p plays an instrumental role in the retardation of nuclear export and promotion of consequent nuclear localization of *SKS1* and other NR mRNAs.

To validate our observation further, we quantified both the Hoechst (indicator of localization of the nucleus) and GFP (indicator of the distribution of the *SKS1/PGK1* mRNA) signals and subsequently calculated the co-localization index (CI) (GFP signals that overlap with the Hoechst signals) as described in the materials and methods as a measure of nuclear-retained message. As shown in Fig. 5.5C and Table 5.1, the CI of the Hoechst and GFP signals from the three typical

messages *CYC1, CYH2* and *PGK1* in wild-type and *dbp2-Δ* strains are very similar, whereas, the CI of the five NR mRNAs, *SKS1, IMP3, SAS4, NCA3* and *NCW2* estimated in wild-type yeast strain are significantly higher relative to that estimated in *dbp2-Δ* strain. Notably, the CI values of all the NR mRNAs determined in the wild-type strain are significantly higher than the CI values of all of the typical messages in this strain. These data, thus, strongly indicate that *SKS1* and other NR mRNAs are strongly arrested in the nucleus in the wild-type yeast strain in a Dbp2p dependent manner under normal condition. However, it displays a primarily cytoplasmic distribution in a *dbp2-Δ* strain lacking this RNA helicase, thereby indicating that Dbp2p plays an important functional role in retarding export of NR mRNAs in general.

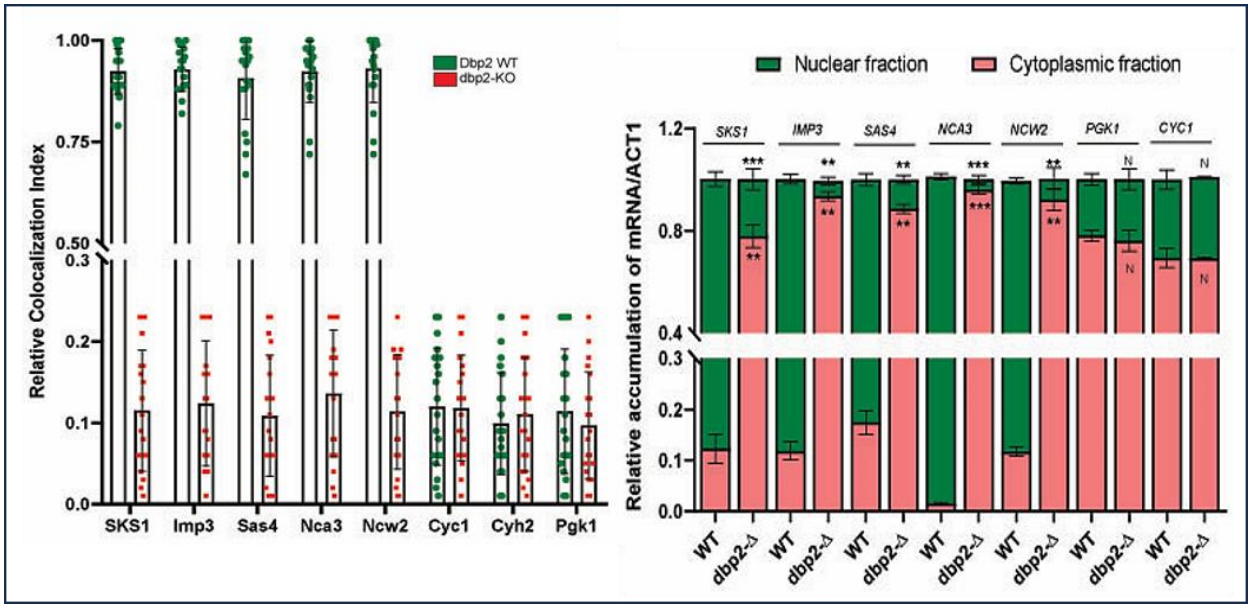

Fig.5.5C-D: Analysis of Co-localization Index and Biochemical analysis of nuclear and cytoplasmic fractions confirm the nuclear retention of NR messages in WT yeast cells. *C. Bar graphs depicting the co-localization (CI, expressed in arbitrary units) of the Hoechst (stains nucleus) and the GFP signals (mRNA) in the WT and dbp2-Δyeast strains for the five NR and three typical mRNAs. Means and standard error of the mean were determined from n=20 cells. CI (Pearson correlation coefficient, PCC) were determined as described in the method section. D. Stacked bar showing the nuclear and cytoplasmic distribution of five NR and two typical mRNAs in wild type (DBP2+) and dbp2-Δstrains determined by biochemical fractionation of the nuclear and cytoplasmic fractions of these yeast strains as described in materials and methods. The statistical significance of the difference in values reflected in the ranges of p-values estimated from Student's two-tailed t-tests for a given pair of test strains for each message are presented with following symbols, * <0.05, **<0.005 and ***<0.001, N= not significant.*

TABLE 5.1: Co-localization Index (CI) values of NR and typical messages in *DBP2*$^{+}$ and *dbp2*-Δ strains under normal nutrient-rich medium:

mRNA	WT (*DBP2*$^{+}$)		*dbp2*-Δ	
	CI Mean (+/- SEM)	N	CI Mean (+/- SEM)	N
SKS1	0.924 (+/-0.0123)	20	0.115(+/-0.0166)	20
IMP3	0.928947 (+/-0.0124)	20	0.1235(+/-0.0171)	20
SAS4	0.907(+/-0. 023)	20	0.1085(+/-0.0166)	20
NCA3	0.923(+/-0.017)	20	0.136(+/-0.0174)	20
NCW2	0.9305(+/-0.0188)	20	0.1135(+/-0.0157)	20
CYC1	0.12(+/-0.0161)	20	0.118(+/-0.0146)	20
CYH2	0.099(+/-0.014)	20	0.1105(+/-0.0157)	20
PGK1	0.114(+/-0.0171)	20	0.0965(+/-0.0147)	20

To establish Dbp2p-driven nuclear arrest of NR mRNAs on a sound foundation, we addressed this problem using biochemical approach. We precisely fractionated the nuclear and cytoplasmic fractions from the wild-type and *dbp2-Δ* yeast strains using biochemical procedure [160] and estimated the abundance of all of these NR and typical mRNAs in the nuclear and cytoplasmic fractions. Remarkably, in the wild-type yeast strain, the abundance of all of the tested NR mRNAs were found to be significantly higher in the nuclear fraction (84 to 98 percent relative to their total cellular abundance), which was reversed in the *dbp2-Δ* yeast strain (4 to 22 percent in nuclear fraction relative to their total cellular abundance) (Fig. 5.5D). The distribution of two typical mRNAs, in contrast, remained largely cytoplasmic (only 4 to 29 percent in nuclear fraction relative to their total cellular abundance) in both wild-type and *dbp2-Δ* yeast strains, which resembles the cellular distributions of the NR mRNAs in *dbp2-Δ* yeast strain (Fig. 5.5D). This finding thereby indicates that while typical/bulk-normal messages are efficiently exported from nucleus to cytoplasm in both the wild-type as well as *dbp2-Δ* yeast strains, all the arbitrarily selected NR mRNAs are extremely export-incompetent and preferentially retained in the nucleus in wild-type yeast strain under normal condition, which requires Dbp2p. Collective data from these sets of experiments are therefore consistent with the view that DEAD-box RNA helicase Dbp2p plays a crucial role in retaining these NR mRNAs in the nucleus under normal condition in a selective manner.

5.5 Dbp2p determines the cellular repertoire of the *SKS1* and several other NR mRNAs by promoting their nuclear retention and stimulating their nuclear decay:

Previous research from our laboratory speculates that Dbp2p triggers the nuclear degradation of the *SKS1* and other NR mRNAs by the nuclear exosome/CTEXT [(133)] by promoting their strong nuclear retention. Consequently, it is expected that this RNA helicase may determine the cellular repertoire of *SKS1* and other NR mRNAs. To validate this speculation, we determined the steady-state levels of these randomly selected NR messages in the WT and *dbp2-Δ* yeast strains by quantitative and end point PCR. As shown in Fig. 5.6, analyses of their steady-state levels revealed a significant up-regulation of *SKS1* (≈.5 fold), *IMP3* (≈ 2.1 folds), *SAS4* (≈ 4.2 folds), *NCA3* (≈ 5.5 folds), *NCW2* (≈ 2.4 folds) and *GRE1* (≈ 5.4 folds) mRNAs in dbp2-Δ strain relative to WT strain. These observations are consistent with the idea that Dbp2p by promoting the nuclear retention and exosome/CTEXT dependent nuclear decay of these NR mRNAs, destabilized all of these transcripts and thereby imposing significant impact on the expression levels of these NR messages.

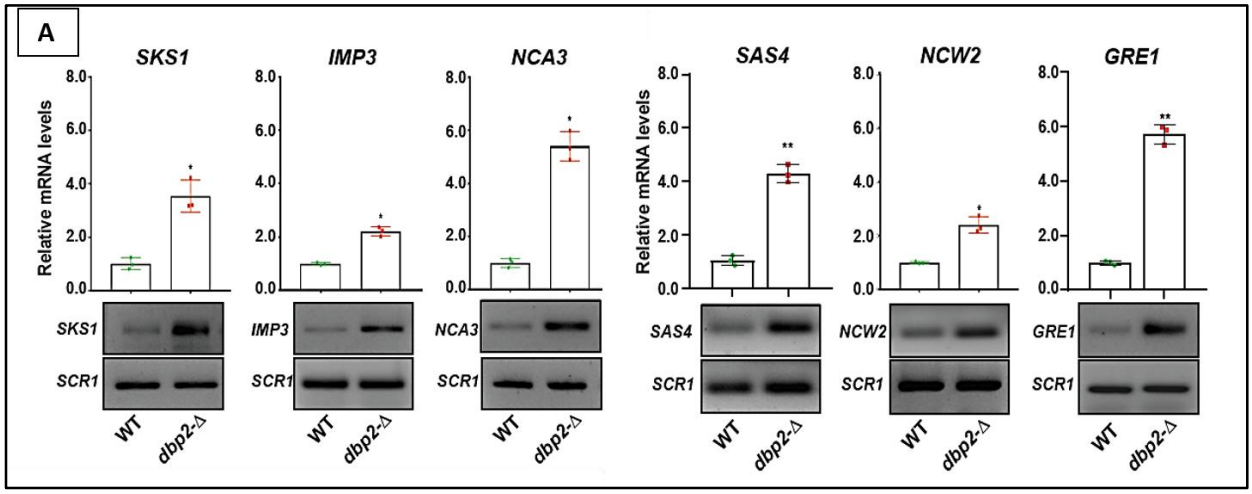

Fig.5.6: Dbp2p plays a crucial role in dictating the cellular repertoire of NR mRNAs in vivo. *Top panels show the bar graphs depicting the relative steady-state levels of six NR mRNAs in wild type (DBP2⁺) and dbp2-Δ yeast strains (biological replicates, n=3). Normalized values of each mRNA with respect to SCR1 signal in the wild type (DBP2⁺) strain was set to one. The statistical significance of the difference in values reflected in the ranges of p-values estimated from Student's two-tailed t-tests for a given pair of test strains for each message are presented with following symbols, * <0.05, **<0.005 and ***<0.001, N= not significant. The bottom panels show the levels of these mRNAs along with SCR1 RNA in wild type (DBP2⁺) and dbp2-Δ yeast strains determined by semi-quantitative RT-PCR followed by gel analysis of the PCR product.*

Next, we wanted to examine if these NR mRNAs, which were selected from the previous microarray datasets of transcripts upregulated in cbc1-Δ and rrp6-Δ mutant yeast strains [(100)]

were also upregulated in the transcriptome-wide analysis of steady-state levels of transcripts in RNA-seq datasets reported by Beck *et al*. (2014) (GEO accession: GSE58097). Consequently, we carried out a rigorous reanalysis of RNA-Seq datasets in WT and *dbp2-Δ* yeast strains. [110] Our analysis revealed that except for *SAS4* mRNA, all five of the six NR mRNAs, *SKS1, IMP3, NCA3, NCW2* and *GRE1* mRNAs displayed up-regulation by more than two-folds in dbp2-Δ strain (Log FC change cutoffs = +/- 1, p -value cutoff = 0.05, Fig. 5.7A). For some unknown reason, level of *SAS4* message was found by marginally downregulated in *dbp2-Δ* strain in the RNA-Seq dataset (Fig. 5.7C). Nevertheless, the result and findings from the collective sets of experiment described in Figs. 5.4 and 5.5, further reinforce the idea that Dbp2p not only binds to *SKS1* mRNA but also interacts with other NR messages thereby promoting their nuclear retention and exosome/CTEXT dependent mRNA degradation. Finally, we query if these NR mRNAs displaying upregulation in exosome deficient *rrp6-Δ* and the CTEXT deficient *cbc1-Δ* yeast strains [100] have any overlap with those mRNAs exhibiting enhancement in a *dbp2-Δ* yeast strain. Consequently, we analyzed further three previously published datasets reporting transcriptomic data in a cbc1-Δ strain [100], *rrp6-Δ* strain [166] (GEO Accession: GSE135056) and *dbp2-Δ* strain [110] (GEO accession: GSE58097) relative to wild-type yeast strain. A Venn diagram constructed by combining the mRNAs displaying upregulation in a *rrp6-Δ*, *cbc1-Δ* and *dbp2-Δ* yeast strains depicts that a total of 476, 615 and 705 transcripts were upregulated in *cbc1-Δ*, *rrp6-Δ* and *dbp2-Δ* strains respectively (Fig. 5.7B). Remarkably, a total of 37 mRNAs were found to be upregulated in all three sets, which consists of all of the previously designated transcripts as NR messages as exemplified by *SKS1, IMP3, NCA3, NCW2* and *GRE1* mRNAs except *SAS4* message. Strikingly, all of these messages were previously shown to be stabilized in both *cbc1-Δ* and *rrp6-Δ* strains. [100] Taken, together these findings indicate that the Dbp2p and the nuclear exosome/CTEXT plays a pivotal role in determining the cellular repertoire of these 37 NR messages.

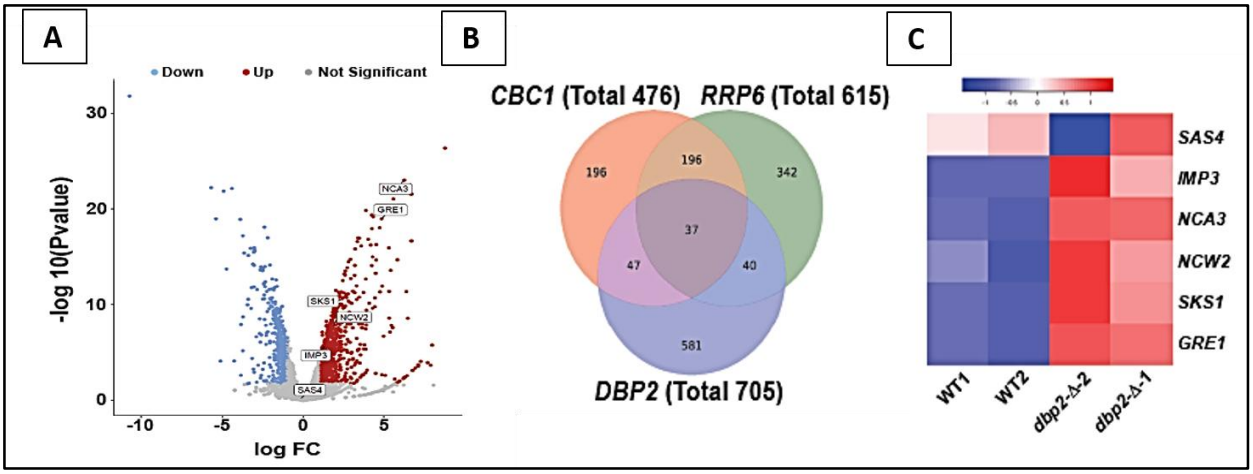

Fig. 5.7 (A-C): RNA-seq analysis further strengthens the role of Dbp2p in maintaining the cellular repertoire of the NR messages. *A. Volcano plot showing the normalized expression levels of transcriptome in dbp2-Δ strain relative to wild type strain revealed by the analysis of the previously done RNA-seq data submitted by Beck et al., (2014). Position of these NR mRNAs are indicated in the plot. The indices at the top indicate the upregulated, down regulated and unaltered transcripts in dbp2-Δ strain. B. Venn diagram showing the total number of transcripts upregulated in cbc1-Δ, rrp6-Δ and dbp2-Δ yeast strains and their overlaps. The datasets used to prepare the Venn diagram was taken from Kuai et al. (2005), and Beck et al., (2014). C. Heat Map showing the expression levels of five NR mRNAs in two independent replicates in wild type (DBP2+) and dbp2-Δ yeast strains.*

To demonstrate experimentally if the upregulation of these mRNAs is associated with their activation of the transcription rates of these respective genes or diminution of the nuclear decay rates of the corresponding messages, we determined both the transcription and decay rates of *SKS1* and other mRNAs in WT and *dbp2- Δ* yeast strains. In order to assess the transcription rate, we determined the occupancy of the elongating (hyper phosphorylated) RNA Polymerase II (RNAPII) in the genomic loci of these respective genes encoding these NR-mRNAs by Chromatin-IP (ChIP) analysis. It should be mentioned here that the occupancy of elongating (hyper phosphorylated) RNA Polymerase II (RNAPII) was previously used as an indicator of transcription rates of these genes [(136) (195)]. Their decay rate was estimated via transcription shut-off method respectively in wild-type and *dbp2-Δ* strains as described in materials and methods. Remarkably, a similar and comparable RNAPII occupancy profiles of these genes were obtained by using a monoclonal antibody against hyper-phosphorylated elongating RNAPII as shown in Fig. 5.8A, which clearly indicated that the transcription rates in the genomic loci of these genes in both of these yeast strains did not undergo any significant alteration (Fig. 5.8A). Thus, the observed up-regulation of the six NR mRNAs in *dbp2-Δ* strain relative to wild-type strain cannot be attributed to their enhanced transcription rate. Further, to demonstrate the enhanced steady-state level of *SKS1* mRNA can be correlated to the diminished decay rate in dbp2-Δ strain, the decay rates

of the these arbitrarily selected NR mRNAs in a wild-type and *dbp2-Δ* yeast strain were determined. As shown in the Fig. 5.9 (A-I), the decay rate of all of these NR messages became diminished in dbp2-Δ strain relative to wild type yeast strain with a concomitant increases their half-life values (Fig. 5.8B).

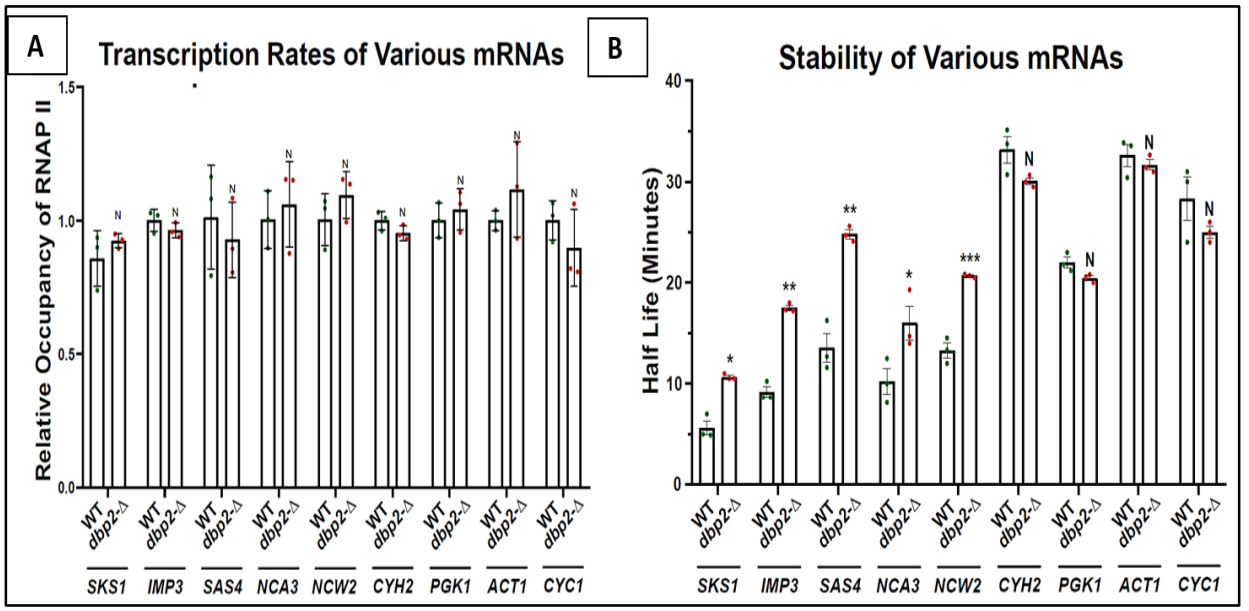

Fig. 5.8A-B: Dbp2p promotes the nuclear decay of the NR messages without altering their transcription rates. *A. Bar graphs showing the relative RNA Polymerase II occupancy at the genomic loci of the five NR and four typical mRNAs in a wild type (DBP2⁺) and dbp2-Δ strains determined by chromatin-immunoprecipitation (ChIP) analysis using the antibody against elongating RNA polymerase II. Mean ChIP signal is presented as means ± SE (n = 3 for each strain). B. Bar graphs depicting the half-life values of five NR and four typical mRNAs in a wild type (DBP2⁺) and dbp2-Δ strains at 30℃. The statistical significance of the difference in values reflected in the ranges of p-values estimated from Student's two-tailed t-tests for a given pair of test strains for each message are presented with following symbols, * <0.05, **<0.005 and ***<0.001, N= not significant.*

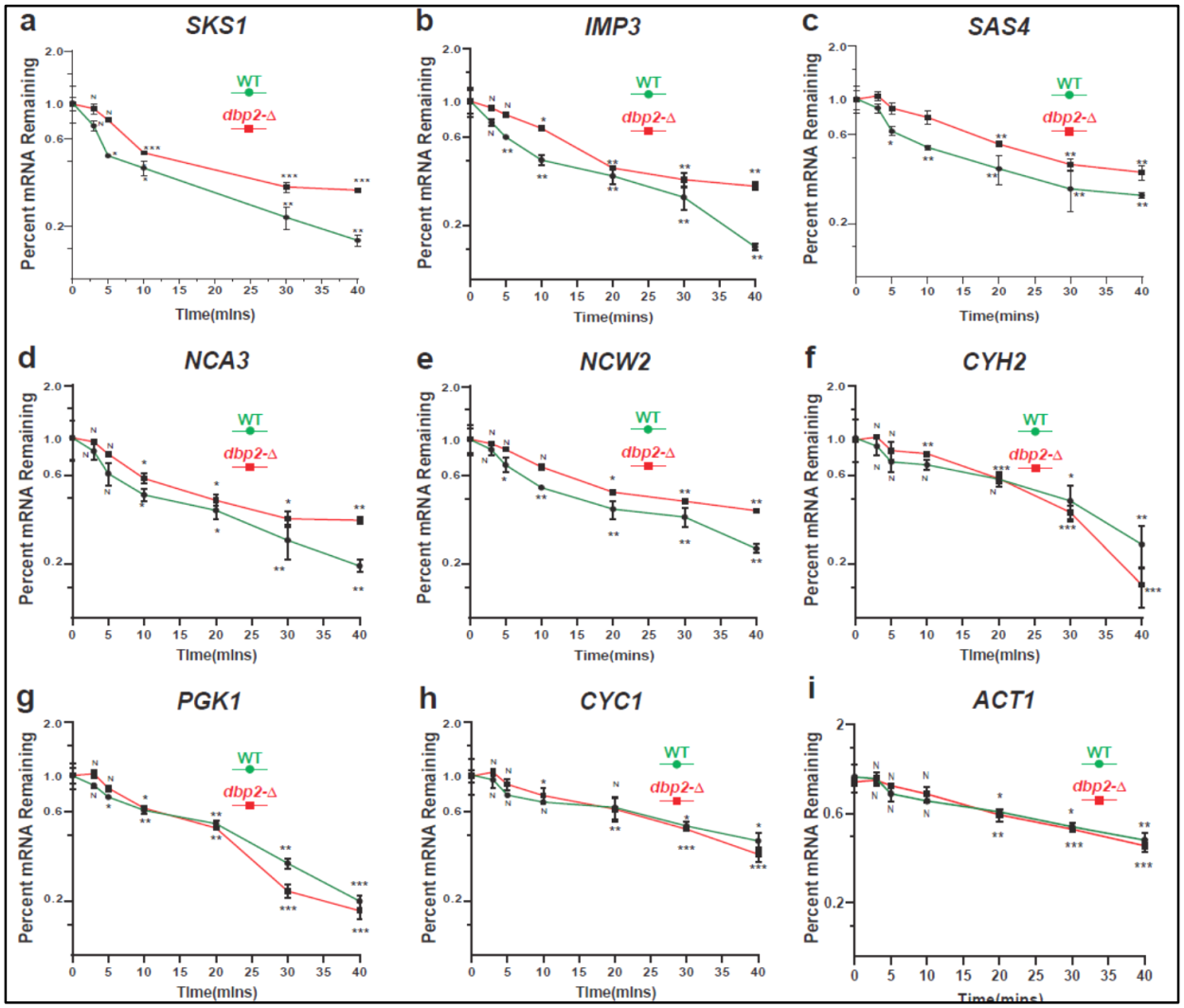

Fig.5.9A-I: Decay rates of the five NR mRNAs and four typical mRNAs, which were determined from WT and dbp2-Δ yeast. *Normalized (to SCR1 RNA) signals (mean values ± SD) were presented as the percent of remaining RNA (with respect to the normalized signal at 0 min) as a function of the time of incubation with transcription inhibitor 1, 10-phenanthroline as described in Materials and Methods. Three independent cDNA preparations (biological replicates, n=3) from RIPs prepared from respective yeast strains were used to determine the levels of these mRNAs. The statistical significance of difference as reflected in the ranges of p-values estimated from Student's two-tailed t-tests for a given pair of test strains for each message are presented with following symbols, * <0.05, **<0.005 and ***<0.001, ns, not significant.*

These data, taken together, supports the argument that Dbp2p by binding to the *SKS1-NZ in vivo* promotes its nuclear retention and thereby further induces their degradation that is dependent on the nuclear exosome/CTEXT. Depletion of Dbp2p leads to the release of these mRNAs from the nuclear retention and facilitate their rapid nuclear export and cytoplasmic distribution. From here onwards, we move towards understanding the mechanism of this Dbp2p mediated nuclear retention and how it can be related to the physiological distribution of *SKS1* mRNA.

Chapter 6

RESULTS (III)

6.1 Association of Dbp2p with the NR messages prevents the association of the export factors Mex67p and Yra1p to these messages:

Having shown that the association of Dbp2p with *SKS1* and other NR mRNAs leads to their preferential nuclear arrest and subsequent promotion of rapid nuclear mRNA decay, we went a step forward to inquire the mechanism of the preferential nuclear retention of these NR mRNAs. Previous research has demonstrated that the association of two major export factors/receptors, the non-importin export factor, Mex67p (TAP in humans) and REF family member, Yra1p with the maturing nuclear mRNPs is crucial for the successful export of the exporting mRNAs. [10] [22] [167-169] Consequently, we addressed if the NR mRNAs are associated with the export receptors, Mex67p and Yra1p under normal condition and if Dbp2p plays any inhibitory role in that association. Towards this quest, we first determined the relative binding/association of these two export receptors with these randomly selected NR mRNAs as well as with four typical mRNAs in wild-type yeast strain under normal condition using RNA immunoprecipitation (RIP) assay. As shown in Fig. 6.1A and C, the relative binding/association of both Mex67p and Yra1p to all the NR mRNAs is significantly lower (8 to 10 times lower) than the relative association of both of these factors with the all tested typical messages.

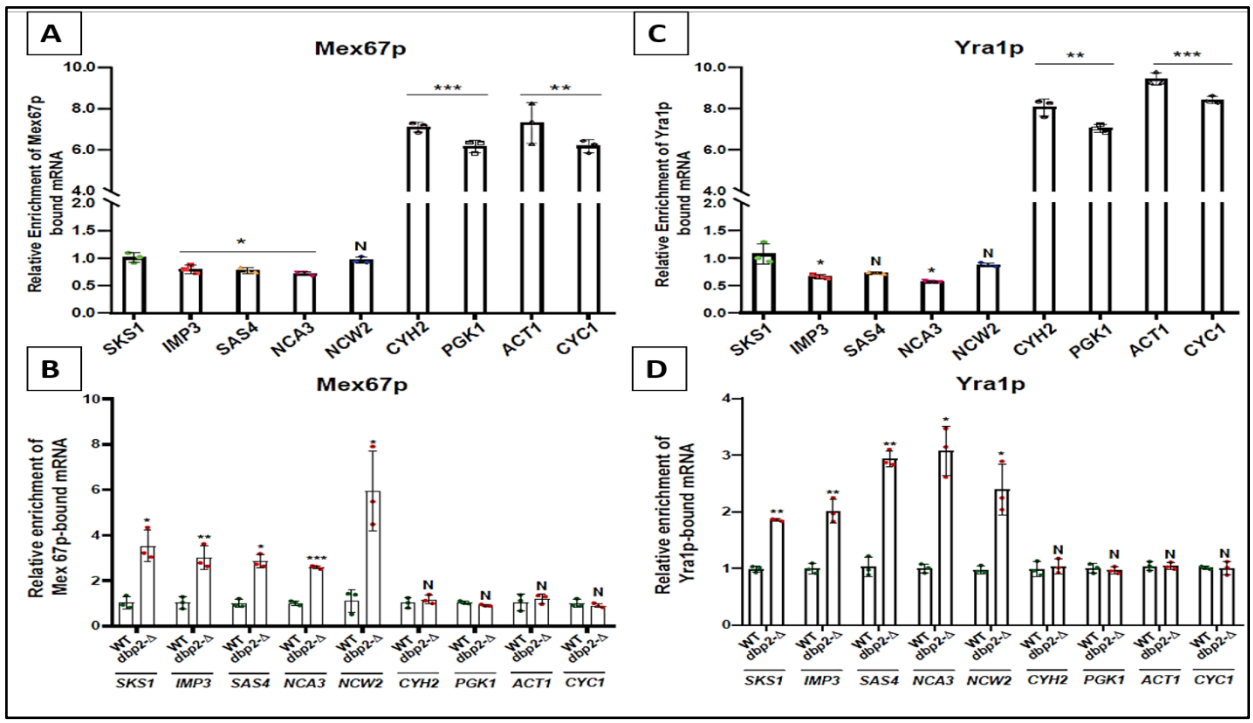

Fig.6.1: Dbp2p binding prevents association of export factors like Mex67p and Yra1p to NR mRNAs. *A) Bar graphs revealing relative association of the five NR and four typical mRNAs to Mex67p (left histograms, and C) Yra1p (right histograms, in WT yeast*

*strain. B) Bar graphs comparing the relative association of the five NR and four typical mRNAs bound to Mex67p (left histograms, and D) Yra1p (right histograms, in WT and dbp2-Δ yeast strain. Three independent cDNA preparations (biological replicates, n=3) from RIP assays prepared from respective yeast strains were used to determine the levels of these mRNAs as described in materials and methods. The statistical significance of difference as reflected in the ranges of p-values estimated from Student's two-tailed t-tests for a given pair of test strains for each message are presented with following symbols, * <0.05, **<0.005 and ***<0.001, N= not significant.*

This finding is consistent with the view that NR mRNAs do not associate with the canonical export factors Mex67p/Yra1p under normal condition. In the next step, we addressed if Dbp2p plays any functional role in the lack of association of the export factors Mex67p/Yra1p with the NR mRNAs and if preferential association of Dbp2p with the NR mRNAs (Fig. 5.4E) preclude the binding of the export factors. Consequently, we analyzed the relative association of the export factors Mex67p/Yra1p with the NR and typical mRNAs in wild-type and *dbp2*-Δ yeast strains lacking functional Dbp2p. As shown in Fig. 6.1B and D, the relative association of both Mex67p/Yra1p with the all five NR mRNAs become significantly higher in the *dbp2*-Δ yeast strain (average binding of Mex67p is ≈3-6 folds and average binding of Yra1p is ≈2-3folds in *dbp2*-Δ strain relative to their binding of NR messages in WT yeast strain) lacking functional Dbp2p. This finding strongly affirms that Dbp2p by preferentially binding to these NR mRNAs further prevent the binding of the export factors Mex67p/Yra1p thereby inhibiting their nuclear export. However, it remains to find out how Dbp2p binding inhibits the association of these export factor (see discussion).

6.2 Cytoplasmic shift of Dbp2p releases *SKS1* mRNA from its nuclear retention by allowing association of the export factors Mex67p and Yra1p under nutrient stress condition:

The above finding again raised questions about the regulation behind this nuclear to cytoplasmic shift of the *SKS1* mRNA with increase in glucose and nitrogen stress. Since the export mechanism of *SKS1* mRNA is being modified between nutrient rich and nutrient stressed conditions, we questioned whether there was any alteration in the binding efficiency of nuclear export factors like Mex67p and Yra1p. RNA-immunoprecipitation (RIP) assay revealed that the relative binding efficiency of both the export factors Mex67p and Yra1p with *SKS1* mRNA increases by 2-2.5 folds when nutrient stress increases in the media (Fig. 6.2 A-B). The binding efficiency of both the export factors starts increasing significantly from the same nutrient concentrations (below 0.25% glucose and 369 µM Ammonium sulphate) where steady state level of *SKS1* mRNA and protein

level Sks1p start increasing. This finding strongly suggests that the two studies co-relate well with each other and indicate towards a cause-and-effect relationship. This finding prompted us to investigate the protein level of Dbp2p under various concentrations of Glucose and Nitrogen sources in the growth media.

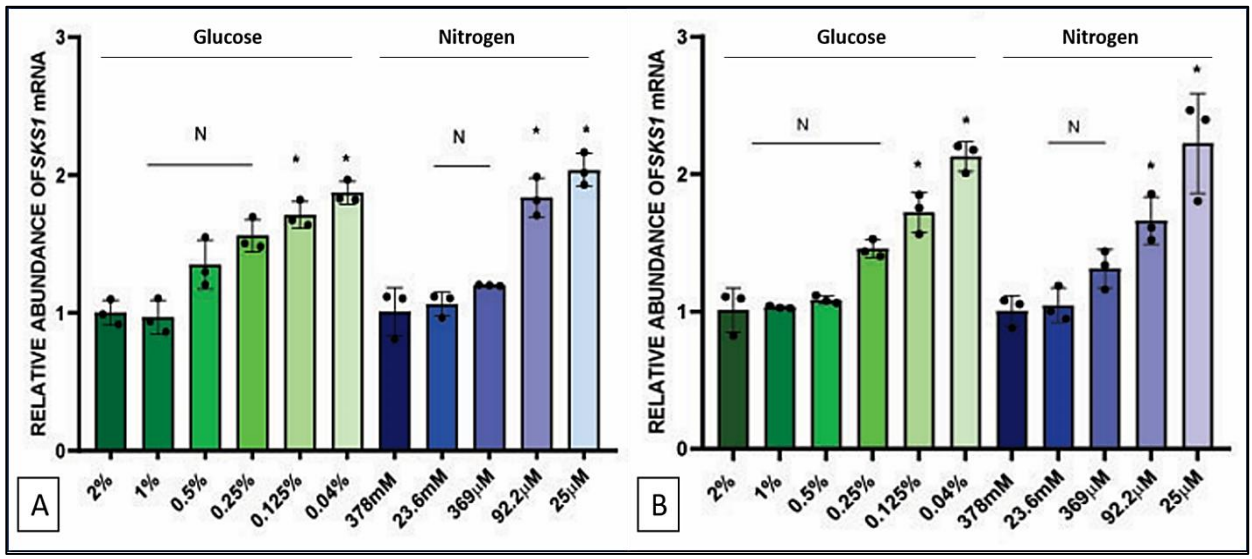

***Fig 6.2*: RNA-Immunoprecipitation assay to measure the binding efficiency of nuclear mRNA-export factors like (A) Mex67p and (B) Yra1p to SKS1 mRNA.** *Yeast strains carrying Mex67p-TAP and Yra1p-HA were grown till O.D.= 0.8 in media with defined concentrations of glucose and nitrogen as mentioned, then the cultures were subjected to UV (254nm) for Crosslinking the closely situated nucleic-acids and proteins. After isolating proteins from each culture, immuno-precipitation of Mex67p-TAP and Yra1p-HA was performed using respective antibodies followed by isolation of RNAs bound to these immuno-precipitated proteins. These RNAs were then converted to cDNA and used for qRT PCR analysis (with 2ng of each cDNA) to check the binding efficiency of the respective proteins with SKS1 mRNA. Histograms show that the with increasing nutrient stress, the binding efficiency of export factors (A) Mex67p-TAP and (B) Yra1p-HA increased up to 2-2.5 folds, thus facilitating the export of SKS1 mRNA from nucleus to cytoplasm under nutrient stress. The concentrations of glucose and nitrogen showing increase in binding efficiency of export factors to SKS1 mRNA co-related well with the concentrations where SKS1 mRNA and Sks1p levels start increasing. The statistical significance of difference as reflected in the ranges of p-values estimated from Student's two-tailed t-tests for a given pair of test strains for each message are presented with following symbols, * <0.05, ** <0.005 and *** <0.001, N= not significant.*

So far, we have uncovered a fascinating dynamic: the interaction between Dbp2p and nuclear retained RNA (NR) messages not only inhibits the binding of export factors but also results in their retention within the nucleus. Conversely, exposure to glucose and nitrogen stress appears to bolster the binding of export factors to *SKS1* mRNA, facilitating its movement to the cytoplasm. Our next aim is to elucidate the connection between these two intriguing phenomena. To delve deeper, we investigated the binding efficiency of Dbp2p with *SKS1* mRNA across varying nutrient concentrations in the growth media, employing a RIP assay. Our findings revealed a gradual decline in the association of Dbp2p with *SKS1* mRNA, dropping to approximately 35% under conditions of 0.04% glucose and 25 µM ammonium sulfate, in stark contrast to nutrient-rich

growth conditions (see Fig. 6.3A). This prompted us to propose an intriguing hypothesis: if nutrient stress destabilizes the association of Dbp2p with *SKS1* mRNA, it could indicate a decrease in cellular Dbp2p levels, ultimately releasing *SKS1* mRNA from its nuclear confines. However, our exploration took an unexpected turn when we assessed the protein levels of Dbp2p under various concentrations of glucose and nitrogen sources. To our surprise, the cellular concentrations of Dbp2p did not alter under these conditions and Dbp2p exhibited remarkable stability across all nutrient conditions (Fig. 6.3B). This revelation opens new avenues for understanding the nuanced roles of nutrient availability in post-transcriptional regulation.

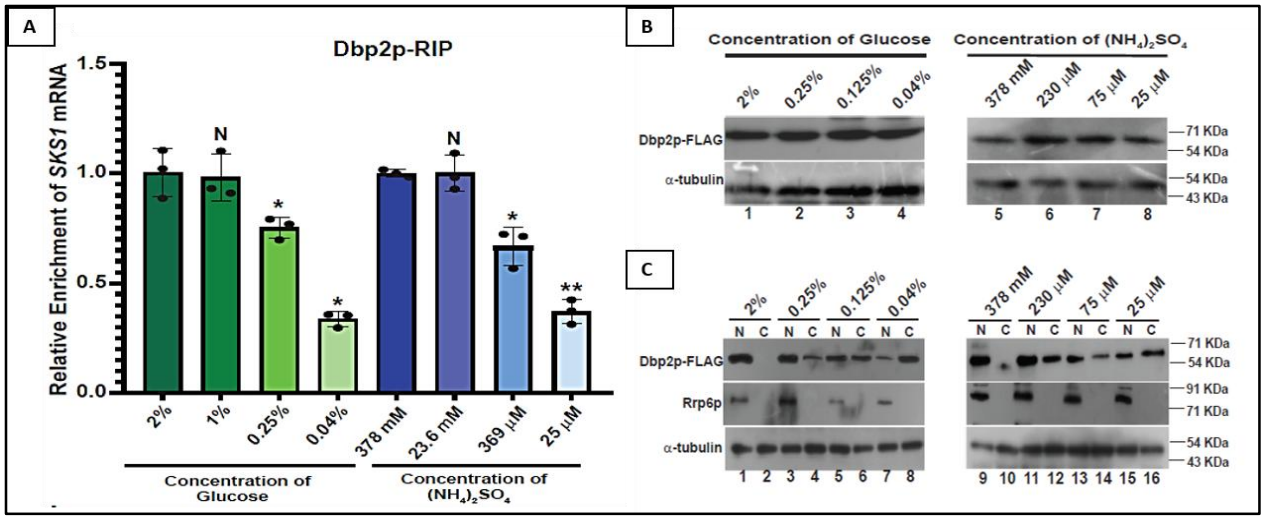

Fig 6.3: Dbp2p re-localizes from nucleus to cytoplasm under nutrient limiting growth conditions thereby allowing enhanced association of export factors Mex67p and Yra1p. *A. Bar Graphs revealing relative association of Dbp2p with SKS1 mRNA under indicated concentrations of glucose and ammonium sulphate, which was determined by RIP assay using the UV-crosslinked cell extracts from wild-type strains expressing Dbp2p-FLAG with the anti-FLAG antibody as described in materials and methods. B. Western Blot showing the relative abundance of total cellular Dbp2p protein in the wild-type yeast strain under indicated concentrations of glucose and ammonium sulphate in the growth medium. C. Western Blot showing the relative abundance of Dbp2p protein in the nuclear and cytoplasmic fractions in the cells grown under indicated concentrations of glucose and ammonium sulphate in the growth medium. After developing the Dbp2p signal, the blot was stripped and re-probed with Rrp6p, which was used as the nuclear marker. For both panels, B and C, α-tubulin was used as the loading control. The statistical significance of difference as reflected in the ranges of p-values estimated from Student's two-tailed t-tests for a given pair of test strains for each message are presented with following symbols, *<0.05, **<0.005 and ***<0.001, N= not significant.*

Next, we took a different approach and studied the protein level of Dbp2p separately in the nuclear and cytoplasmic fractions of yeast cells grown under defined concentrations of Glucose and Nitrogen sources. This analysis clearly pointed out that though the total protein level of Dbp2p is stable under all concentrations of Glucose and Nitrogen sources in growth media, but it gradually re-localizes from nucleus to cytoplasm with increasing nutrient limitations (Fig. 6.3C). Rrp6p has been used as a nuclear marker here while α-Tubulin was the loading control (note that for budding yeast, which exhibits closed mitosis, α-tubulin was reported to be both nuclear and

cytoplasmic). Hence, the cytoplasmic re-localization of Dbp2p loosens its association and allows the binding of export factors with *SKS1* mRNA resulting in the mRNA's nuclear export under nutrient limiting growth conditions.

Thus, we come to our model derived from the investigation done till now. Under nutrient rich conditions when Sks1p is not required by the yeast cell for survival, Dbp2p mostly localizes within the nucleus and binds to the 202 nt *cis*-acting element of *SKS1* mRNA. This association has an antagonizing effect on the binding of mRNA export factors like Mex67p and Yra1p by a mechanism, which needs further investigation. Poor association of export factors with *SKS1* mRNA results in nuclear arrest followed by degradation of the mRNA by the nuclear EXOSOME/CTEXT. But, under glucose and nitrogen limiting growth conditions when Sks1p is essential for survival of the yeast cells, Dbp2p re-localizes into cytoplasm and allows better binding of export factors to the *SKS1* mRNA. Hence, the mRNA escapes the nuclear degradation machinery and is readily exported out of the nucleus into the cytoplasm for translation. (Fig. 6.4A-B)

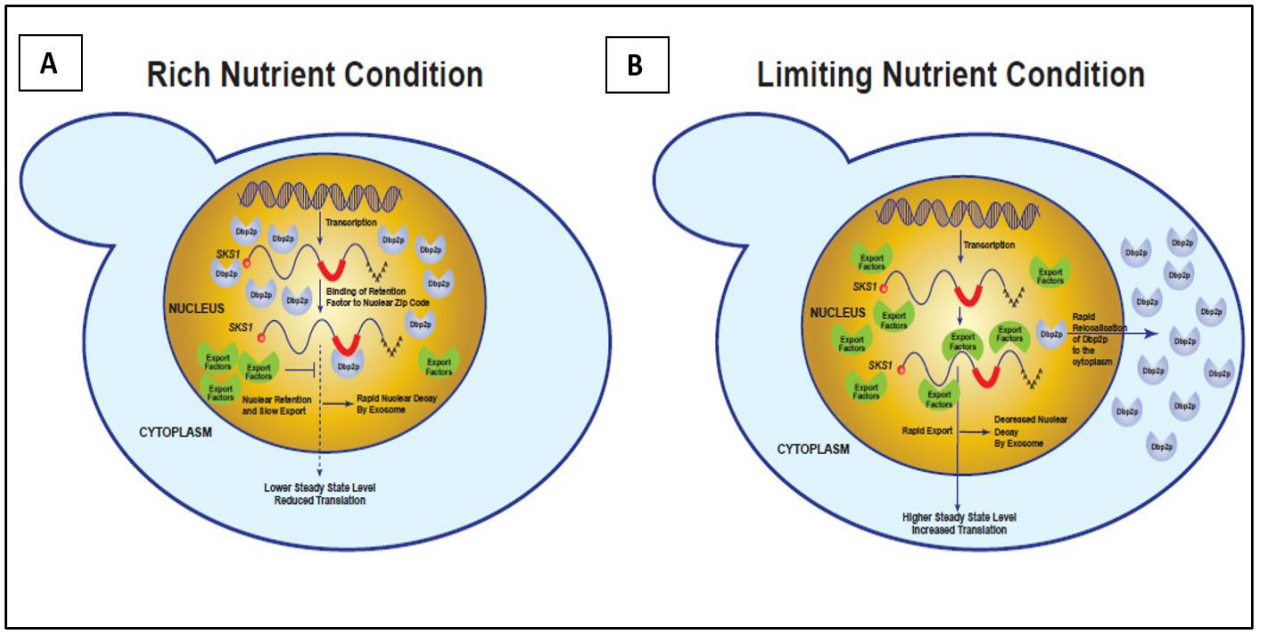

Fig 6.4: Model showing the reversible nuclear retention and export of SKS1 mRNA in response to limiting nutrient concentration. *A. When glucose and nitrogen supply is high, total cellular Dbp2p is principally localized to nucleus and selectively binds to SKS1 mRNA at its 202 nt NZ element (indicated by red box) and thereby antagonizing the binding of the export factors to SKS1 leading to its nuclear retention. Preferential nuclear retention of SKS1 in nutrient rich condition (when Sks1p function is not essential for the cell) in turn promotes its preferential decay by the nuclear exosome/CTEXT. B. Under nutrient limiting condition, Dbp2p itself re-localizes to cytoplasm leading to its physical absence in the nucleus. In the absence of Dbp2p in the nucleus, the export factors can readily bind to SKS1 and facilitates its rapid export and subsequent translation in the cytoplasm.*

Chapter 7

DISCUSSION

Maintaining a delicate equilibrium between energy production and regulated consumption is essential for all forms of life. Severe disruptions in this balance can lead to disastrous cellular events like cancer. Thus, metabolic processes play a critical role in both healthy cell growth and disease states. Adapting gene expression program to maintain energy homeostasis under low nutrient conditions is essential for cell survival under unfavorable conditions. Our findings reveal that the RNA helicase Dbp2p is crucial for regulating gene expression under nutrient-limiting conditions by facilitating the reversible nuclear retention and release of *SKS1* and potentially other mRNAs. Remarkably, *SKS1* encoding a serine/threonine protein kinase implicated in the adaptation of the yeast cells in the low glucose medium [155-157] belongs to the Nuclear Retained ("NR") category of mRNAs that are preferentially arrested in the nucleus. [100] [133] Owing to the existence of a kinetic competition between the processes of the nuclear export and exosome-mediated mRNA degradation, [74] the preferential nuclear arrest of *SKS1* subsequently leads to its rapid degradation dependent on the nuclear exosome/CTEXT. [133]

Our previous analysis demonstrated that a nuclear zip code (*NZ*) consisting of a 202 nt segment spanning from 825 to 1026 nt of the *SKS1* transcript body is responsible for its slow export and preferential nuclear retention/decay [133] thereby contributing to its distinctive cellular repertoire under normal condition. This finding, therefore, suggests that the 'nuclear arrest' of *SKS1* and similar NR messages is a key factor in their physiological regulation. [133] Notably, Sks1p is a vital kinase that participates in the adaptation of yeast cells under very low-glucose conditions. [155-157] In line with previous research, we found that the expression of *SKS1* mRNA increases progressively as the concentrations of glucose or nitrogen decrease. Importantly, this enhancement in steady-state levels of SKS1 mRNA is directly correlated with a reduction in its decay rate, which is influenced by the nuclear exosome/CTEXT (Figs. 4.6 and 4.7). Additionally, we confirmed that the lower decay rate of SKS1 mRNA is associated with its rapid export under conditions of glucose and nitrogen depletion (Figs. 4.8-4.12). This rapid export of SKS1 during nutrient-limited states allows it to outcompete the nuclear exosome/CTEXT in terms of degradation, preventing its decay in the nucleus and increasing its levels in the cytoplasm. To gain an insight into the mechanism of the nuclear retention of NR messages in general, we postulated that a hypothetical nuclear zip-code binding protein (*NZBP*) preferentially binds to their respective zip-code elements (*NZ*) and thereby promotes their nuclear arrest probably by antagonizing with the association of the export factors. Here, we have attempted to identify that

hypothetical universal nuclear zip-code element binding protein using *SKS1* as the model mRNA, since its nuclear zip code has already been delineated. [133] Using the 202 nt long nuclear Zip Code as the bait, we identified Dbp2p, a member of the DEAD-box RNA helicase as the universal zip code binding protein (*NZBP*) by employing the "Streptotag" affinity purification strategy (Figs. 5.1-5.4). Subsequent analysis demonstrated Dbp2p indeed binds to all arbitrarily selected NR mRNAs *in vivo* in a selective fashion thereby promoting their characteristic nuclear retention (Fig. 5.5) and intra-nuclear decay by the nuclear exosome/CTEXT (Figs. 5.8 and 5.9). Additional analyses revealed that selective association of Dbp2p with these messages leads to their decreased association of export factors Mex67p/Yra1p (Figs. 6.1) thereby preventing their nuclear export and facilitating their nuclear retention and subsequent nuclear decay. We established that under nutrient-deprived conditions, Dbp2p, the primary nuclear zipcode-binding protein, redistributes from the nucleus to the cytoplasm, thereby supporting our findings. This redistribution enhances the association of *SKS1* mRNA with the export factors Mex67p and Yra1p (Figs 6.2 and 6.3). The increased interaction of these export factors with SKS1 mRNA promotes its export and leads to heightened translation. This results in the production of a significant amount of Sks1p, which is crucial for cell survival and adaptation in environments with limited glucose and nitrogen (Fig. 6.4). Notably, it has been previously reported that Dbp2p rapidly shifts from the nucleus to the cytoplasm when yeast cells are exposed to decreasing concentrations of glucose.[110]

The study's data did not confirm whether Dbp2p exclusively binds to *SKS1* and nuclear retained mRNAs or as part of a larger protein complex, and it also leaves open the possibility that another unidentified recruiter may facilitate Dbp2p's binding to nuclear zip code element of NR mRNAs, necessitating further experiments to clarify the binding sequence.

It is speculated that representative mRNAs belonging to the thirty seven "NR" mRNAs, which were stabilized and exported efficiently to the cytoplasm in the *dbp2*-Δ null strain are indeed exported to cytoplasm under limiting glucose/nitrogen conditions, although we have not assessed it in our investigation. Notably, loss of glucose/nitrogen in the surrounding medium may suddenly create various kinds of circumstances involving secondary stress on many cellular pathways/organelles/parts that demands the involvement of diverse factors encoded by these NR mRNAs to mitigate such state. For example, Gre1p and Sip18p were implicated in maintaining osmotic balance during various stress responses. [170] Furthermore, Usv1p/Nsf1p, Atg32p were

implicated in the filamentous and invasive growth, mitophagy of damaged mitochondria during glucose limiting non-fermentative conditions, [171-172] Tip41p negatively regulates TORC1 signalling pathway[173] that occurs during nitrogen stress [174] and Spl1p and Hal1p was desmonstrated to upregulate during carbon and nitrogen stress respectively with poorly understood functional roles. [175-176] In this investigation, we meticulously examined the Dbp2p-dependent intranuclear localization of *SKS1* under nutrient-rich conditions, along with its carefully orchestrated release during the depletion of glucose and nitrogen in the growth medium. It is essential to underscore the pivotal role that Dbp2p plays as a central regulator of the gene expression program in the face of glucose and nitrogen stress, deftly controlling the expression of genes critical for survival during nutrient scarcity. Furthermore, nutrient depletion elicits a cascade of stress responses and various distressed metabolic states within the cell. This scenario demands an immediate and precise mobilization of specific proteins to navigate the challenges of a resource-limited environment. Consequently, a post-transcriptional strategy, rather than a transcriptional alteration strategy ,has emerged as a more effective means of meeting this urgent need for survival. This approach embraces dynamic and reversible processes—including nuclear retention, degradation, export of these proteins, and swift translation—ensuring that the cell can adeptly respond to the pressing survival demands posed by nutrient stress.

Notably, previous studies implicated Dbp2p in various aspects of mRNA surveillance and transcription termination. [102][105] Like other DEAD-box helicases, Dbp2p has a highly conserved helicase core that is involved in ATP binding, hydrolysis, and RNA binding and a DEAD box that is characterized by the repeating Asp-Glu-Ala-Asp (DEAD) motif. [177] These proteins also display an ATP-dependent RNA helicase activity [178], which is responsible for the unwinding of RNA duplex, [179-180] remodeling of RNPs [104] [181] as well as ATP-dependent fastening of multiprotein complexes. [182-183] Remarkably, our discovery of Dbp2p as an mRNA retention factor adds another new functional role of this protein to the list of its already existing activities in RNA metabolism. To our knowledge, this is the first report of a protein that serves as a nuclear mRNA retention/export-retarding factor. This conclusion was based on the following observations. First, the genetic inactivation of Dbp2p resulting in the loss of Dbp2p leads to the redistribution of *SKS1* mRNA from the nucleus to the cytoplasm (Fig. 5.5A). Moreover, an imposition of the nutrient deprivation condition, which causes the nucleus to cytoplasmic shuttling of Dbp2p with

its concomitant nuclear depletion also accompanied by the rapid nuclear export of *SKS1* mRNA (Figs. 4.11 and 6.3). As mentioned in the introduction, we have also identified Dbp2p as a novel component of CTEXT [72] that assists targeting and recruitment of export-defective nuclear mRNAs to the nuclear exosome. [70] Looking at the novel role of Dbp2p, that involves the nuclear arrest of the "NR" mRNAs in general, it won't be unreasonable to speculate that perhaps Dbp2p also perform a similar function of retaining the 3′-end defective messages with aberrantly long 3′-extension and export defective messages. [70]

Although several instances of nuclear retention of mammalian/viral mRNAs were reported [69] [184-191] their mechanism of nuclear retention is currently obscure except the *CTN-RNA*. *CTN-RNA* provides an example of a nucleus-retained (within the nuclear paraspeckles) transcript in the unstressed mouse liver cells with a unique retention mechanism that involves adenosine to inosine editing of the bases in its 3′-UTR. [185] However, the identity of any protein factor that facilitates the nuclear retention of these messages is still unknown to date. The Discovery of Dbp2p as the mRNA nuclear retention factor thus marks a significant finding from this investigation.

It should be underscored here that previous work from Tran laboratory showed that (i) overexpression of Dbp2p in export defective *mex67-5* yeast strain led to the accumulation poly(A)$^+$ RNA in the nucleus at the permissive temperature and (ii) Dbp2p facilitates the formation and export competent mRNP by physically associating with Yra1 [104]. Although these two observations appear to contradict our findings, a careful interpretation of our findings with previous findings does not controvert the earlier results. First, in the preceding study, the poly(A)$^+$ RNA accumulation within the nucleus was also documented even in a wild-type (*MEX67*$^+$) yeast strain upon over-expression of Dbp2p, albeit the extent of nuclear accumulation was much less relative to *mex67-5* strain [104]. Although this observation was explained as a secondary effect, we would like to interpret this finding in a different light. It should be emphasized here that Dbp2p binds to the "NR" mRNAs with very high affinity and the "Typical" or "Bulk-normal" message with lower affinity under physiological concentration (Fig. 5.4E). Therefore, while Dbp2p does bind weakly to all of the tested "typical" or bulk-normal mRNAs (Fig. 5.4E) belonging to the general poly(A)$^+$ mRNAome, it will not be unreasonable to speculate that Dbp2p may associate with them rather strongly at high concentrations when overexpressed. This increased Dbp2p-poly(A)$^+$ mRNAome association would prevent their association with

Mex67p/Yra1p thereby resulting in their weak nuclear accumulation even at the non-permissive temperature of 25°C. Therefore, the observation that overexpression of Dbp2p triggered the nuclear accumulation of poly(A)$^+$ RNA in the *mex67-5* yeast strain in fact supports the newly demonstrated role of Dbp2p – its ability to retain specific messages in the nucleus.

Second, in the same investigation, Dbp2p was demonstrated to promote export-competent mRNP formation in poly(A)$^+$ RNA fraction by stimulating association with Yra1p, Nab2p, and Mex67p thereby aiding in their nuclear export [(104)]. In this connection, it should be highlighted that the functional impact of Dbp2p in the context of any specific function of Dbp2p may not be universal for the total cellular mRNAome. For example, Dbp2p facilitates the transcription termination, promotes depositions of 3′-end processing factors, and aids in the maturation of only a subset of mRNAs. [(109)] Under this context, we would like to argue that while the observation by Ma et al. (2013) [(104)] that Dbp2p facilitating export-competent mRNP formation and their efficient export is only pertinent for general poly(A)$^+$ RNA fraction belonging to the "Typical" category, it is not relevant for the "NR" category of the mRNAs. We believe that Dbp2p imposes differential impacts on the "Typical" and the "NR" categories of mRNAs. As our findings suggest, Dbp2p binds weakly with the "Typical" mRNAs as exemplified by *CYC1*, *CYH2* and *PGK1* mRNA (Fig. 5.4E) and under the condition of the weak association of Dbp2p, these typical mRNAs can associate with the other export factors (Fig. 6.1) and become export-competent and exported efficiently under normal condition (Fig. 5.5B). In contrast, Dbp2p binds strongly with "NR" mRNAs as exemplified by *SKS1*, *IMP3*, *SAS4*, *NCA3* and *NCW2* and the association of Dbp2p to these NR mRNAs further prevents the binding of the export factors under normal growth condition thereby inhibiting their nuclear export and nuclear retention. It should also be noted here that, Dbp2p instead of binding alone, may bind to the "NR" messages in association with other uncharacterized zip code binding proteins, which were identified in our StreptoTag purification procedure (Fig. 5.3). Collective actions of these nuclear zip code binding proteins to "NR" mRNAs may have a different consequences with respect to the association of export factors, Mex67p/Yra1p to these subsets of mRNAs, which is antagonistic to the their nuclear export. Future experiments involving identification and functional characterization of these uncharacterized zip code binding factors will resolve this issue.

Typically glucose sensing in budding yeast is accomplished by several pathways including the Rtg1-Snf3 pathway, TOR pathway, and AMP-dependent protein kinase (Snf1) pathway. [(192-194)]

These signaling pathways communicate the status of the intracellular glucose concentration between the energy-generating and energy-consuming metabolic processes. While the Snf1 pathway promotes energy availability during nutrient-limiting situations, the TOR pathway favors the energy-demanding biogenesis events during nutrient-rich conditions. Our finding that Dbp2p rapidly redistributes to the cytoplasm upon imposition of glucose/nitrogen limiting condition is reminiscent of the earlier finding that glucose deprivation in the medium leads to rapid relocalization of Dbp2p from the nucleus to the cytoplasm. [(110)] Remarkably, these authors also showed that rapid nucleocytoplasmic relocalization of Dbp2p is independent of Snf1, Hog1, or TOR signaling pathways [(110)]. The intricate communication between cellular glucose and nitrogen levels and the nuclear protein Dbp2p remains a fascinating mystery. One compelling question that emerges from this research is the molecular mechanism driving Dbp2p's relocation from the nucleus to the cytoplasm during periods of glucose and nitrogen deprivation—an enigma we have yet to unravel. Remarkably, Dbp2p is adorned with numerous residues that could serve as potential sites for critical protein modifications, such as phosphorylation. These modifications may play an essential role in its dynamic movement between the nucleus and cytoplasm in response to the stresses of glucose and nitrogen scarcity. It is essential to explore whether the regulated phosphorylation of Dbp2p influences its ability to sense glucose and facilitate its swift transition from nucleus to cytoplasm—a process that lies at the very heart of the post-transcriptional regulation of glucose- and nitrogen-dependent expression of *SKS1.*

LIST OF PUBLICATIONS:

1. Anusha Chaudhuri, **Soumita Paul***, Mayukh Banerjea and Biswadip Das (2024). Polyadenylated versions of small non-coding RNAs in Saccharomyces cerevisiae are degraded by Rrp6p/Rrp47p independent of the core nuclear exosome. **Microbial Cell** 11: 155-186. doi: 10.15698/mic2024.05.823. (*Equal Contribution)

2. **Soumita Paul**, Subhadeep Das, Mayukh Banerjea, Shouvik Chaudhuri, Biswadip Das, The ATP-dependent DEAD-box RNA Helicase Dbp2 regulates the glucose/nitrogen stress response in baker's yeast by modulating reversible nuclear retention and decay of *SKS1* mRNA, **Genetics**, 2024;, iyae221, https://doi.org/10.1093/genetics/iyae221

3. Mayukh Banerjea, **Soumita Paul** and Biswadip Das, The nuclear mRNA surveillance system regulates telomere length by modulating levels of specific mRNAs encoding key telomere regulators in *Saccharomyces cerevisiae*., ***FEBS J***, 2025, (Under Revision)

REFERENCES:

1. Goffeau A, Barrell BG, Bussey H, et al.,1996 Life with 6000 genes. Science. 274:563–547.
2. Wood V, Rutherford KM, Ivens A, et al., 2001 A re-annotation of the *Saccharomyces cerevisiae* genome. *Comp Funct Genomics.* 2:143–154.
3. Parapouli M, *et. al*. *Saccharomyces cerevisiae* and its industrial applications. doi: 10.3934/microbiol.2020001.
4. Nandy S.K, Srivastava R.K, 2018 A review on sustainable yeast biotechnological processes and applications, Microbiological Research.
5. Bird G., N. Fong, J. C. Gatlin, S. Farabaugh, and D. L. Bentley, 2005 Ribozyme cleavage reveals connections between mRNA release from the site of transcription and pre-mRNA processing. Mol Cell. 20: 747–758. https://doi.org/S1097-2765(05)01769-7 10.1016/j.molcel.2005.11.009.
6. Luna R., H. Gaillard, C. Gonzalez-Aguilera, and A. Aguilera, 2008 Biogenesis of mRNPs: integrating different processes in the eukaryotic nucleus. Chromosoma. 117: 319–331. https://doi.org/10.1007/s00412-008-0158-4.
7. Perales R., and D. Bentley, 2009 “Cotranscriptionality”: the transcription elongation complex as a nexus for nuclear transactions. Mol Cell. 36: 178–191. https://doi.org/10.1016/j.molcel.2009.09.018S1097-2765(09)00676-5
8. Bjork P., and L. Wieslander, 2014 Mechanisms of mRNA export. Semin Cell Dev Biol. 32: 47–54. https://doi.org/10.1016/j.semcdb.2014.04.027S1084-9521(14)00098-6
9. Bentley D. L., 2015 The union of transcription and mRNA processing: 20 years of coupling. RNA. 21: 569–570. https://doi.org/10.1261/rna.050740.115.
10. Fasken MB, Corbett AH, 2016 Links between mRNA splicing, mRNA quality control, and intellectual disability. RNA Dis.3(4): e1448. Epub 2016 Nov 7. PMID: 27868086; PMCID: PMC5113822.
11. Wahle E.,1991 A novel poly(A)-binding protein acts as a specificity factor in the second phase of messenger RNA polyadenylation. Cell. 66: 759–68.
12. Kataoka N., J. Yong, V. N. Kim, F. Velazquez, R. A. Perkinson, et al., 2000 Pre-mRNA splicing imprints mRNA in the nucleus with a novel RNA-binding protein that persists in the cytoplasm. Mol. Cell. 6: 673–82.
13. Le Hir H, Gatfield D, Izaurralde E, Moore MJ, 2001 The exon-exon junction complex provides a binding platform for factors involved in mRNA export and nonsense-mediated mRNA decay. EMBO J.;20(17):4987-97. doi: 10.1093/emboj/20.17.4987. PMID: 11532962; PMCID: PMC125616.

14. Muller-McNicoll M., and K. M. Neugebauer, 2013 How cells get the message: dynamic assembly and function of mRNA-protein complexes. Nat Rev Genet. 14: 275–287. https://doi.org/10.1038/nrg3434nrg3434.

15. Gonatopoulos-Pournatzis T., and V. H. Cowling, 2014 Cap-binding complex (CBC). Biochem. J. 457: 231–42. https://doi.org/10.1042/BJ20131214

16. Singh G., G. Pratt, G. W. Yeo, and M. J. More, 2015 The Clothes Make the mRNA: Past and Present Trends in mRNP Fashion. Annu. Rev. Biochem. 84: 325–354. https://doi.org/10.1146/annurev-biochem-080111-092106.

17. Vinciguerra P., and F. Stutz, 2004 mRNA export: an assembly line from genes to nuclear pores. Curr Opin Cell Biol. 16: 285–292. https://doi.org/10.1016/j.ceb.2004.03.013S0955067404000511

18. Kohler A., and E. Hurt, 2007 Exporting RNA from the nucleus to the cytoplasm. Nat Rev Mol Cell Biol. 8: 761–773. https://doi.org/nrm2255 10.1038/nrm2255.

19. Perales R., and D. Bentley, 2009 "Cotranscriptionality": the transcription elongation complex as a nexus for nuclear transactions. Mol Cell. 36: 178–191. https://doi.org/10.1016/j.molcel.2009.09.018S1097-2765(09)00676-5

20. Proudfoot N. J., A. Furger, and M. J. Dye, 2002 Integrating mRNA processing with transcription. Cell. 108: 501–512. https://doi.org/S0092867402006177

21. Stutz F., and E. Izaurralde, 2003 The interplay of nuclear mRNP assembly, mRNA surveillance and export. Trends Cell Biol. 13: 319–327. https://doi.org/S0962892403001065.

22. Moore M. J., and N. J., 2009 Proudfoot, Pre-mRNA processing reaches back to transcription and ahead to translation. Cell. 136: 688–700. https://doi.org/10.1016/j.cell.2009.02.001S0092-8674(09)00133-0

23. Dimaano C., and K. S. Ullman, 2004 Nucleocytoplasmic transport: integrating mRNA production and turnover with export through the nuclear pore. Mol Cell Biol. 24: 3069–3076.

24. Tran E. J., and S. R. Wente, 2006 Dynamic nuclear pore complexes: life on the edge. Cell. 125: 1041–1053. https://doi.org/S0092-8674(06)00674-X 10.1016/j.cell.2006.05.027

25. Kohler A., and E. Hurt, 2007 Exporting RNA from the nucleus to the cytoplasm. Nat Rev Mol Cell Biol. 8: 761–773. https://doi.org/nrm2255 [pii]10.1038/nrm2255

26. Rodriguez-Navarro S., and E. Hurt, 2011 Linking gene regulation to mRNA production and export. Curr Opin Cell Biol. 23: 302–309. https://doi.org/10.1016/j.ceb.2010.12.002S0955-0674(10)00215-2

27. Schnell S. J., J. Ma, and W. Yang, 2014 Three-Dimensional Mapping of mRNA Export through the Nuclear Pore Complex. Genes (Basel). 5: 1032–49. https://doi.org/10.3390/genes5041032

28. Ishigaki Y, Li X, Serin G, Maquat LE, 2001 Evidence for a pioneer round of mRNA translation: mRNAs subject to nonsense-mediated decay in mammalian cells are bound by CBP80 and CBP20. Cell.; 106(5):607-617.

29. Gao Q, Das B, Sherman F, Maquat LE, 2005 Cap-binding protein 1-mediated and eukaryotic translation initiation factor 4E-mediated pioneer rounds of translation in yeast. Proc Natl Acad Sci U S A. 102(12): 4258-4263.
30. Maquat LE, Hwang J, Sato H, Tang Y.,2010 CBP80-promoted mRNP rearrangements during the pioneer round of translation, nonsense-mediated mRNA decay, and thereafter. Cold Spring Harb Symp Quant Biol. 75:127-134.
31. Nover L, Scharf KD, Neumann D, 1983 Formation of cytoplasmic heat shock granules in tomato cell cultures and leaves. Mol Cell Biol. 3(9): 1648-1655
32. Kedersha NL, Gupta M, Li W, Miller I, Anderson P., 1999 RNA binding proteins TIA-1 and TIAR link the phosphorylation of eIF-2 alpha to the assembly of mammalian stress granules. J Cell Biol. 147(7): 1431-1442.
33. Parker R., 2012 RNA degradation in Saccharomyces cerevisiae. Genetics. 191(3): 671-702.
34. Sheth U, Parker R.,2006 Targeting of aberrant mRNAs to cytoplasmic processing bodies. Cell. 125(6): 1095-1109.
35. Balagopal V, Parker R., 2009 Polysomes, P bodies and stress granules: states and fates of eukaryotic mRNAs. Curr Opin Cell Biol. 21(3): 403-408.
36. Beelman CA, Parker R, 1994 Differential effects of translational inhibition in cis and in trans on the decay of the unstable yeast MFA2 mRNA. J Biol Chem. 269(13): 9687-9692.
37. Beelman CA, Stevens A, Caponigro G, LaGrandeur TE, Hatfield L, Fortner DM, Parker R., 1996 An essential component of the decapping enzyme required for normal rates of mRNA turnover. Nature. 382(6592): 642-646.
38. Caponigro G, Parker R., 1996 Mechanisms and control of mRNA turnover in Saccharomyces cerevisiae. Microbiol Rev. 60(1): 233-249.
39. Wahle E, Winkler GS., 2013 RNA decay machines: deadenylation by the Ccr4-not and Pan2-Pan3 complexes. Biochim Biophys Acta. 1829(6-7): 561-570.
40. Chen CY, Shyu AB., 2011 Mechanisms of deadenylation dependent decay. Wiley Interdiscip Rev RNA. 2(2): 167-183.
41. Schwartz DC, Parker R., 2000 mRNA decapping in yeast requires dissociation of the cap binding protein, eukaryotic translation initiation factor 4E. Mol Cell Biol. 20(21): 7933-7942.
42. She M, Decker CJ, Sundra murthy K, Liu Y, Chen N, Parker R, Song H., 2004 Crystal structure of Dcp1p and its functional implications in mRNA decapping. Nat Struct Mol Biol. 11(3): 249-256.
43. She M, Decker CJ, Svergun DI, Round A, Chen N, Muhlrad D, Parker R, Song H., 2008 Structural basis of dcp2 recognition and activation by dcp1. Mol Cell. 29(3): 337-349.

44. Coller JM, Tucker M, Sheth U, Valencia-Sanchez MA, Parker R., 2001 The DEAD box helicase, Dhh1p, functions in mRNA decapping and interacts with both the decapping and deadenylase complexes. RNA. 7(12): 1717-1727.
45. Arribas-Layton M, Wu D, Lykke-Andersen J, Song H., 2013 Structural and functional control of the eukaryotic mRNA decapping machinery. Biochim Biophys Acta. 1829(6-7): 580-589.
46. Poole TL, Stevens A., 1995 Comparison of features of the RNase activity of 5'-exonuclease-1 and 5'-exonuclease-2 of Saccharomyces cerevisiae. Nucleic Acids Symp Ser. 33): 79-81.
47. Anderson JS, Parker RP., 1998 The 3' to 5' degradation of yeast mRNAs is a general mechanism for mRNA turnover that requires the SKI2 DEVH box protein and 3' to 5' exonucleases of the exosome complex. EMBO J. 17(5): 1497-1506.
48. Araki Y, Takahashi S, Kobayashi T, Kajiho H, Hoshino S, Katada T., 2001 Ski7p G protein interacts with the exosome and the Ski complex for 3'-to-5' mRNA decay in yeast. EMBO J. 20(17): 4684-4693.
49. Van Hoof A, Staples RR, Baker RE, Parker R., 2000 Function of the ski4p (Csl4p) and Ski7p proteins in 3'-to-5' degradation of mRNA. Mol Cell Biol. 20(21): 8230-8243.
50. Liu H, Rodgers ND, Jiao X, Kiledjian M., 2002 The scavenger mRNA decapping enzyme DcpS is a member of the HIT family of pyrophosphatases. EMBO. 21(17): 4699-4708.
51. Maniatis T., and R. Reed, 2002 An extensive network of coupling among gene expression machines. Nature. 416: 499–506. https://doi.org/10.1038/416499a416499a
52. Reed R., 2003 Coupling transcription, splicing and mRNA export. Curr Opin Cell Biol. 15: 326–331. https://doi.org/S0955067403000486.
53. Aguilera A., 2005 Co-transcriptional mRNP assembly: from the DNA to the nuclear pore. Curr Opin Cell Biol.; 17: 242–250. https://doi.org/S0955-0674(05)00041-4 10.1016/j.ceb.2005.03.001
54. Bentley D. L.,2005 Rules of engagement: co-transcriptional recruitment of pre-mRNA processing factors. Curr Opin Cell Biol. 17: 251–256. https://doi.org/S0955-0674(05)00048-7 10.1016/j.ceb.2005.04.006.
55. Bentley D. L.,2014 Coupling mRNA processing with transcription in time and space. Nat. Rev. Genet. 15: 163–175. https://doi.org/10.1038/nrg3662.
56. Reed R., and H. Cheng. TREX, 2005 SR proteins and export of mRNA. Curr Opin Cell Biol. 17: 269–273. https://doi.org/S0955-0674(05)00053-0 10.1016/j.ceb.2005.04.011.
57. Saguez C., J. R. Olesen, and T. H. Jensen,2005 Formation of export-competent mRNP: escaping nuclear destruction. Curr Opin Cell Biol. 17: 287–293. https://doi.org/S0955-0674(05)00051-7 10.1016/j.ceb.2005.04.009.
58. Lykke-Andersen S., R. Tomecki, T. H. Jensen, and A. Dziembowski, 2011 The eukaryotic RNA exosome: same scaffold but variable catalytic subunits. RNA Biol. 8: 61–66. https://doi.org/14237.

59. Tuck A. C., and D. Tollervey,2011 RNA in pieces. Trends Genet. 27: 422–432. https://doi.org/10.1016/j.tig.2011.06.001S0168-9525(11)00089-8.

60. Klauer A. A., and A. van Hoof,2012 Degradation of mRNAs that lack a stop codon: a decade of nonstop progress. Wiley Interdiscip Rev RNA. 3: 649–660. https://doi.org/10.1002/wrna.1124.

61. Chlebowski A., M. Lubas, T. H. Jensen, and A. Dziembowski,2013 RNA decay machines: the exosome. Biochim Biophys Acta. 1829: 552–560. https://doi.org/10.1016/j.bbagrm.2013.01.006S1874-9399(13)00016-3.

62. Das S., and B. Das, 2013 mRNA quality control pathways in Saccharomyces cerevisiae. J. Biosci. 38. https://doi.org/10.1007/s12038-013-9337-4.

63. Schmidt K., and J. S. Butler,2013 Nuclear RNA surveillance: role of TRAMP in controlling exosome specificity. Wiley Interdiscip Rev RNA. 4: 217–231. https://doi.org/10.1002/wrna.1155.

64. Schneider C., and D. Tollervey, 2013 Threading the barrel of the RNA exosome. Trends Biochem Sci. 38: 485–493. https://doi.org/10.1016/j.tibs.2013.06.013S0968-0004(13)00105-9.

65. Lykke-Andersen S., and T. H. Jensen, 2015 Nonsense-mediated mRNA decay: an intricate machinery that shapes transcriptomes. Nat Rev Mol Cell Biol. 16: 665–677. https://doi.org/10.1038/nrm4063nrm4063.

66. Schmid M., 2018 Controlling nuclear RNA levels.

67. Schmid M., and T. H. Jensen, 2008 Quality control of mRNP in the nucleus. Chromosoma. 117: 419–429. https://doi.org/10.1007/s00412-008-0166-4.

68. Schmid M., and T. H. Jensen, 2013 Transcription-associated quality control of mRNP. Biochim Biophys Acta. 1829: 158–168. https://doi.org/10.1016/j.bbagrm.2012.08.012S1874-9399(12)00155-1.

69. Kilchert C., S. Wittmann, and L. Vasiljeva, 2016 The regulation and functions of the nuclear RNA exosome complex. Nat Rev Mol Cell Biol. 17: 227–239. https://doi.org/10.1038/nrm.2015.15nrm.2015.15.

70. Maity A., A. Chaudhuri, and B. Das, 2016 DRN and TRAMP degrade specific and overlapping aberrant mRNAs formed at various stages of mRNP biogenesis in Saccharomyces cerevisiae. FEMS Yeast Res. 16. https://doi.org/10.1093/femsyr/fow088.

71. Singh P., A. Chaudhuri, M. Banerjea, N. Marathe, and B. Das,2021 Nrd1p identifies aberrant and natural exosomal target messages during the nuclear mRNA surveillance in Saccharomyces cerevisiae. Nucleic Acids Res. 49: 11512. https://doi.org/10.1093/NAR/GKAB930

72. Saha U., G. R, P. S., D. S. and D. B, 2024 RRM1 and PAB domains of translation initiation factor gamma, Tif4631p play crucial role in the nuclear degradation of export-defective mRNAs in Saccharomyces cerevisiae. FEBS J. 291: 897–926

73. Butler J. S., 2002 The yin and yang of the exosome. Trends Cell Biol. 12: 90–96. https://doi.org/S0962892401022255

74. Das B., J. S. Butler, and F. Sherman, 2003 Degradation of normal mRNA in the nucleus of Saccharomyces cerevisiae. Mol. Cell. Biol. 23. https://doi.org/10.1128/MCB.23.16.5502-5515.2003

75. Das B., S. Das, and F. Sherman, 2006 Mutant LYS2 mRNAs retained and degraded in the nucleus of Saccharomyces cerevisiae. Proc. Natl. Acad. Sci. U. S. A. 103. https://doi.org/10.1073/pnas.0604562103

76. Liu Q., J. C. Greimann, and C. D. Lima, 2006 Reconstitution, activities, and structure of the eukaryotic RNA exosome. Cell. 127: 1223–1237. https://doi.org/S0092-8674(06)01427-9 10.1016/j.cell.2006.10.037

77. Dziembowski A., E. Lorentzen, E. Conti, and B. Seraphin, 2007 A single subunit, Dis3, is essentially responsible for yeast exosome core activity. Nat Struct Mol Biol. 14: 15–22. https://doi.org/nsmb1184 10.1038/nsmb1184

78. Makino D. L., M. Baumgartner, and E. Conti, 2013 Crystal structure of an RNA-bound 11-subunit eukaryotic exosome complex. Nature. 495: 70–75. https://doi.org/10.1038/nature11870nature11870.

79. Schuch B., M. Feigenbutz, D. L. Makino, S. Falk, C. Basquin, et al., 2014 The exosome-binding factors Rrp6 and Rrp47 form a composite surface for recruiting the Mtr4 helicase. EMBO J. 33: 2829–2846. https://doi.org/10.15252/embj.201488757embj.201488757

80. Mitchell P, Petfalski E, Shevchenko A, Mann M, and Tollervey D., 1997 The exosome: A conserved eukaryotic RNA processing complex containing multiple 3'→5' exoribonucleases. Cell. 91(4): 457–466. doi: 10.1016/S0092-8674(00)80432-8.

81. Allmang C, Kufel J, Chanfreau G, Mitchell P, Petfalski E, and Tollervey D., 1999 Functions of the exosome in rRNA, snoRNA and snRNA synthesis. EMBO J. 18(19): 5399–5410. doi: 10.1093/emboj/18.19.5399.)

82. LaCava, J., Houseley, J., Saveanu, C., Petfalski, E., Thompson, E., Jacquier, A., & Tollervey, D., 2005 RNA degradation by the exosome is promoted by a nuclear polyadenylation complex. Cell. 121(5), 713–724. https://doi.org/S0092-8674(05)00442-3 10.1016/j.cell.2005.04.029

83. Schulz, D., Schwalb, B., Kiesel, A., Baejen, C., Torkler, P., Gagneur, J., Soeding, J., & Cramer, P., 2013 XTranscriptome surveillance by selective termination of noncoding RNA synthesis. Cell. 155(5), 1075. https://doi.org/10.1016/j.cell.2013.10.024

84. Gudipati, Rajani Kanth, Villa, T., Boulay, J., & Libri, D., 2008 Phosphorylation of the RNA polymerase II C-terminal domain dictates transcription termination choice. Nature Structural & Molecular Biology. 15(8), 786–794. https://doi.org/10.1038/nsmb.1460.

85. Porrua, O., Hobor, F., Boulay, J., Kubicek, K., D'Aubenton-Carafa, Y., Gudipati, R. K., Stefl, R., & Libri, D., 2012 In vivo SELEX reveals novel sequence and structural determinants of Nrd1-Nab3-Sen1-dependent

transcription termination. The EMBO Journal. (2012); 31(19), 3935–3948. https://doi.org/10.1038/emboj.2012.237.

86. San Paolo, S., Vanacova, S., Schenk, L., Scherrer, T., Blank, D., Keller, W., & Gerber, A. P., 2009 Distinct roles of non-canonical poly(A) polymerases in RNA metabolism. PLoS Genetics. 5(7), e1000555–e1000555. https://doi.org/10.1371/journal.pgen.1000555.

87. Tudek, A., Porrua, O., Kabzinski, T., Lidschreiber, M., Kubicek, K., Fortova, A., Lacroute, F., Vanacova, S., Cramer, P., Stefl, R., & Libri, D., 2009 Molecular basis for coordinating transcription termination with noncoding RNA degradation. Mol Cell. 55(3), 467–481. https://doi.org/10.1016/j.molcel.2014.05.031S1097-2765(14)00532-2

88. Vasiljeva, L., & Buratowski, S., 2006 Nrd1 interacts with the nuclear exosome for 3' processing of RNA polymerase II transcripts. Mol Cell. 21(2), 239–248. https://doi.org/S1097-2765(05)01816-2 10.1016/j.molcel.2005.11.028

89. Callahan, K P, & Butler, J. S., 2010 TRAMP complex enhances RNA degradation by the nuclear exosome component Rrp6. J Biol Chem. 285(6), 3540–3547. https://doi.org/10.1074/jbc.M109.058396M109.058396

90. Dez, C., Houseley, J., & Tollervey, D., 2006 Surveillance of nuclear-restricted pre-ribosomes within a subnucleolar region of Saccharomyces cerevisiae. The EMBO Journal. 25(7), 1534–1546. https://doi.org/10.1038/sj.emboj.7601035.

91. Houseley, J, & Tollervey, D., 2006 Yeast Trf5p is a nuclear poly(A) polymerase. EMBO Rep, 7(2), 205–211. https://doi.org/7400612 10.1038/sj.embor.7400612

92. Wyers, F., Rougemaille, M., Badis, G., Rousselle, J. C., Dufour, M. E., Boulay, J., Régnault, B., Devaux, F., Namane, A., Séraphin, B., Libri, D., & Jacquier, A., 2005 Cryptic Pol II transcripts are degraded by a nuclear quality control pathway involving a new poly(A) polymerase. Cell. 121(5), 725–737. https://doi.org/10.1016/j.cell.2005.04.030.

93. Egecioglu, D. E., Henras, A. K., & Chanfreau, G. F., 2006 Contributions of Trf4p- And Trf5p-dependent polyadenylation to the processing and degradative functions of the yeast nuclear exosome. RNA. 12(1), 26–32. https://doi.org/10.1261/rna.2207206.

94. Kadaba, S., Krueger, A., Trice, T., Krecic, A. M., Hinnebusch, A. G., & Anderson, J., 2004 Nuclear surveillance and degradation of hypomodified initiator tRNA Met in S. cerevisiae. Genes and Development. 18(11), 1227–1240. https://doi.org/10.1101/gad.1183804.

95. Vanacova, S., Wolf, J., Martin, G., Blank, D., Dettwiler, S., Friedlein, A., Langen, H., Keith, G., & Keller, W., 2005 A new yeast poly(A) polymerase complex involved in RNA quality control. PLoS Biol. 3(6), e189. https://doi.org/05-PLBI-RA-0095R2 10.1371/journal.pbio.0030189.

96. Wang, X., Jia, H., Jankowsky, E., & Anderson, J. T., 2008 Degradation of hypomodified tRNA(iMet) in vivo involves RNA-dependent ATPase activity of the DExH helicase Mtr4p. RNA (New York, N.Y.). 14(1), 107–116. https://doi.org/10.1261/rna.808608.

97. Roth, K. M., Byam, J., Fang, F., & Butler, J. S.,2009 Regulation of NAB2 mRNA 3'-end formation requires the core exosome and the Trf4p component of the TRAMP complex. RNA (New York, N.Y.). 15(6), 1045–1058. https://doi.org/10.1261/rna.709609.

98. Das, B., Guo, Z., Russo, P., Chartrand, P., & Sherman, F.,2000 The role of nuclear cap binding protein Cbc1p of yeast in mRNA termination and degradation. Molecular and Cellular Biology. 20(8). https://doi.org/10.1128/MCB.20.8.2827-2838.2000.

99. Das, S., Saha, U., & Das, B., 2014 Cbc2p, Upf3p and eIF4G are components of the DRN (Degradation of mRNA in the Nucleus) in Saccharomyces cerevisiae. FEMS Yeast Research. 14(6). https://doi.org/10.1111/1567-1364.12180

100. Kuai, L., Das, B., & Sherman, F., 2005 A nuclear degradation pathway controls the abundance of normal mRNAs in Saccharomyces cerevisiae. Proceedings of the National Academy of Sciences of the United States of America. 102(39). https://doi.org/10.1073/pnas.0506518102

101. Xing Z., W. K. Ma, and E. J. Tran, 2019 The DDX5/Dbp2 subfamily of DEAD-box RNA helicases. WIREs RNA. 10. https://doi.org/10.1002/wrna.1519.

102. Cloutier S. C., W. K. Ma, L. T. Nguyen, and E. J. Tran, 2012 The DEAD-box RNA helicase Dbp2 connects RNA quality control with repression of aberrant transcription. J. Biol. Chem. 287: 26155–26166. https://doi.org/10.1074/jbc.M112.383075

103. Xing Z., S. Wang, and E. J. Tran, 2017 Characterization of the mammalian DEAD-box protein DDX5 reveals functional conservation with S. cerevisiae ortholog Dbp2 in transcriptional control and glucose metabolism. RNA. 23: 1125–1138. https://doi.org/10.1261/rna.060335.116

104. Ma W. K., S. C. Cloutier, and E. J. Tran, 2013 The DEAD-box protein Dbp2 functions with the RNA-binding protein Yra1 to promote mRNP assembly. J. Mol. Biol. 425: 3824–3838. https://doi.org/10.1016/j.jmb.2013.05.016

105. Bond A. T., D. A. Mangus, F. He, and A. Jacobson, 2001 Absence of Dbp2p Alters Both Nonsense-Mediated mRNA Decay and rRNA Processing. Mol. Cell. Biol. 21: 7366–7379. https://doi.org/10.1128/mcb.21.21.7366-7379.2001.

106. Nissan T. A. B. J. P. E. T. D. & H. E., 2002 60S pre-ribosome formation viewed from assembly in the nucleolus until export to the cytoplasm. EMBO J. 21: 5539–5547.

107. Tedeschi F. A., S. C. Cloutier, E. J. Tran, and E. Jankowsky, 2018 The DEAD-box protein Dbp2p is linked to noncoding RNAs, the helicase Sen1p, and R-loops. RNA. 24: 1693–1705. https://doi.org/10.1261/rna.067249.118.

108. Ma W. K., B. P. Paudel, Z. Xing, I. G. Sabath, D. Rueda, et al., 2016 Recruitment, Duplex Unwinding and Protein-Mediated Inhibition of the Dead-Box RNA Helicase Dbp2 at Actively Transcribed Chromatin. J. Mol. Biol. 428: 1091–1106. https://doi.org/10.1016/j.jmb.2016.02.005

109. Lai Y.-H., K. Choudhary, S. C. Cloutier, Z. Xing, S. Aviran, et al., 2019 Genome-Wide Discovery of DEAD-Box RNA Helicase Targets Reveals RNA Structural Remodeling in Transcription Termination. Genetics. 212: 153–174. https://doi.org/10.1534/genetics.119.302058.

110. Beck Z. T., S. C. Cloutier, M. J. Schipma, C. J. Petell, W. K. Ma, et al., 2014 Regulation of glucose-dependent gene expression by the RNA helicase Dbp2 in Saccharomyces cerevisiae. Genetics. 198: 1001–1014. https://doi.org/10.1534/genetics.114.170019.

111. Micheline Fromont-Racine, Cosmin Saveanu, 2014 mRNA Degradation and Decay. Fungal RNA biology, Springer, pp.159-193, 978-3-319-05686-9 (Print) 978-3-319-05687-6 (Online). 10.1007/978-3-319-05687-6_7.http://link.springer.com/chapter/10.1007/978-3-319-05687-6_7. pasteur-01496708.

112. Mager WH, De Kruijff AJ., 1995 Stress-induced transcriptional activation. Microbiol Rev. 59(3):506-31. doi: 10.1128/mr.59.3.506-531.1995. PMID: 7565416; PMCID: PMC239371.

113. Ruis H, Schüller C., 1995 Stress signaling in yeast. Bioessays. 17(11):959-65. doi: 10.1002/bies.950171109. PMID: 8526890.

114. Audrey P. Gasch, Paul T. Spellman, Camilla M. Kao, Orna Carmel-Harel, Michael B. Eisen, Gisela Storz, David Botstein, and Patrick O. Brown, 2000 Genomic Expression Programs in the Response of Yeast Cells to Environmental Changes. Vol. 11, 4241–4257.

115. Nelson MA, Metzenberg RL., 1992 Sexual development genes of Neurospora crassa. Genetics. 132(1):149-62. doi: 10.1093/genetics/132.1.149. PMID: 1356883; PMCID: PMC1205113.

116. Alspaugh JA, Perfect JR, Heitman J., 1997 Cryptococcus neoformans mating and virulence are regulated by the G-protein alpha subunit GPA1 and cAMP. Genes Dev. 11(23):3206-17. doi: 10.1101/gad.11.23.3206. PMID: 9389652; PMCID: PMC316752.

117. Werner-Washburne M, Braun E, Johnston GC, Singer RA., 1993 Stationary phase in the yeast Saccharomyces cerevisiae. Microbiol Rev. 57(2):383-401. doi: 10.1128/mr.57.2.383-401.1993. PMID: 8393130; PMCID: PMC372915.

118. Braun EL, Fuge EK, Padilla PA, Werner-Washburne M., 1996 A stationary-phase gene in Saccharomyces cerevisiae is a member of a novel, highly conserved gene family. J Bacteriol. 178(23):6865-72. doi: 10.1128/jb.178.23.6865-6872.1996. PMID: 8955308; PMCID: PMC178587.

119. Cullen PJ, Sprague GF, Jr., 2012 The regulation of filamentous growth in yeast. Genetics 190: 23–49.

120. Pan X, Heitman J., 1999 Cyclic AMP-dependent protein kinase regulates pseudohyphal differentiation in Saccharomyces cerevisiae. Mol Cell Biol. 19: 4874–4887.

121. Zaragoza O, Gancedo JM., 2000 Pseudohyphal growth is induced in Saccharomyces cerevisiae by a combination of stress and cAMP signalling. Antonie Van Leeuwenhoek. 78(2):187-94. doi: 10.1023/a:1026594407609. PMID: 11204770.

122. Estruch F., 2000 Stress-controlled transcription factors, stress-induced genes and stress tolerance in budding yeast. FEMS Microbiol Rev. 24(4):469-86. doi: 10.1111/j.1574-6976.2000.tb00551.x. PMID: 10978547.

123. Igual, Juan Carlos;Estruch, Francisco, 2000 Signalling Stress in Yeast. Food technology and biotechnology. Vol. 38, Issue 4, pages 263 – 276.

124. DeRisi JL, Iyer VR, Brown PO., 1997 Exploring the metabolic and genetic control of gene expression on a genomic scale. Science. 278(5338):680-6. doi: 10.1126/science.278.5338.680. PMID: 9381177.

125. Fuge EK, Braun EL, Werner-Washburne M., 1994 Protein synthesis in long-term stationary-phase cultures of Saccharomyces cerevisiae. J Bacteriol. 176: https://doi.org/10.1128/jb.176.18.5802-5813.1994.

126. Ashe MP, De Long SK, Sachs AB., 2000 Glucose depletion rapidly inhibits translation initiation in yeast. Mol Biol Cell. 11(3):833-48. doi: 10.1091/mbc.11.3.833. PMID: 10712503; PMCID: PMC14814.

127. François J, Parrou JL., 2001 Reserve carbohydrates metabolism in the yeast Saccharomyces cerevisiae. FEMS Microbiol Rev. 25(1):125-45. doi: 10.1111/j.1574-6976.2001.tb00574.x. PMID: 11152943.

128. Albig AR, Decker CJ., 2001 The target of rapamycin signaling pathway regulates mRNA turnover in the yeast Saccharomyces cerevisiae. Mol Biol Cell. 12(11):3428-38. doi: 10.1091/mbc.12.11.3428. PMID: 11694578; PMCID: PMC60265.

129. Vasudevan S, Peltz SW., 2001 Regulated ARE-mediated mRNA decay in Saccharomyces cerevisiae. Mol Cell. 7(6):1191-200. doi: 10.1016/s1097-2765(01)00279-9. PMID: 11430822.

130. Causton HC, Ren B, Koh SS, Harbison CT, Kanin E, Jennings EG, Lee TI, True HL, Lander ES, Young RA., 2001 Remodeling of yeast genome expression in response to environmental changes. Mol Biol Cell. 12(2):323-37. doi: 10.1091/mbc.12.2.323. PMID: 11179418; PMCID: PMC30946.

131. Gasch AP, Werner-Washburne M., 2002 The genomics of yeast responses to environmental stress and starvation. Funct Integr Genomics. 2(4-5):181-92. doi: 10.1007/s10142-002-0058-2. Epub 2002 Apr 30. PMID: 12192591.

132. Chaudhuri A, Das S, Das B., 2020 Localization elements and zip codes in the intracellular transport and localization of messenger RNAs in Saccharomyces cerevisiae. Wiley Interdiscip Rev RNA. 11(4):e1591. doi: 10.1002/wrna.1591. Epub 2020 Feb 26. PMID: 32101377.

133. Das, S., Biswas, S., Chaudhuri, S., Bhattacharya, A. and Das, B., 2019 A nuclear zip code in SKS1 mRNA promotes its slow export, nuclear retention and degradation by the Nuclear exosome/DRN in Saccharomyces cerevisiae. J. Mol. Biol. 431, 3626-3646.

134. Maity, J., Das, B., Bohr, V., and Karmakar, P., 2018 Acidic domain of WRNp is critical for autophagy and up-regulates age associated proteins. DNA Repair. 68, 1-11, https://doi.org/10.1016/j.dnarep.2018.05.003.
135. Singh, P., Saha, U., Paira, S. and Das, B., 2018 Nuclear mRNA Surveillance mechanisms: Function and links to human diseases. J. Mol. Biol. 430, 1993-2013, doi:10.1016/j.jmb.2018.05.009.
136. Sarkar, D. Paira, S. and Das, B., 2018 Nuclear mRNA degradation tunes the gain of the unfolded protein response in Saccharomyces cerevisiae. Nucleic Acids Res. 46, 1139-1156, doi: 10.1093/nar/gkx1160.
137. Das, S., Sarkar, D. & Das, B., 2017 The Interplay between Transcription and mRNA Degradation in Saccharomyces cerevisiae. Microbial Cell. 4(7), 212-228.
138. Das S, Das B.,2016 eIF4G-an integrator of mRNA metabolism? FEMS Yeast Res. 16(7):fow087. doi: 10.1093/femsyr/fow087. Epub 2016 Sep 29. PMID: 27694156.
139. Wang, Y-K., Das, B, Huber, D. H., Sherman, F. and Ruschenko, E. P. (2004) Role of the 14-3-3 protein in carbon metabolism of the pathogenic yeast Candida albicans. Yeast, 21, 685-702).
140. Das B, Guo Z, Russo P, Chartrand P, Sherman F., 2000 The role of nuclear cap binding protein Cbc1p of yeast in mRNA termination and degradation. Mol Cell Biol. 20(8):2827-38. doi: 10.1128/MCB.20.8.2827-2838.2000. PMID: 10733586; PMCID: PMC85501.
141. Polevoda B, Martzen MR, Das B, Phizicky EM, Sherman F., 2000 Cytochrome c methyltransferase, Ctm1p, of yeast. J Biol Chem. 275(27):20508-13. doi: 10.1074/jbc.M001891200. PMID: 10791961.
142. Pearce DA, Carr CJ, Das B, Sherman F. Phenotypic reversal of the btn1 defects in yeast by chloroquine: a yeast model for Batten disease. Proc Natl Acad Sci U S A. 1999 Sep 28;96(20):11341-5. doi: 10.1073/pnas.96.20.11341. PMID: 10500178; PMCID: PMC18035.
143. Maity A, Das B., 2016 N6-methyladenosine modification in mRNA: machinery, function and implications for health and diseases. FEBS J. 283(9):1607-30. doi: 10.1111/febs.13614. Epub 2015 Dec 31. PMID: 26645578.
144. Chakrabarti, Abhijit, Aloke K. Bera, Biswadip Das, Subrata Chattopadhyay, Dibyendu Sarkar, and Chanchal DasGupta. “Binding and Conformation of Denatured Horseradish Peroxidase during E. Coli Ribosome Mediated Folding.” Current Science 76, no. 9 (1999): 1235–38. http://www.jstor.org/stable/24101949.
145. Pearce, D.A., Ferea, T., Nosel, S. A., Das, B. and Sherman, F., 1999 DNA microarray analysis of strains lacking BTN1, the yeast. ortholog of the human Batten disease gene. Nature Genet. 23, 73-73 (2017 SCI Impact factor: 27.95).
146. Pearce DA, Ferea T, Nosel SA, Das B, Sherman F., 1999 Action of BTN1, the yeast orthologue of the gene mutated in Batten disease. Nat Genet. 22(1):55-8. doi: 10.1038/8861. PMID: 10319861.

147. Chattopadhyay S, Das B, Dasgupta C., 1996 Reactivation of denatured proteins by 23S ribosomal RNA: role of domain V. Proc Natl Acad Sci U S A. 93(16):8284-7. doi: 10.1073/pnas.93.16.8284. PMID: 8710862; PMCID: PMC38662.

148. Bharatula V, Broach JR., 2018 The nutrient stress response in yeast. In Stress Response Mechanisms in Fungi: Theoretical and Practical Aspects. Springer International Publishing. p. 131-159 doi: 10.1007/978-3-030-00683-9_4

149. Kresnowati MT, van Winden WA, Almering MJ, ten Pierick A, Ras C, Knijnenburg TA, Daran-Lapujade P, Pronk JT, Heijnen JJ, Daran JM., 2006 When transcriptome meets metabolome: fast cellular responses of yeast to sudden relief of glucose limitation. Mol Syst Biol. 2:49. doi: 10.1038/msb4100083. Epub 2006 Sep 12. PMID: 16969341; PMCID: PMC1681515.

150. Zaman S, Lippman SI, Schneper L, Slonim N, Broach JR., 2009 Glucose regulates transcription in yeast through a network of signaling pathways. Mol Syst Biol. 5:245. doi: 10.1038/msb.2009.2. Epub 2009 Feb 17. Erratum in: Mol Syst Biol. 2009;5:257. PMID: 19225458; PMCID: PMC2657534.

151. Kaniak A, Xue Z, Macool D, Kim JH, Johnston M., 2004 Regulatory network connecting two glucose signal transduction pathways in Saccharomyces cerevisiae. Eukaryot Cell. 3(1):221-31. doi: 10.1128/EC.3.1.221-231.2004. PMID: 14871952; PMCID: PMC329515.

152. Karhumaa K, Wu B, Kielland-Brandt MC., 2010 Conditions with high intracellular glucose inhibit sensing through glucose sensor Snf3 in Saccharomyces cerevisiae. J Cell Biochem. 110(4):920-5. doi: 10.1002/jcb.22605. PMID: 20564191.

153. Snowdon C, Johnston M., 2016 A novel role for yeast casein kinases in glucose sensing and signaling. Mol Biol Cell. 27(21):3369-3375. doi: 10.1091/mbc.E16-05-0342. Epub 2016 Sep 14. PMID: 27630263; PMCID: PMC5170868.

154. Wu H, Zheng X, Araki Y, Sahara H, Takagi H, Shimoi H., 2006 Global gene expression analysis of yeast cells during sake brewing. Appl Environ Microbiol. 72(11):7353-8. doi: 10.1128/AEM.01097-06. Epub 2006 Sep 22. PMID: 16997994; PMCID: PMC1636205.

155. Yang Z, Bisson LF, 1996 The SKS1 protein kinase is a multicopy suppressor of the snf3 mutation of Saccharomyces cerevisiae. Yeast. 12(14):1407-19. doi: 10.1002/(SICI)1097-0061(199611)12:14%3C1407::AID-YEA36%3E3.0.CO;2-1. PMID: 8948096.

156. Vagnoli P, Bisson LF., 1998 The SKS1 gene of Saccharomyces cerevisiae is required for long-term adaptation of snf3 null strains to low glucose. Yeast. 14(4):359-69. doi: 10.1002/(SICI)1097-0061(19980315)14:4<359::AID-YEA227>3.0.CO;2-#. PMID: 9559544.

157. Johnson C, Kweon HK, Sheidy D, Shively CA, Mellacheruvu D, Nesvizhskii AI, Andrews PC, Kumar A., 2014 The yeast Sks1p kinase signaling network regulates pseudohyphal growth and glucose response.

PLoS Genet. 10(3):e1004183. doi: 10.1371/journal.pgen.1004183. PMID: 24603354; PMCID: PMC3945295.

158. Sherman F., 1991 Getting started with yeast. Methods Enzymol. 194:3-21. doi: 10.1016/0076-6879(91)94004-v. PMID: 2005794.
159. Janke C, Magiera MM, Rathfelder N, Taxis C, Reber S, Maekawa H, Moreno-Borchart A, Doenges G, Schwob E, Schiebel E, Knop M., 2004 A versatile toolbox for PCR-based tagging of yeast genes: new fluorescent proteins, more markers and promoter substitution cassettes. Yeast. 21(11):947-62. doi: 10.1002/yea.1142. PMID: 15334558.
160. Kizer KO, Xiao T, Strahl BD., 2006 Accelerated nuclei preparation and methods for analysis of histone modifications in yeast. Methods. 40(4):296-302. doi: 10.1016/j.ymeth.2006.06.022. PMID: 17101440; PMCID: PMC1698964.
161. Brodsky AS, Silver PA., 2000 Pre-mRNA processing factors are required for nuclear export. RNA. 6(12):1737-49. doi: 10.1017/s1355838200001059. PMID: 11142374; PMCID: PMC1370044.
162. Tang J, Abovich N, Rosbash M., 1996 Identification and characterization of a yeast gene encoding the U2 small nuclear ribonucleoprotein particle B" protein. Mol Cell Biol. 2787-95. doi: 10.1128/MCB.16.6.2787. PMID: 8649387; PMCID: PMC231270.
163. Bachler M, Schroeder R, Von Ahsen U., 1999 StreptoTag: A novel method for the isolation of RNA-binding proteins. RNA. 5(11):1509-1516. doi:10.1017/S1355838299991574
164. Windbichler N, Schroeder R., 2006 Isolation of specific RNA-binding proteins using the streptomycin-binding RNA aptamer. Nat Protoc. 1(2):637-40. doi: 10.1038/nprot.2006.95. PMID: 17406291. https://doi.org/10.1002/(SICI)1097-0061(19980315)14:4<359::AID-YEA227>3.0.
165. Perez-Riverol Y., A. Csordas, J. Bai, M. Bernal-Llinares, S. Hewapathirana, et al., 2019 The PRIDE database and related tools and resources in 2019: improving support for quantification data. Nucleic Acids Res. 47: D442–D450. https://doi.org/10.1093/NAR/GKY1106
166. Victorino J. F., M. J. Fox, W. R. Smith-Kinnaman, S. A. Peck Justice, K. H. Burriss, *et al.*, 2020 RNA Polymerase II CTD phosphatase Rtr1 fine-tunes transcription termination. PLOS Genet. 16: e1008317.
167. Hogan D. J., D. P. Riordan, A. P. Gerber, D. Herschlag, and P. O. Brown, 2008 Diverse RNA-binding proteins interact with functionally related sets of RNAs, suggesting an extensive regulatory system. PLoS Biol. 6: e255. https://doi.org/10.1371/journal.pbio.0060255
168. Qu X., S. Lykke-Andersen, T. Nasser, C. Saguez, E. Bertrand, et al., 2009 Assembly of an export-competent mRNP is needed for efficient release of the 3'-end processing complexes after polyadenylation. Mol Cell Biol. 29: 5327–5338. https://doi.org/10.1128/MCB.00468-09MCB.00468-09

169. Tomecki R., M. S. Kristiansen, S. Lykke-Andersen, A. Chlebowski, K. M. Larsen, *et al.,* 2010 The human core exosome interacts with differentially localized processive RNases: hDIS3 and hDIS3L. EMBO J. 29: 2342–2357. https://doi.org/10.1038/emboj.2010.121emboj2010121

170. Garay-Arroyo A., and A. A. Covarrubias, 1999 Three genes whose expression is induced by stress inSaccharomyces cerevisiae. Yeast. 15: 879–892. https://doi.org/10.1002/(SICI)1097-0061(199907)15:10A<879::AID-YEA428>3.0.CO;2-Q

171. Hlynialuk C., R. Schierholtz, A. Vernooy, and G. van der Merwe, 2008 Nsf1/Ypl230w participates in transcriptional activation during non-fermentative growth and in response to salt stress in Saccharomyces cerevisiae. Microbiology. 154: 2482–2491. https://doi.org/10.1099/mic.0.2008/019976-0

172. Okamoto K., N. Kondo-Okamoto, and Y. Ohsumi, 2009 Mitochondria-Anchored Receptor Atg32 Mediates Degradation of Mitochondria via Selective Autophagy. Dev. Cell. 17: 87–97. https://doi.org/10.1016/j.devcel.2009.06.013

173. Jacinto E., B. Guo, K. T. Arndt, T. Schmelzle, and M. N. Hall, 2001 TIP41 Interacts with TAP42 and Negatively Regulates the TOR Signaling Pathway. Mol. Cell. 8: 1017–1026. https://doi.org/10.1016/S1097-2765(01)00386-0

174. Davie E., G. M. A. Forte, and J. Petersen, 2015 Nitrogen Regulates AMPK to Control TORC1 Signaling. Curr. Biol. 25: 445–454. https://doi.org/10.1016/j.cub.2014.12.034

175. Puig S., and J. E. Perez-Ortin, 2000 Stress response and expression patterns in wine fermentations of yeast genes induced at the diauxic shift. Yeast. 16: 139–148. https://doi.org/10.1002/(SICI)1097-0061(20000130)16:2<139::AID-YEA512>3.0.CO;2-J

176. Pascual-Ahuir A., R. Serrano, and M. Proft., 2001 The Sko1p Repressor and Gcn4p Activator Antagonistically Modulate Stress-Regulated Transcription in Saccharomyces cerevisiae. Mol. Cell. Biol. 21: 16–25. https://doi.org/10.1128/MCB.21.1.16-25.2001

177. Linder P., and E. Jankowsky, 2011 From unwinding to clamping the DEAD box RNA helicase family. Nat. Rev. Mol. Cell Biol. 12: 505–516.

178. Putnam A. A., and E. Jankowsky, 2013 DEAD-box helicases as integrators of RNA, nucleotide and protein binding. Biochim. Biophys. Acta - Gene Regul. Mech. 1829: 884–893.

179. Rogers G. W., N. J. Richter, and W. C. Merrick. 1999.Biochemical and Kinetic Characterization of the RNA Helicase Activity of Eukaryotic Initiation Factor 4A.

180. Yang Q., and E. Jankowsky, 2006 The DEAD-box protein Ded1 unwinds RNA duplexes by a mode distinct from translocating helicases. Nat. Struct. Mol. Biol. 13: 981–986. https://doi.org/10.1038/nsmb1165.

181. Fairman M. E., P. A. Maroney, W. Wang, H. A. Bowers, P. Gollnick, et al., 1999 Protein Displacement by DExH/D "RNA Helicases" Without Duplex Unwinding Downloaded from. 24. C. J. Hueck, Microbiol. Mol. Biol. Rev. 167: 5979. https://doi.org/10.1126/science.1096330.

182. Nielsen K. H., H. Chamieh, C. B. F. Andersen, F. Fredslund, K. Hamborg, et al., 2009 Mechanism of ATP turnover inhibition in the EJC. RNA. 15: 67–75. https://doi.org/10.1261/rna.1283109.

183. Ballut L., B. Marchadier, A. Baguet, C. Tomasetto, B. Séraphin, et al., 2005 The exon junction core complex is locked onto RNA by inhibition of eIF4AIII ATPase activity. Nat. Struct. Mol. Biol. 12: 861–869. https://doi.org/10.1038/nsmb990.

184. Zolotukhin A., D. Michalowski, J. Bear, S. V. Smulevitch, A. M. Traish, et al., 2003 PSF acts through the human immunodeficiency virus type 1 mRNA instability elements to regulate virus expression. Mol. Cell. Biol. 23: 6618–6630. https://doi.org/10.1128/MCB.23.18.6618

185. Prasanth K. V., S. G. Prasanth, Z. Xuan, S. Hearn, S. M. Freier, et al., 2005 Regulating gene expression through RNA nuclear retention. Cell. 123: 249–263. https://doi.org/10.1016/j.cell.2005.08.033.

186. Lassen K. G., K. X. Ramyar, J. R. Bailey, Y. Zhou, and R. F. Siliciano, 2006 Nuclear retention of multiply spliced HIV-1 RNA in resting CD4+ T cells. PLoS Pathog. 2: 0650–0661. https://doi.org/10.1371/journal.ppat.0020068.

187. Dunscombe P., C. Grau, N. Defourny, J. Malicki, J. M. Borras, et al., 2014 Guidelines for equipment and staffing of radiotherapy facilities in the European countries: final results of the ESTRO-HERO survey. Radiother Oncol. 112: 165–177. https://doi.org/10.1016/j.radonc.2014.08.032S0167-8140(14)00362-4.

188. Halpern K. B., I. Caspi, D. Lemze, E. Elinav, I. Ulitsky, et al., 2015 Nuclear Retention of mRNA in Mammalian Tissues Report Nuclear Retention of mRNA in Mammalian Tissues. Cell Reports. 1–10. https://doi.org/10.1016/j.celrep.2015.11.036.

189. Bresson S. M., O. V Hunter, A. C. Hunter, and N. K. Conrad, 2015 Canonical Poly(A) Polymerase Activity Promotes the Decay of a Wide Variety of Mammalian Nuclear RNAs., (T. Jensen, Ed.). PLoS Genet. 11: e1005610. https://doi.org/10.1371/journal.pgen.1005610

190. Akef A., E. S. Lee, and A. F. Palazzo, 2015 Splicing promotes the nuclear export of β-globin mRNA by overcoming nuclear retention elements. RNA. 21: 1908–20. https://doi.org/10.1261/rna.051987.115.

191. Ma G., J. Yasunaga, K. Shimura, K. Takemoto, M. Watanabe, et al., 2021 Human retroviral antisense mRNAs are retained in the nuclei of infected cells for viral persistence. Proc. Natl. Acad. Sci. 118: e2014783118. https://doi.org/10.1073/pnas.2014783118.

192. Woods A, Munday MR, Scott J, Yang X, Carlson M, Carling D. ,1994 Yeast SNF1 is functionally related to mammalian AMP-activated protein kinase and regulates acetyl-CoA carboxylase in vivo. J Biol Chem. 269(30):19509-15. PMID: 7913470.

193. James R Broach,2012 Nutritional Control of Growth and Development in Yeast. Genetics. Pages 73–105, https://doi.org/10.1534/genetics.111.135731

194. González A, Hall MN, Lin SC, Hardie DG., 2020 AMPK and TOR: The Yin and Yang of Cellular Nutrient Sensing and Growth Control. Cell Metab. Mar 3;31(3):472-492. doi: 10.1016/j.cmet.2020.01.015. PMID: 32130880.

195. Sandoval J., J. L. Rodriguez, G. Tur, G. Serviddio, J. Pereda, et al., 2004 RNAPol-ChIP: a novel application of chromatin immunoprecipitation to the analysis of real-time gene transcription. Nucleic Acids Res 32: e88. https://doi.org/10.1093/nar/gnh09132/11/e88

196. Ho CK, Shuman S., 1999 Distinct roles for CTD Ser-2 and Ser-5 phosphorylation in the recruitment and allosteric activation of mammalian mRNA capping enzyme. *Mol Cell*. 3(3):405-411. doi:10.1016/s1097-2765(00)80468-2

microbial cell

Research Article

www.microbialcell.com

Polyadenylated versions of small non-coding RNAs in *Saccharomyces cerevisiae* are degraded by Rrp6p/Rrp47p independent of the core nuclear exosome

Anusha Chaudhuri[1,#], Soumita Paul[2,#], Mayukh Banerjea[2] and Biswadip Das[2,*]

[1] Present Position: Zentrum für Molekulare, Medizin, Institut für Kardiovaskuläre Regeneration, Haus 25B, Goethe-Universität, Theodor -Stern-Kai 7, Universitätsklinikum, 60590 Frankfurt am Main, Germany. [2] Department of Life Science and Biotechnology, Jadavpur University, 188 Raja S.C. Mullick Road, Kolkata – 700 032, West Bengal, India.

[#] These authors contributed equally to this work.
* Corresponding Author:
Dr. Biswadip Das, Professor, Department of Life Science and Biotechnology, Jadavpur University, 188 Raja S.C. Mullick Road, Kolkata – 700 032, West Bengal, India; Phone: 91-9748908607 (Cell); E-mail: biswadipdas22@gmail.com, biswadip.das@jadavpuruniversity.in

ABSTRACT In *Saccharomyces cerevisiae*, polyadenylated forms of mature (and not precursor) small non-coding RNAs (sncRNAs) those fail to undergo proper 3′-end maturation are subject to an active degradation by Rrp6p and Rrp47p, which does not require the involvement of core exosome and TRAMP components. In agreement with this finding, Rrp6p/Rrp47p is demonstrated to exist as an exosome-independent complex, which preferentially associates with mature polyadenylated forms of these sncRNAs. Consistent with this observation, a C-terminally truncated version of Rrp6p (Rrp6p-ΔC2) lacking physical association with the core nuclear exosome supports their decay just like its full-length version. Polyadenylation is catalyzed by both the canonical and non-canonical poly(A) polymerases, Pap1p and Trf4p. Analysis of the polyadenylation profiles in WT and *rrp6*-Δ strains revealed that the majority of the polyadenylation sites correspond to either one to three nucleotides upstream or downstream of their mature ends and their poly(A) tails ranges from 10-15 adenylate residues. Most interestingly, the accumulated polyadenylated snRNAs are functional in the *rrp6*-Δ strain and are assembled into spliceosomes. Thus, Rrp6p-Rrp47p defines a core nuclear exosome-independent novel RNA turnover system in baker's yeast targeting imperfectly processed polyadenylated sncRNAs that accumulate in the absence of Rrp6p.

doi: 10.15698/mic2024.05.823
Received originally: 13.02.2024;
in revised form: 03.03.2024,
Accepted 05.03.2024,
Published 22.05.2024.

Keywords: rRNA, snoRNA, snRNA, Nuclear Exosome, Rrp6p, Rrp47p, Mpp6p, Nuclear RNA turnover.

Abbreviations:
CTEXT – Cbc1p-Tif4631p-dependent EXosomal Targeting,
LM-PAT – Ligation-Mediated PolyA Tail,
NNS complex – Nrd1p-Nab3p-Sen1p complex,
rRNA – ribosomal RNA,
sncRNA – small non-coding RNA,
snRNA – small nuclear RNA,
snoRNA – small nucleolar RNA,
TRAMP – TRf4p/5p-Air1p/2p-Mtr4p-Polyadenylation,
WT – wild type.

INTRODUCTION

In baker's yeast *Saccharomyces cerevisiae*, ribosomal RNAs (rRNAs), small nuclear RNAs (snRNAs), and small nucleolar RNAs (snoRNAs) comprise the major class of untranslated RNAs that serve diverse functions at distinct phases of the gene expression pipeline. The rDNA locus encoding rRNAs consists of a 9.1 kb long DNA segment that expresses 100 to 200 copies of the 35S rRNA precursor unit. Each 35S rRNA precursor unit consists of 18S, 5.8S, and 25S rRNA genes and two non-transcribed spacer units (NTSs) separated by the 5S rRNA (reviewed in Refs. [1] and [2]). The 5S rRNA gene is transcribed in the opposite direction by RNA polymerase III to generate a precursor that is extended by ten nucleotides at its 3′-end. Their maturation involves exonucleolytic removal of the 3′-end extension by the product of the *RNA82* gene [3] and several modification events.

Two other prominent classes of small non-coding RNAs (sncRNAs), as exemplified by snRNAs and snoRNAs, encode small nuclear RNAs (comprise the RNA components of spliceosome machinery) and small nucleolar RNAs (serve as the guide RNAs for site-specific modification events in the ribo-

OXFORD GENETICS

GENETICS, 2025, 229(3), iyae221
https://doi.org/10.1093/genetics/iyae221
Advance Access Publication Date: 31 December 2024
Investigation

The ATP-dependent DEAD-box RNA helicase Dbp2 regulates the glucose/nitrogen stress response in baker's yeast by modulating reversible nuclear retention and decay of *SKS1* mRNA

Soumita Paul [1], Subhadeep Das [1,3], Mayukh Banerjea [1], Shouvik Chaudhuri,[2,4] Biswadip Das [1,*]

[1]Department of Life Science and Biotechnology, Jadavpur University, Kolkata 700032, India
[2]Department of Mechanical Engineering, Jadavpur University, Kolkata 700032, India
[3]Present address: Department of Biochemistry, Purdue University, BCHM A343, 175 South University Street, West Lafayette, IN 47907, USA
[4]Present address: Department of Mechanical and Electrical Engineering, University of Southern Denmark, Alsion 2, DK-6400 Sonderborg, Denmark

*Corresponding author: Department of Life Science and Biotechnology, Jadavpur University, 188 Raja S.C. Mullick Road, Kolkata 700032, West Bengal, India.
Email: biswadip.das@jadavpuruniversity.in

In *Saccharomyces cerevisiae*, *SKS1* mRNA encoding a glucose-sensing serine/threonine kinase belongs to "nucleus-retained" (NR) mRNAs representing a subset of otherwise normal transcripts, which exhibits slow nuclear export and excessively long nuclear dwell time. Nuclear retention of the *SKS1* mRNA triggered by a 202 nt "export-retarding" nuclear zip code element promotes its rapid degradation in the nucleus by the nuclear exosome/CTEXT. In this investigation, we demonstrate that Dbp2p, an ATP-dependent DEAD-box RNA helicase binds to *SKS1* and other NR-mRNAs and thereby inhibits their export by antagonizing with the binding of the export factors Mex67p/Yra1p. Consistent with this observation, a significant portion of these NR-mRNAs was found to localize into the cytoplasm in a yeast strain carrying a deletion in the *DBP2* gene with the concomitant enhancement of its steady-state level and stability. This observation supports the view that Dbp2p promotes the nuclear retention of NR-mRNAs to trigger their subsequent nuclear degradation. Further analysis revealed that Dbp2p-dependent nuclear retention of *SKS1* mRNA is reversible, which plays a crucial role in the adaptability and viability of the yeast cells in low concentrations of glucose/nitrogen in the growth medium. At high nutrient levels when the function of Sks1p is not necessary, *SKS1* mRNA is retained in the nucleus and degraded. In contrast, during low glucose/nitrogen levels when Sks1p is vital to respond to such situations, the nuclear retention of *SKS1* mRNA is relieved to permit its increased nuclear export and translation leading to a huge burst of cytoplasmic Sks1p.

Keywords: nuclear retention; Dbp2; *SKS1* mRNA; glucose/nitrogen stress; mRNA export; nuclear zip code

Introduction

Nuclear mRNP biogenesis events comprise the capping of the nascent RNA transcript at the 5′-end, pre-mRNA splicing, and cleavage/polyadenylation at the 3′-end of the message (Bird *et al.* 2005; Luna *et al.* 2008; Perales and Bentley 2009; Bjork and Wieslander 2014; Bentley 2015; Fasken and Corbett 2016), These events are accompanied by the association of the nascent transcripts with a wide repertoire of mRNA maturation factors and heterogeneous nuclear ribonucleoproteins (hnRNPs) (Wahle 1991; Kataoka *et al.* 2000; Hir *et al.* 2001; Muller-McNicoll and Neugebauer 2013; Gonatopoulos-Pournatzis and Cowling 2014; Singh *et al.* 2015). This vibrant RNA–protein association initiates with the interaction and binding of the heterodimeric nuclear cap-binding complex (CBC) to the m^7G cap (Gonatopoulos-Pournatzis and Cowling 2014) followed by the deposition of the transcription/export (TREX) complex onto the maturing message that consists of THO proteins, (Hpr1p, Mft1p, Tho2p, and Thp2p), mRNA export factor RNA helicase Sub2p (UAP56 in human); RNA-binding protein (RBP) Yra1p (REF/ALY in human) (Vinciguerra and Stutz 2004; Kohler and Hurt 2007; Perales and Bentley 2009). Cotranscriptional recruitment of these proteins/factors onto the transcribing/maturing message further aids splicing (if intron is present) and 3′-end maturation process followed by the consequent association of the transcript with the export receptor Mex67p:Mtr2p (NXF1:p15 in human), various hnRNPs, and poly(A) tail-binding protein Pab1p (Muller-McNicoll and Neugebauer 2013; Singh *et al.* 2015). The collective and concerted action of the whole spectrum of RBPs ultimately leads to the formation of mature export-competent mRNPs (Proudfoot *et al.* 2002; Stutz and Izaurralde 2003; Vinciguerra and Stutz 2004; Moore and Proudfoot 2009) followed by its release from the transcription site at the chromatin and gradual movement through the interchromatin space to the nuclear periphery. At the nuclear periphery, the export-competent mRNPs dock at the nuclear pore complex, travel through it, and are eventually released into the cytoplasm (Dimaano and Ullman 2004; Tran and Wente 2006; Kohler and Hurt 2007; Rodriguez-Navarro and Hurt 2011; Bjork and Wieslander 2014; Schnell *et al.* 2014). Remarkably, every

Received on 23 October 2024; accepted on 23 December 2024

ORIGINAL ARTICLE **Submitted to *FEBS Journal***

The nuclear mRNA surveillance system regulates telomere length by modulating levels of specific mRNAs encoding key telomere regulators in *Saccharomyces cerevisiae*

Mayukh Banerjea, Soumita Paul[¥] and Biswadip Das[*]

Department of Life Science and Biotechnology, Jadavpur University, Kolkata, India.

[*]**Correspondence**:
Dr. Biswadip Das
Department of Life Science and Biotechnology, Jadavpur University
188 Raja S.C. Mullick Road, Kolkata – 700 032
West Bengal, India
Phone: 91-9748908607 (Cell)
E. mail: biswadip.das@jadavpuruniversity.in

[¥]Present Address: Agrivet Research and Advisory Private Limited, 714 Block-A, Lake Town, South Dumdum, West Bengal - 700089

Running title: CTEXT complex regulates telomere length and silencing.

Abbreviations: CTEXT, **C**BC-**T**if4631p-dependent **ex**osomal **t**argeting,
TRAMP, **TR**f4p/5p-**A**ir1p/2p-**M**tr4p-**P**olyadenylation,
TPE, **T**elomere **P**osition **E**ffect
TLM, **T**elomere **L**ength **M**aintenance

Keywords: Telomere length, Telomere Position Effect, mRNA degradation, Nuclear Exosome, CTEXT, Tif4631p, Rrp6p, Cbc1p.

Conflict of Interest: The authors declare no conflict of Interest.

This file includes: Manuscript File: BanerjeaM25 FEBS Res Art Manuscript.doc (Title page + Abstract + Introduction + Results + Discussion + Materials and methods + Acknowledgement + Data Availability Statement + Author Contributions + Competing Interest Statement + Funding + References + Tables + Legends to Figures)
Figures: BanerjeaM25 FEBS Res Art Manuscript Fig. 1 to 8